Characterization of the Antibacterial Activity of the Type VI Secretion System

Characterization of the Antibacterial Activity of the Type VI Secretion System

A dissertation presented

by

Brian Thomas Ho

to

The Division of Medical Sciences

in partial fulfillment of the requirements

for the degree of

Doctor of Philosophy

in the subject of

Microbiology and Molecular Genetics

Harvard University

Cambridge, Massachusetts

December, 2013

Dissertation Advisor: Professor John J. Mekalanos Brian Thomas Ho

Characterization of the Antibacterial Activity of the Type VI Secretion System

Abstract

This dissertation summarizes advances made toward understanding of the composition, structure, mechanism, and regulation of the bacterial type VI secretion system (T6SS). The T6SS is a widely conserved bacterial nanomachine used by Gram-negative bacteria to deliver toxic effector proteins into the extracellular environment or into adjacent target cells. Systematic deletion of open reading frames present in the *Vibrio cholerae* T6SS gene cluster revealed the genes essential for T6SS activity and provided key insights into understanding the mechanism by which this organelle is assembled and its components are recycled. Characterization of one phage-related T6SS component yielded insight into the mechanism by which many effectors associate with the T6SS organelle and are delivered into target cells. This T6SS component serves both to sharpen the tip of the membrane-puncturing T6SS spike complex and as a vehicle for attaching a diverse set of effector proteins. Time-lapse fluorescence microscopy of GFP-labeled T6SS components revealed key insights into the behavior and regulation of the T6SS in *Pseudomonas aeruginosa*. The T6SS in this organism assembled in response to exogenous T6SS attack by adjacent sister cells as well as heterologous T6SS$^+$ species *V. cholerae* and *Acinetobacter baylyi*. This retaliatory T6SS counterattack was precisely aimed and caused no collateral damage to neighboring, non-aggressive bacteria. These counterattacks are mediated by

phosphorylation cascade that recognizes exogenous attacks and post-translationally activates the T6SS in *P. aeruginosa*. Deletion of genes in this pathway eliminated the retaliatory response while retaining T6SS functionality. This pathway also induced T6SS counterattacks in response to mating pair formation associated with type IV secretion system (T4SS)-mediated DNA conjugation as well as treatment with membrane-disrupting natural product polymyxin B, suggesting that the signal needed to induce T6SS activity was mechanical perturbation of the *P. aeruginosa* cell membrane. Interestingly, these T4SS-induced counterattacks were able to confer resistance to the acquisition of horizontally transferred foreign DNA by selectively killing conjugative donor cells. As such, the T6SS of *P. aeruginosa* may represent a type of general bacterial innate immune system capable of responding to a wide range of exogenous threats.

Table of Contents

Figure Listing

Table Listing

Chapter 1. A view to a kill: the bacterial type 6 secretion system

Advances in the understanding of the structure, mechanical function, assembly, and regulation of the bacterial type 6 secretion system (T6SS) are summarized. This newly recognized bacterial organelle is structurally and mechanistically analogous to an intracellular membrane-attached contractile phage tail. A rapid conformation change in the structure of a sheath protein complex propels T6SS spike and tube components along with a diverse set of anti-bacterial and anti-eukaryotic effectors out of predatory T6SS$^+$ cells and into prey cells. The contracted organelle is then recycled in an ATP-dependent process. T6SS is regulated at both transcriptional and post-translational levels, the latter involving detection of signals associated with membrane perturbation in some species. In addition to directly targeting eukaryotic cells, the T6SS can also target other bacteria co-infecting a mammalian host, highlighting the importance of the T6SS not only for bacterial survival in environmental ecosystems but also in the context of infection and disease.

Foreword

A modified version of this chapter has been submitted as a review to Cell Host & Microbe.

I would like to thank Dr. Tao Dong for contributing to the initial draft of this chapter, specifically to the sections discussing effector discovery strategies and transcriptional regulation. I would also like to thank Professor Mekalanos for considerable help in the editing and revising of this chapter.

Introduction

Several different types of protein secretion systems exist in Gram-negative bacteria that function to translocate proteins outside of their cells, into the extracellular milieu, and sometimes into other cells. The type 6 secretion system (T6SS) represents one of the most recently recognized examples of these organelles. It was first defined functionally in 2006 in *Vibrio cholerae* through genetic identification of several of its critical components and canonical substrates (Pukatzki et al., 2006), but genes now known to be integrally associated with the T6SS had been identified as playing roles in virulence as early as 2002 for *Salmonella* (Folkesson et al., 2002), *Rhizobium* (Bladergroen et al., 2003), *Fracisella* (Nano et al., 2004) and *Edwardsiella* (Rao et al., 2004), while several bioinformatics studies had identified their high conservation and broad distribution in nearly 25% of all Gram-negative bacteria (Das and Chaudhuri, 2003; Pallen et al., 2002; Schlieker et al., 2005). An explosion of interest in T6SS has led to its rapid study in *Pseudomonas* (Mougous et al., 2006), *Escherichia* (Dudley et al., 2006), *Burkholderia* (Schell et al., 2007), *Agrobacterium* (Wu et al., 2008), *Aeromonas* (Suarez et al., 2008), *Helicobacter* (Bartonickova et al., 2012), and *Campylobacter* (Lertpiriyapong et al., 2012) as well as other organisms. Although these initial studies were understandably focused on the role of T6SS in virulence, more recently, T6SSs have been implicated in inter-bacterial interactions ranging from bactericidal activity (Hood et al., 2010; MacIntyre et al., 2010) and competitive growth in mixed-culture biofilms (Schwarz et al., 2010) to self versus non-self discrimination (Alteri et al., 2013; Wenren et al., 2013). Like the type 4 secretion system (T4SS), T6SS can translocate proteins into both prokaryotic and eukaryotic cells, underlining the versatility of the T6SS nanomachine. This review will focus on advances in understanding the structure, mechanical function, assembly, and regulation of this remarkable secretion organelle.

Components, structure, and energetics

The first two canonical substrates of the T6SS belong to protein superfamilies commonly called Hcp (Haemolysin co-regulated protein) and VgrG (Valine-glycine repeat G) (Pukatzki et al., 2006). These proteins are unusual in that they are both secreted and required for T6SS apparatus functionality (Mougous et al., 2006; Pukatzki et al., 2006). Structure prediction algorithms indicated that VgrG proteins show significant structural homology to a complex called $(gp27)_3$-$(gp5)_3$, which corresponds to the tail spike or "needle" of the T4 phage tail (Pukatzki et al., 2007). Early evidence suggested that different VgrG proteins could form complexes (Pukatzki et al., 2007) and eventual evidence for homotrimeric complexes was obtained through crystallographic (Leiman et al., 2009) and biochemical analysis (Hachani et al., 2011). However, the first T6SS protein to be crystalized was the Hcp1 protein of *P. aeruginosa*, and its atomic structure suggested that this protein could form tubes composed of stacked rings of Hcp hexamers (Mougous et al., 2006). Additional evidence for Hcp tube formation was obtained through cross-linking studies (Ballister et al., 2008) and further structural analysis of the Hcp protein fold showed its similarity to a duplicated 'b-tube' domain within the VgrG N-terminal gp27-like domain of VgrG (Leiman et al., 2009). These analyses predicted that if Hcp formed a tube in the context of the functional apparatus, then that tube would likely dock with the 'pseudo hexameric' b-tube domain of a VgrG trimer (Leiman et al., 2009). The NMR structure of the lambda phage tube protein p5 revealed it to be a structural homolog of Hcp (Pell et al., 2009), and indeed bioinformatic analysis of genes encoding Hcp orthologs suggests that they are as closely related to predicted phage tube proteins as other T6SS-encoded Hcp orthologs (Leiman et al., 2009). Such phage tube proteins include gp19 of T4 phage, which lacks a crystal structure but forms tubes similar in appearance to Hcp tubes (Leiman et al., 2009).

A third component of the T6SS apparatus, now known as TssE (Type six subunit E), showed significant homology to the T4 phage base plate component gp25 (Leiman et al., 2009), which is known to reside near the interface between the phage spike and the tube complex (Kanamaru et al., 2002). The similarities between T6SS components and phage pointed to a model predicting that the T6SS represented at least in part a phage tail-like structure in an orientation that is opposite that of phage infection (Leiman et al., 2009) (Figure 1.1) and supported earlier suggestions (Mougous et al., 2006) that Hcp in its tubular conformation might

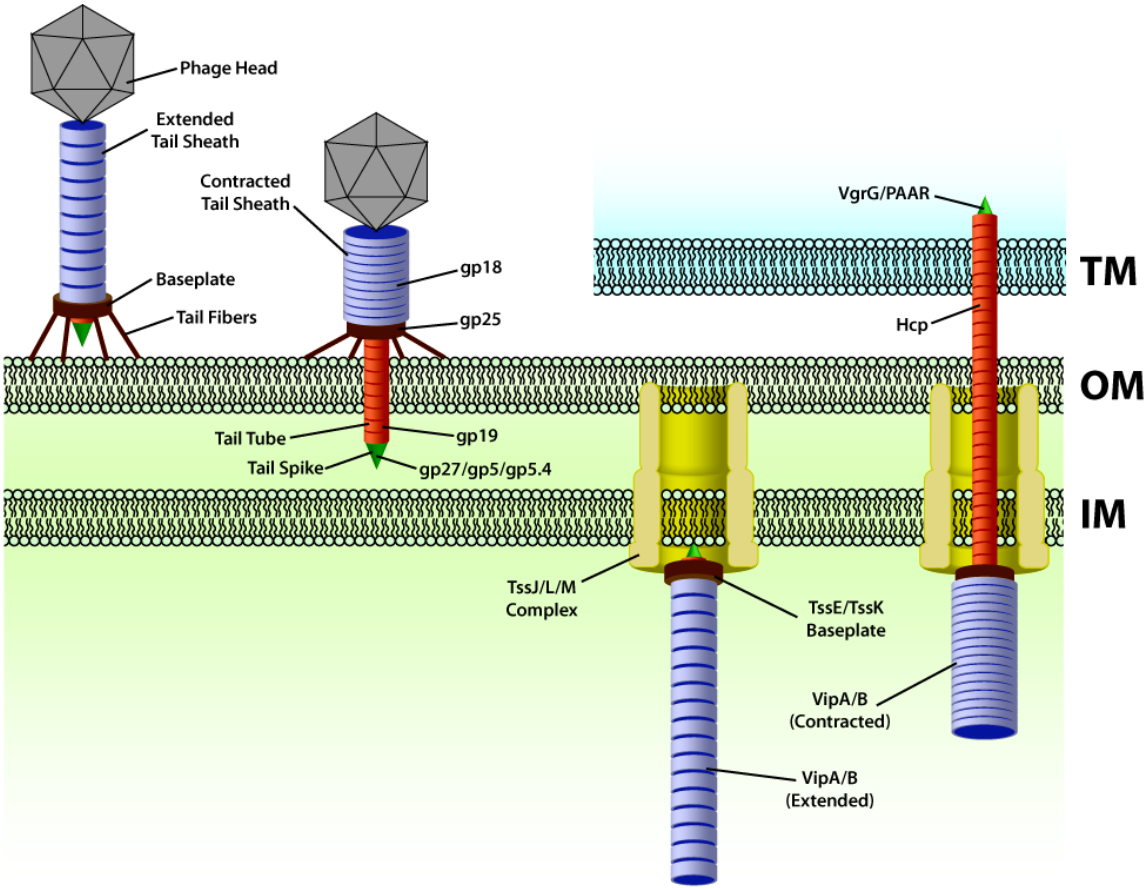

Figure 1.1 Contractile phage tails and the contractile T6SS organelle. T6SS and contractile phage share a number of core structural components. Homologous components are depicted in the same color. While phage attach to the outer membrane (OM) via tail fibers connected to its baseplate, T6SS baseplate attaches to an inner membrane (IM) complex that spans the periplasm and associates with the outer membrane. Contraction of phage sheath delivers the phage spike into a target cell, while contraction of T6SS sheath forces the T6SS spike out of the cell and potentially across a target membrane (TM). Phage T4 gene names of components conserved in T6SS are labeled.

act as a conduit for protein transport by the T6SS machine once extruded from the cell.

Support for the phage tail model for the T6SS organelle came through a series of observations that revolved around three additional essential T6SS components. In a seminal study, Mogk and colleagues determined that in *V. cholerae*, the Clp family AAA+ ATPase ClpV recognized two other T6SS components, VipA and VipB (named for ClpV-interacting protein), the latter two of which formed tubular structures in both *Escherichia coli* and *V. cholerae* (Bonemann et al., 2009). When viewed down the long axis under electron microscopy, VipA/B tubules formed 12-tooth cogwheel-like shapes that were completely disintegrated by a process dependent on ClpV-mediated ATP hydrolysis (Bonemann et al., 2009). It was first noted by Leiman et al. (2009) that the VipA/B tubule structures described by Bonemann et al. (2009) were highly similar to 'contracted' T4 phage tail sheaths, further suggesting that a VipA/B sheath contraction mechanism might provide the energy for T6SS protein transport. With this new information, several models appeared in reviews envisioning how the apparatus might be organized and might actually work (Bonemann et al., 2010; Filloux, 2009; Records, 2011). However, further insights into the functional mechanism of protein translocation by the T6SS organelle would require cell biological analysis and visualization of the dynamic action of intact organelles in living cells as well as super-high resolution visualization of flash-frozen cells.

Basler et al. (2012) were the first to report direct visualization of the T6SS organelle dynamics in *V. cholerae* using a combination of time-lapse fluorescence light microscopy and electron cryotomography. Utilizing functional, fluorescent VipA-GFP fusion proteins, these investigators were able to show that a large VipA-containing sheath structure exists inside cells and undergoes cycles of extension, contraction, disassembly, and re-assembly. The T6SS sheath polymerizes from a membrane-bound complex in an extended conformation, and like phage, the

extended sheath structure then undergoes a rapid contraction event, estimated to occur over less than 5 milliseconds (Basler et al., 2012) (Figure 1.1). Disassembly of the contracted sheath structure is driven by ClpV, which recognizes only the contracted form of the T6SS sheath in both *V. cholerae* and *P. aeruginosa* (Basler and Mekalanos, 2012; Basler et al., 2012). The contraction event is correlated with protein secretion and delivery of effectors and attack signals into target cells (Basler et al., 2013; Basler and Mekalanos, 2012; Basler et al., 2012; Ho et al., 2013). Both the extended and contracted sheath structures are observed attached to the membrane and can be differentiated from each other by their dimensions, surface topology and internal density, the last of which has been hypothesized to correspond minimally to the Hcp tube (Basler et al., 2012).

As with phage, the T6SS apparatus needs a way to attach the tube and sheath complex to a membrane in order to translocate molecules across it. In phage, this is achieved via a large baseplate complex that serves both as a platform for assembly of the tube and sheath, as well as a place for tail fibers to attach (Kostyuchenko et al., 2003) (Figure 1.1). In T6SS, gp25-like TssE is the only homolog to phage baseplate components present (Leiman et al., 2009; Lossi et al., 2011). Instead of a fully phage-like baseplate complex, the T6SS tube and sheath are anchored to the membrane via a complex related to the Dot/Icm T4SS found in *Legionella* (Figure 1.1). This complex consists of two inner membrane components, TssL (DotU-related) and TssM (IcmF-related) (Durand et al., 2012; Ma et al., 2009b; VanRheenen et al., 2004), and an outer-membrane lipoprotein (TssJ) (Felisberto-Rodrigues et al., 2011) (Figure 1.2). In some organisms this complex is thought to be anchored to the peptidoglycan through an extension domain of TssL or through an additional accessory protein (Aschtgen et al., 2010). Although it remains unclear how the T6SS tube and sheath attach to the baseplate, two-hybrid interaction studies

indicate that the essential cytoplasmic protein TssK interacts with both the membrane-bound TssJ-TssL-TssM complex as well as the Hcp tube and VipA/B sheath and may serve as an adaptor between the two (Zoued et al., 2013). There are 3 other essential proteins that are virtually universally conserved, TssF, TssG, and TssA (Boyer et al., 2009; Zheng et al., 2011;

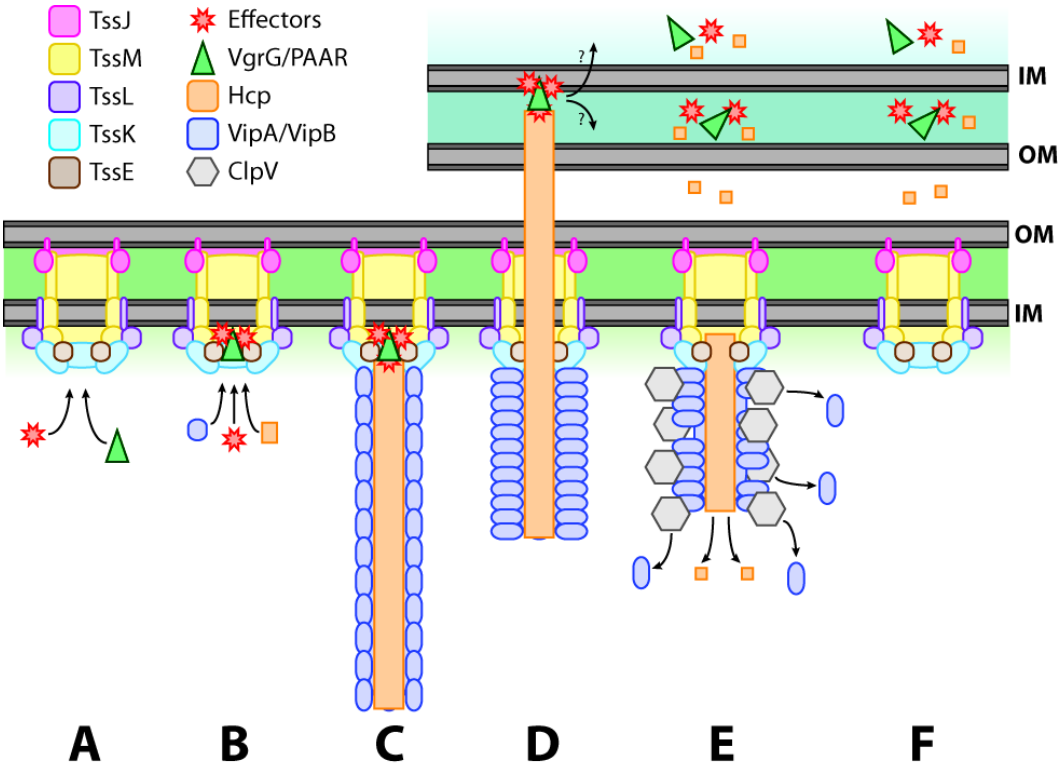

Figure 1.2 T6SS assembly, effector translocation, and component recycling. (**A**) Baseplate complex forms consisting of TssE, TssJ, TssK, TssL and TssM. Other components not pictured include TssA, TssF, and TssG. In some T6SSs, Fha is an essential part of this complex. TssJ, TssK, TssL and TssM are placed in this drawing based on protein localization and interaction studies (Felisberto-Rodrigues et al., 2011; Zoued et al., 2013), while TssE position is inferred from phage homolog (Kostyuchenko et al., 2003) (**B**) VgrG, PAAR, and effector proteins are recruited to this complex and assemble into the structure. VgrG interaction with PAAR or effectors likely contributes to the overall stability of the apparatus assembly. Although these components are pictures here as being cytosolic, it is unclear whether there is an opening into the periplasm. (**C**) Hcp tube polymerizes from VgrG while VipA/VipB sheath polymerizes around it. (**D**) Analogous to phage, a conformation change in the sheath structure results in a contraction event that launches the Hcp tube out of the cell and across a target membrane. This contraction event delivers the loaded VgrG-effector "warhead" through the layers of the cell envelope, however it is not known how often penetration into the cytosol occurs if at all. It is also unknown how much Hcp is lost outside the cell and how much is retained within the cytosol. (**E**) ClpV uses ATP to remodel the contracted sheath, restoring the pool of available sheath subunits. The now unsheathed Hcp tube disassembles; parts of the tube that not expelled from the cell are recycled within the cytosol. (**F**) The naked baseplate complex is then ready to be recycled or disassembled, depending on the T6SS and its activation state.

Zheng and Leung, 2007), but it is unclear what roles they play in T6SS assembly, structure, or function.

Other genes are clearly accessory in regard to their contribution to T6SS function. For example, the protein Fha (Forkhead-associated) (Pallen et al., 2002) is absent in more than half of the bioinformatically identified T6SSs (Boyer et al., 2009) (Figure 1.3A), several of which

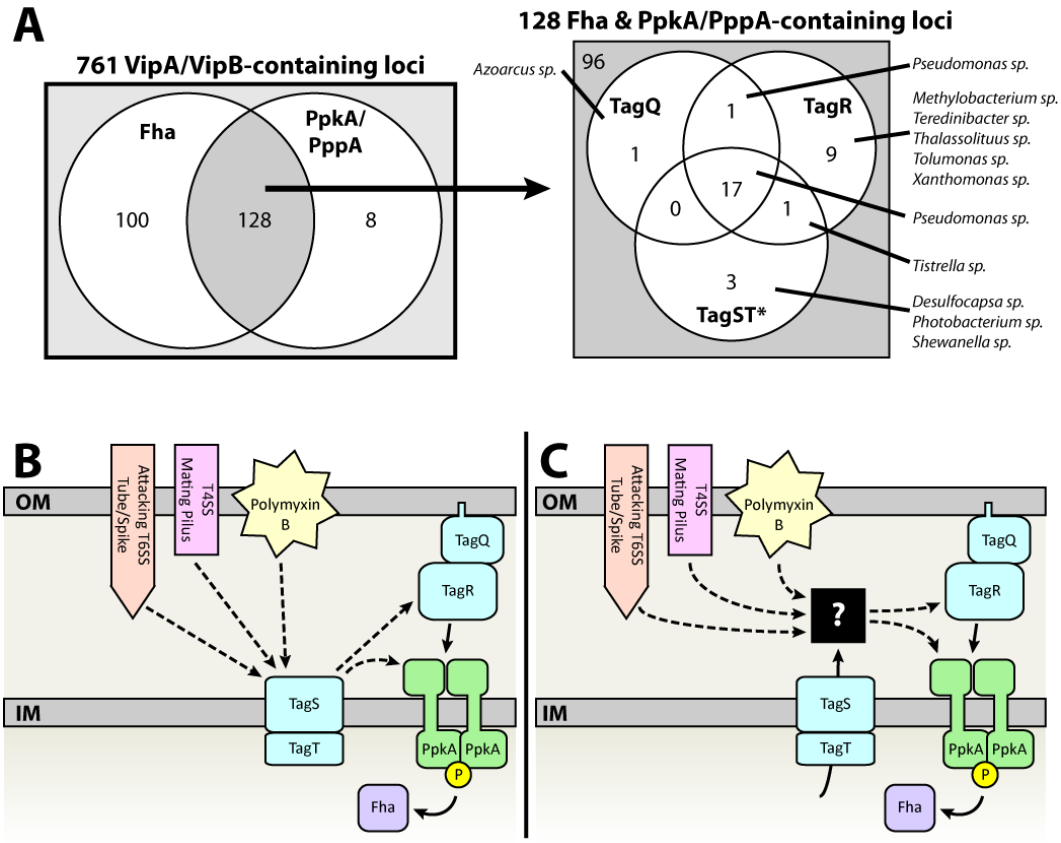

Figure 1.3 T6SS counterattack sensing pathway. (**A**) Hmmsearch (Finn et al., 2011) was used to identify 761 VipA (pfam05591)/VipB (pfam05943)-containing gene loci identified in sequenced bacterial genomes (ftp://ftp.ncbi.nih.gov/genomes/bacteria). 128 of these loci contained nearby (within 40kb) Fha (pfam00498), PpkA (PF00069 or PF13519), and PppA (PF13672) genes. Subsets of these loci carrying different combinations of TagQ (pfam13488), TagR (pfam03781), TagS (pfam02687), or TagT (pfam00005) homologs were also identified. All loci with TagS also had TagT (*). (**B** and **C**) Various signals involving membrane perturbation including exogenous T6SS attack, T4SS mating pair formation and certain membrane disrupting antibiotics like polymyxin B can trigger Fha phosphorylation by PpkA. TagR directly activates PpkA, while TagQ positions TagR in the periplasm and associates it with the outer membrane. TagS and TagT comprise an inner membrane ABC transporter. It is possible that TagS and TagT directly sense the membrane perturbation signal (**B**) or are responsible for localization of the actual signal sensor (**C**). It should be noted that TagS and TagT are not required for delivery of TagQ and TagR to the periplasmic space (Casabona et al., 2012)

have been confirmed to be functional and active without it, such as in *A. baylyi* (Basler et al., 2013) and *E. tarda* (Zheng and Leung, 2007). However, in at least some of the T6SS that do have Fha, such as *P. aeruginosa* (Mougous et al., 2007) and *V. cholerae* (Zheng et al., 2011), the Fha protein has been shown to be essential. In a subset of these organisms (Figure 1.3A), Fha has evolved to play a critical role in mediating post-translational regulation of T6SS activity (Basler et al., 2013; Fritsch et al., 2013; Ho et al., 2013; Mougous et al., 2007).

Based on early data showing subcellular co-localization of Fha and ClpV (Mougous et al., 2007), most models that followed hypothesized that Fha orthologs trigger formation of a membrane-associated complex that is critical to formation of a functional T6SS organelle. As such, one way to conceptualize the T6SS organelle is as a complex composed of two distinct assemblies – one analogous to a contractile phage tail and baseplate and the other a trans-membrane complex (Cascales and Cambillau, 2012; Silverman et al., 2012). However, other than using structural or sequence homology as a guide to differentiate the proteins belonging to these two complexes, there is no data supporting the concept that these two assemblies can form independently. For this reason, we prefer to refer to the entire membrane-associated complex excluding the spike, tube, sheath and ClpV components as the "baseplate complex."

Clearly, energy is required for the function of the T6SS organelle as a protein translocation machine. In this regard, there has been significant controversy in the T6SS field as to what role ClpV plays in the process. ClpV was initially identified as a member of the Clp family of AAA+ ATPases found almost exclusively in pathogenic bacteria (Schlieker et al., 2005) before being implicated in T6SS function (Mougous et al., 2006) and recognized as being widely conserved in nearly all T6SSs (Boyer et al., 2009). Early localization studies of fluorescent ClpV-GFP fusions suggested that ClpV was recruited to specific complexes on the

bacterial membrane containing Fha (Mougous et al., 2007). Members of the Clp family form hexameric ring structures that bind and unfold protein substrates by threading them through their central channel (Mogk et al., 2008). The elegant biochemical studies of Bonemann et al. (2009) confirmed these activities in the context of T6SS, but some models for T6SS function have perhaps overreached on these observations by suggesting that ClpV also drives effector recognition and translocation. For example, one model postulates that after contraction of the VipA/B sheath launches the Hcp tube into a target cell to form an intercellular bridge, ClpV is recruited to power the translocation of effector proteins by threading them down the Hcp tube (Silverman et al., 2012). However, we now know this model is likely incorrect. First, ClpV is not essential for T6SS-dependent bacterial killing, but rather it merely increases T6SS efficiency (Basler et al., 2012; Zheng et al., 2011). Second, ClpV specifically recognizes and remodels VipB (and by association, VipA) in contracted sheaths and not other secreted substrates (Bonemann et al., 2009; Pietrosiuk et al., 2011). Third, when observed in time-lapse ClpV-GFP visibly coats the entire length of the contracted sheath (Basler and Mekalanos, 2012), an observation further confirmed through high-resolution thin-section electron microscopy (Kapitein et al., 2013). Binding along the length of a contracted sheath would be unnecessary if ClpV were merely translocating effectors down the channel of the Hcp tube. Rather than playing a direct role in substrate translocation, these observations suggest that the role of ClpV may actually be to recycle T6SS sheath components, allowing for efficient turnover of at least the contracted sheath if not the entire organelle (Basler and Mekalanos, 2012; Basler et al., 2012) (Figure 1.2). All of the energy required for protein secretion and translocation is contained intrinsically within the assembly of the extended sheath structure. All available evidence indicates ClpV simply allows the cell to re-access this energy potential by ATP-driven

remodeling of VipB/VipB that are trapped in contracted, low energy sheaths (Basler et al., 2012; Bonemann et al., 2009; Pietrosiuk et al., 2011).

The presence of ClpV in the T6SS represents an interesting evolutionary adaptation from its phage relatives. Contractile phages utilize a "one-and-done" mechanism, where a single contraction even is sufficient for penetration of a host membrane and delivery of components needed for successful infection. Unlike phage, bacterial cells benefit greatly from being able to reuse intracellular components of the T6SS. Indeed, fluorescence microscopy has revealed that sheath components can be limiting for *V. cholerae* T6SS. Complementation of a *vipA* mutant with low levels of VipA expression from an inducible plasmid reduced the number of T6SS structures per cell significantly (Basler et al., 2012). Furthermore, nonfunctional ClpV mutants or ClpV mutants unable to recognize VipB show accumulation of contracted sheath structures as well as reduced formation of new T6SS structures (Basler and Mekalanos, 2012). This observation also explains why residual T6SS activity is still observed in ClpV knockouts (Basler et al., 2012; Zheng et al., 2011). In such situations, T6SS structures still form, and assembled sheaths still contract, however after this process occurs once, the T6SS structure is locked in a contracted form and cannot be recycled.

Another key difference between phage and T6SS is the inherent difference in penetration depth provided by the contraction event. T4 Phage tails, for example, are only about 100 nm in length (Duda et al., 1985), while T6SS sheaths can be more than 10 times that length, extending across the entire width and sometimes length of a cell (Basler et al., 2012) (Figure 1.4A). This difference in assembly length results in a contraction-driven tube extrusion for phage like T4 that is only about 50 nanometers. In contrast, T6SS can attack an area up to half the width of the cell and therefore possibly penetrate target cells as deep as 500 nanometers (Figure 1.4B). Like

phage, which must ultimately deliver genetic information into the cytosol, some T6SS nuclease effectors have clear cytosolic targets (Koskiniemi et al., 2013). Although direct delivery into the cytosol by a single T6SS contraction event has never been shown, the calculated penetration depth of the T6SS spike/tube complex suggests that it could commonly occur. If so, one wonders how the tube/spike complex is able to cross the peptidoglycan. Many phage (e.g., T4) carry lysozyme domains fused to their tail spike complexes (Arisaka et al., 2003), but T6SS VgrG proteins lack equivalent domains (Pukatzki et al., 2007) and those that have lysozyme-like effector domains do not need them for target cell intoxication (Zheng et al., 2011). It is possible that phages need to digest their way through the peptidoglycan barrier, while the T6SS can use brute force to puncture this layer to gain access to the cytosol in one contraction event. Ultimately, high-resolution imaging and more precise biophysical measurements of the forces involved will be needed to fully resolve these possibilities.

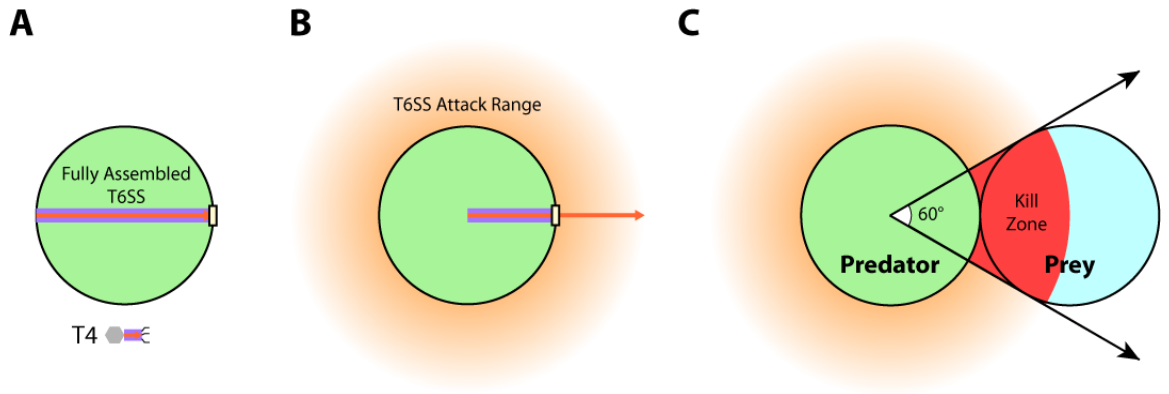

Figure 1.4 Spatial geometry of anti-bacterial T6SS attacks. (**A**) Fully assembled T6SS tube (orange arrow) and sheath (purple rectangle) can extends across the diameter of the cell. By comparison, T4 phage tails are typically only ~100 nm (~1/10 cell width). Phage tail length is drawn approximately to scale. (**B**) After contraction, sheath length is reduced by close to 50%. Assuming the inner Hcp completely fills the sheath, the full range of the T6SS (orange halo) is a zone approximately 500 nm wide (~1/2 cell width) surrounding the cell. (**C**) Assuming perfectly cylindrical cellular geometry and tight spatial packing, at most 1/6th of the T6SS$^+$ attack range will contain a given prey cell. This number is even smaller the larger the distance between the T6SS$^+$ predator and the prey cell, highlighting the need for proper aiming of T6SS attacks. If a prey cell cannot be sensed, the attacker must fire repeatedly in all directions, wasting a majority of the attack potential.

Effector identification, T6SS secretion recognition signals, and mechanism of translocation

The first T6SS effector with confirmed enzymatic activity was the VgrG-1 protein of *V. cholerae* (Pukatzki et al., 2007). This VgrG has become the prototypical example of "evolved VgrGs" carrying additional enzymatic domains fused to the C-terminus of their gp5-like b-helix domain (Leiman et al., 2009) (Figure 1.5). Other examples include *V. cholerae* VgrG-3, which carries a lysozyme-like domain (Brooks et al., 2013; Dong et al., 2013), *A. hydrophila* VgrG-1, which carries an ADP-ribosylating toxin domain (Suarez et al., 2010), and bioinformatically

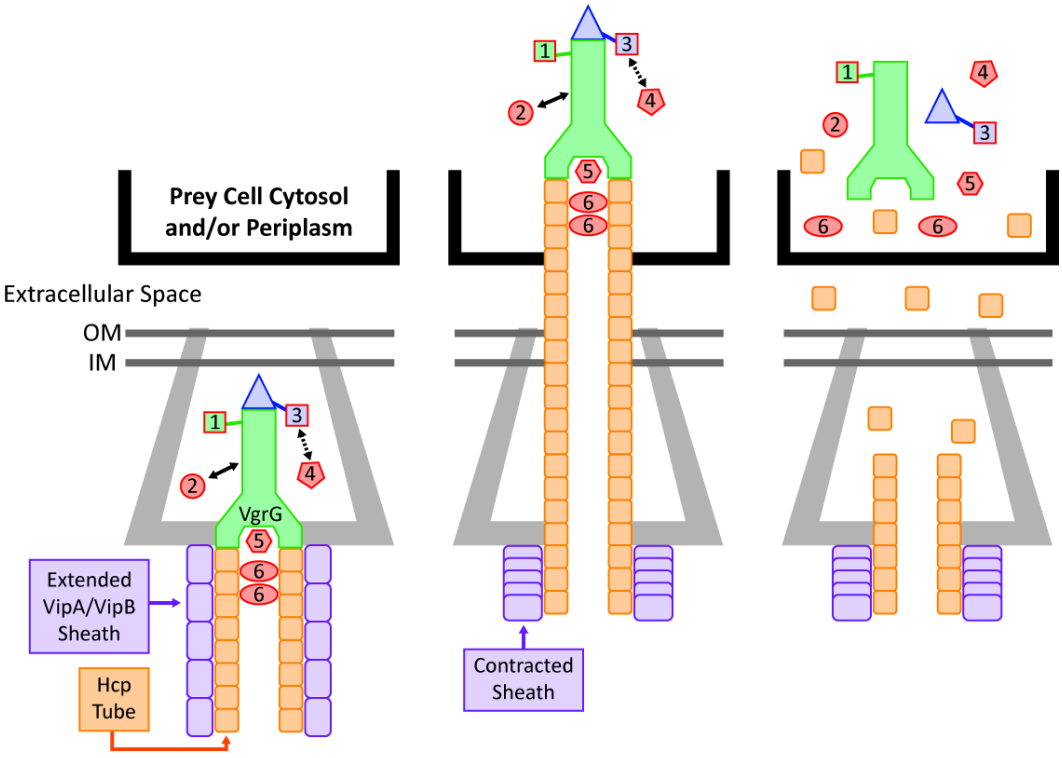

Figure 1.5 Modified MERV model for effector loading and delivery. T6SS effectors are loaded onto the VgrG spike complex or within the distal end of the Hcp tube (left panel). Sheath contraction leads to the simultaneous delivery of the VgrG spike and all associated effectors (middle panel), abrogating the need for the Hcp tube to be stably maintained (right panel). Prototypical examples of effector classes 1-3 have been characterized: *V. cholerae* VgrG-1 and VgrG-3 (Class 1), *V. cholerae* TseL (Class 2), *D. dadantii* RhsA (Class 3). Effector classes 4-6 represent hypothetical mechanisms that are likely to exist. Class 4 effectors associate with PAAR protein extensions such as transthyretin-like domains (Shneider et al., 2013) or Rhs-repeat domains (Koskiniemi et al., 2013). Class 5 effectors bind to the inside of the cup-shaped opening in the gp27-like domain of VgrG. Class 6 effectors bind to the lumenal side of the Hcp tube; although it has not yet been experimentally confirmed, it is likely that *P. aeruginosa* effector Tse2 falls into this category.

identified S-type pyocin nuclease VgrG in *Salmonella* (Blondel et al., 2009) and VgrG-lipase in *Burkholderia* (Pukatzki et al., 2009). These domain extensions can be further modified through interaction with additional effector proteins (Figure 1.5). For example, in *V. cholerae*, T6SS effector TseL (Type six effector Lipase) interacts with VgrG-3 and requires it for its secretion (Dong et al., 2013). The modular nature of these C-terminal extension domains and interacting proteins suggests that VgrG may be employed as a delivery vehicle for translocation of other heterologous functional domains. Indeed, in *V. cholerae* a b-lactamase domain replacing the actin-crosslinking domain of VgrG-1 can be delivered into host cells by the T6SS (Ma et al., 2009a).

In both *V. cholerae* (Pukatzki et al., 2007) and *P. aeruginosa* (Hachani et al., 2011), there is evidence that VgrG forms a trimeric complex with other non-identical VgrG proteins (Hachani et al., 2011). Indeed, both hetero- and homo-trimeric VgrG complexes can be observed in *P. aeruginosa* (Hachani et al., 2011), while in *V. cholerae*, T6SS activity requires that at least two distinct VgrG proteins be present for T6SS activity to occur. *V. cholerae* VgrG-2 is required along with at least one of VgrG-1 and VgrG-3 (Zheng et al., 2011), suggesting that formation of hetero-trimeric complexes of VgrG-2 and VgrG-1 or VgrG-2 and VgrG-3 is required. Differences in spike complex assembly in different organisms may reflect differences in how the complex integrates itself within the T6SS apparatus along with other associated effector proteins. Indeed, in *V. cholerae* deletion of VgrG-3 along with secreted effector VasX abolishes T6SS activity including Hcp secretion (Dong et al., 2013), suggesting that the associations with VgrG complexes may play a direct role in T6SS assembly. These effector-VgrG interactions may partially explain why some organisms only have a single copy of VgrG (*Rhizobium leguminosarum*), while others have 3 (*V. cholerae*), 10 (*P. aeruginosa*), or even 32 (*Sorangium*

cellulosum) distinct VgrG genes, as incorporation and delivery of different effectors may require a specifically adapted VgrG protein. Collectively, these observations suggest that heterotrimeric VgrG complexes have, in theory, the ability to deliver more than one effector domain in the context of a single spike trimer.

The first cytotoxic non-VgrG effectors were identified by Mougous and colleagues (Hood et al., 2010) and included enzymes that attacked glycan and peptide bonds in bacterial peptidoglycan (Russell et al., 2011). Collectively, VgrG and non-VgrG T6SS effectors exhibit a diverse range of functions targeting both eukaryotic hosts and bacterial competitors. Known effector activities include actin modification (Pukatzki et al., 2007; Suarez et al., 2010), muramidases and peptidases that attack the bacterial cell wall (Chou et al., 2012; Dong et al., 2013; English et al., 2012; Hood et al., 2010; Russell et al., 2011; Russell et al., 2012; Whitney et al., 2013), nucleases (Koskiniemi et al., 2013), lipases (Dong et al., 2013; Russell et al., 2013), and proteins facilitating eukaryotic membrane fusion (French et al., 2011). In order to prevent self or sister cell intoxication, T6SS$^+$ organisms also encode immunity proteins to neutralize their cognate antibacterial effectors (Brooks et al., 2013; Dong et al., 2013; English et al., 2012; Hood et al., 2010).

Effectors have been identified using mass spectrometry-based approaches in a number of bacteria, including *P. aeruginosa* (Hood et al., 2010), *Serratia marcescens* (Fritsch et al., 2013), and *V. cholerae* (Miyata et al., 2011). Interestingly, *P. aeruginosa* mutants lacking all three effectors identified in this manner (Hood et al., 2010) are still able to kill *V. cholerae* and *E. coli* (Basler et al., 2013; Ho et al., 2013). Although cell envelope puncturing can lead to cell death as in the case of R-type pyocins (Michel-Briand and Baysse, 2002), Gram-negative bacteria have been reported to survive multiple cell envelope puncturing events where an open channel is not

maintained (Suo et al., 2009), suggesting that Tse-independent killing may still involve other effectors that have escaped detection by the previously employed proteomic approaches due to either low expression levels or their intrinsic properties. Tn-seq (transposon mutagenesis coupled with massively parallel sequencing) has recently been employed as an alternative to proteomics to detect three pairs of effectors and their cognate immunity proteins in *V. cholerae* (Dong et al., 2013). This method takes advantage of the incidental sister cell-sister cell T6SS attacks, as cells carrying transposon disruptions of effector immunity genes drop out of mixed populations of $T6SS^+$ but not $T6SS^-$ cells in a manner detectable by deep sequencing.

Bioinformatic analyses using the physical properties (i.e., molecular weight, isoelectric point and operon structure) of known *P. aeruginosa* effectors have predicted a large group of potential T6SS effectors (Russell et al., 2012). However, these analyses did not identify all of the effectors in *V. cholerae* and *S. marcescens*, indicating again the diversity of T6SS effectors. Notably, T6SS effector genes are often found immediately downstream of orphan *hcp-vgrG* gene pairs not encoded within the main T6SS gene clusters in several organisms, including *V. cholerae* (Dong et al., 2013; Miyata et al., 2011; Zheng et al., 2011), *Dickeya dadantii* (Koskiniemi et al., 2013) and *Proteus mirabilis* (Alteri et al., 2013; Wenren et al., 2013). By extension, genes downstream of these *hcp-vgrG* gene pairs may encode T6SS effectors in other organisms as well. Indeed, many of these downstream genes belong to a diverse family of lipase effectors (Russell et al., 2013).

Recently, another gene product frequently found adjacent to T6SS genes has been implicated as both a structural component of the T6SS organelle and as a secreted substrate. Specifically, PAAR (Proline Alanine-Alanine-aRginine)-motif-containing proteins have been identified as metal-binding, cone shaped proteins that effectively sharpen the b-helical tip of the

VgrG trimer (Shneider et al., 2013) (Figure 1.5). Like VgrG, PAAR proteins can also have additional extension domains with various predicted effector activities suggesting that the hundreds of PAAR proteins identifiable in genome databases may be T6SS effectors as well (Shneider et al., 2013). Because the interaction between PAAR proteins and the C-terminal end of the VgrG trimer is driven by hydrogen bonding between the backbones of the respective proteins, it has been proposed that various PAAR proteins might be able to bind to any given VgrG trimer (Shneider et al., 2013). Indeed, an effector nuclease RhsA delivered to target cells by the T6SS *D. dadantii* (Koskiniemi et al., 2013) has been identified to be a PAAR protein (Shneider et al., 2013). This nuclease effector requires either of two VgrG genes to be delivered to sensitive target cells (Koskiniemi et al., 2013), suggesting that this PAAR protein is capable of recognizing distinct VgrG trimers. Furthermore, as with Hcp and VgrG, there are frequently multiple genes encoding PAAR proteins in bacterial species that encode T6SS (Shneider et al., 2013), suggesting that like VgrG effectors, genes encoding PAAR effector proteins have been subject to extensive horizontal transmission among organisms.

The T6SS is also capable of translocating proteins lacking identifiable signals for VgrG association such as PAAR motifs. Although it has been suggested that the Hcp tube may function as a passive conduit through which these effectors might be translocated (Mougous et al., 2006; Silverman et al., 2012), the opening in the Hcp tube is only 40Å wide (Mougous et al., 2006) and is too small for all but the smallest effectors to pass through in a folded state (Benz et al., 2012). Early on, the triple AAA+ ATPase ClpV was suggested to power unfolded proteins down an intercellular Hcp tube (Mougous et al., 2006; Silverman et al., 2012), however, such a mechanism would require stable assembly of unsheathed extracellular Hcp tubes, which has never been observed. Recent elegant biochemical and electron-microscopy evidence (Silverman

et al., 2013) suggests that some effectors can bind to residues displayed on the inside of Hcp1 hexamers. Given that this interaction stabilizes some effectors such as Tse2, Hcp has been designated to have chaperone function (Silverman et al., 2013). Additionally, alteration of residues on the lumenal side of the Hcp tube prevents secretion of Tse2 and Tse3 and reduces secretion of Tse1. Given that Tse3 (44.4 kDa) is too large to fit into the Hcp tube in a folded conformation, Silverman et al. (2013) suggested that Tse3 may be interacting with lumenal Hcp residues while in an unfolded state. These Hcp-effector interactions are not without precedent as early biochemical analysis of the T6SS in *E. tarda* showed that secreted T6SS substrate EvpP also interacted with Hcp (Zheng and Leung, 2007). Thus, Hcp "effector chaperone" activity may be the first step in a process that recruits effectors into fully assembled Hcp tubes. These observations suggest that some effectors may be loaded into the Hcp tube during assembly of the T6SS structure and may be injected into target cells along with the tube. The effectors that reside in the Hcp tube in an unfolded conformation may also act analogously to phage tail "tape measure" proteins (Rodriguez-Rubio et al., 2012) and thus control the length of the extended T6SS tail/tube complex.

Another group of potential T6SS effectors whose members are also too large to reside within the Hcp tube in a folded confirmation include members of the extended Rhs-repeat-containing protein family (Koskiniemi et al., 2013). Recently, structural analysis has determined that the Rhs-repeat domain of one bacterial toxin forms a shell-like structure that completely encloses and protects the toxin's folded enzymatically active effector domain (Busby et al., 2013). Given that many PAAR proteins display Rhs-repeat domains as well as putative effector domains (Shneider et al., 2013), it seems likely that these caged effector molecules are completely folded structures that decorate the VgrG tip. Together these data suggest a refinement

of a model termed the Multiple Effector Translocation VgrG (MERV) model (Shneider et al., 2013). According to this model (Figure 1.5**)**, effectors can be secreted and delivered to target cells by the T6SS organelle using as many as five functionally distinct mechanisms. In accordance with this model, we propose that effectors can be delivered to target cells as a complex of cargo proteins that decorate the VgrG/PAAR spike or reside within the proximal part of the Hcp tube lumen (Figure 1.5). A key aspect of this model is that the entire cytotoxic load can be delivered in a single T6SS firing event, thereby abrogating the need for a stable intercellular channel and prolonged cell-cell association. Rather than providing more time for additional effectors to be transferred through a tube, longer cell-cell associations allow for repeated T6SS firing events to hit a given prey cell. It is also worth noting that certain large toxins also utilize a strategy that involves delivery of multiple effector domains in a presumably a single membrane translocation event (Satchell, 2011).

Regulation of T6SS expression and assembly

Because the assembly, contraction, disassembly and re-assembly cycle of the T6SS organelle is likely to be energetically costly to the bacterial cell, it is not surprising that both expression and assembly of this organelle is tightly regulated. In most cases, bacteria have some sort of transcriptional control over T6SS tied to quorum sensing (Kitaoka et al., 2011; Salomon et al., 2013; Zheng et al., 2010), biofilm formation (Aubert et al., 2008; Moscoso et al., 2011), iron-depletion (Brunet et al., 2011; Chakraborty et al., 2011), thermoregulation (Pieper et al., 2009; Salomon et al., 2013), salinity (Salomon et al., 2013) or other stress responses (Brooks et al., 2013; Gueguen et al., 2013)**.** In *V. cholerae*, the major T6SS cluster encodes an essential regulator of T6SS, VasH, which acts as a σ^{54} (RpoN) activator. Indeed, both RpoN and VasH are

required for T6SS function (Pukatzki et al., 2006; Zheng et al., 2011), but interestingly RpoN and VasH only control the transcription of the two *hcp* operons but not the major cluster (Dong and Mekalanos, 2012). It is worth noting that VasH and RpoN were originally reported to directly bind to the main T6SS gene cluster in addition to the *hcp2* promoter (Bernard et al., 2011). However, the authors of this study reached this conclusion using in vitro gel-shift assays and heterologous expression of transcriptional reporter fusions in *E. coli* rather than assaying these regulators under native conditions. That RpoN and VasH only control the *hcp* operons and not the main cluster suggests a two-tiered regulatory cascade. Environmental signals first need to trigger the transcription of the major cluster so that *vasH* is expressed, which subsequently activates the transcription of the *hcp* operons by RpoN. Because the *hcp* operons carry many of the secreted T6SS components, namely Hcp, VgrG and their downstream effector proteins, while the main cluster contains mostly structural components, this two-tiered regulation may be important for maintaining different levels of expression for components that can be internally recycled versus those that are secreted and thus consumed by the functioning system. Despite this tight control, transcriptional regulation still has its limitations. Given the number of independent components of the T6SS apparatus and the multiplicity of subunits required, transcriptional regulation does not allow for rapid response to new stimuli. Furthermore, because of cellular geometry, T6SS firing events are inherently inefficient at hitting target cells. Even assuming perfectly cylindrical geometry and tight spatial packing of adjacent cells, a T6SS$^+$ attacker would require on average six randomly positioned T6SS firing events in order to actually hit a given neighboring cell (Figure 1.4C). The consequence is that cells are forced into one of two states, a docile one with an inactive or ineffective T6SS or an aggressive one with an excessively active T6SS that indiscriminately attacks all neighbors.

P. aeruginosa addresses both T6SS efficiency and target selection through a post-translational regulatory system. The T6SS in *P. aeruginosa* requires the phosphorylation of Fha by threonine kinase PpkA (Mougous et al., 2007) (Figure 1.3B, C). PpkA activity requires outer membrane lipoprotein TagQ (Type six secretion-associated gene Q) and outer membrane-associated protein TagR (Silverman et al., 2011). TagR was originally identified as a protein bioinformatically predicted to interact with the periplasmic domain of PpkA (Hsu et al., 2009), while TagQ was shown to be required for proper localization of TagR (Casabona et al., 2012). Two additional proteins, TagS and TagT, comprise a membrane-bound complex related to bacterial ABC transporters and are both required for full activation of PpkA (Casabona et al., 2012). Deactivation of the T6SS is achieved through dephosphorylation of Fha by protein phosphatase PppA (Mougous et al., 2007). Deletion mutants of PppA exhibit elevated levels of T6SS activity when measured by either the Hcp secretion level (Mougous et al., 2007) or by ClpV dynamics (Basler et al., 2013).

It was initially hypothesized that surface growth triggered this post-translational regulation of the T6SS (Silverman et al., 2011), however time-lapse visualization of T6SS dynamics through fluorescence microscopy has revealed *P. aeruginosa* to have a more fascinating regulatory system (Basler and Mekalanos, 2012). When grown on a solid surface, a *P. aeruginosa* cell that spontaneously fires its T6SS apparatus will frequently strike a neighboring sister cell. This attacked sister cell then builds its own T6SS organelle and fires a retaliatory T6SS counterattack. The initial attackers then sense this T6SS counterattack and retaliate in turn. Because *P. aeruginosa* encodes immunity proteins to its own T6SS effectors, none of these T6SS attacks between sister cells are lethal, allowing for this reciprocal interaction to be stably maintained for several minutes. This phenomenon has been named ‘T6SS dueling’

(Basler and Mekalanos, 2012). Further genetic analysis of this dueling activity confirmed the involvement of the threonine phosphorylation pathway (Basler et al., 2013). As expected, mutations in PpkA, TagQ, or TagR caused complete loss of all T6SS activation. However, deletion of TagT maintained basal levels of T6SS activity but completely suppressed dueling activity. In contrast, although a PppA deletion mutant exhibited high levels of T6SS activity in virtually all cells, almost none of this activity was associated with T6SS dueling, suggesting that dephosphorylation of Fha is required to reposition the T6SS apparatus in response to newly sensed attacks. Because dueling activity can only occur if neighboring cells remain adjacent to each other, it is not surprising that this phenomenon is manifest only on solid surfaces and not in liquid culture. As such, it is highly likely that the observed correlation between surface growth and increased PpkA activity (Casabona et al., 2012) is due to accumulation of dueling sister cells within a given surface-growing population.

Although sister cell dueling might play some role in cell signaling involving non-T6SS targets of PpkA regulation (Goldova et al., 2011), responding to sister cell attacks is probably not the intended use of the T6SS response pathway. Indeed, *P. aeruginosa* T6SS is capable of responding to T6SS attack from heterologous organisms lacking cognate immunity proteins to *P. aeruginosa* T6SS effectors. When grown in competition with *P. aeruginosa*, T6SS$^+$ *V. cholerae* and *A. baylyi* but not T6SS$^-$ mutants of these organisms were both killed in a TagT-dependent manner (Basler et al., 2013). A similar differentiation between T6SS$^+$ and T6SS$^-$ *Burkholderia thailandensis* has been reported, although this observation was attributed by the authors to different degrees of susceptibility to *P. aeruginosa* T6SS (Leroux et al., 2012). Perhaps the most critical aspect of this T6SS response mechanism is its ability to precisely aim the retaliatory T6SS response directly at the source of the initial attack. When mixtures of both

T6SS$^+$ and T6SS$^-$ *V. cholerae* were mixed with *P. aeruginosa*, only the T6SS$^+$ *V. cholerae* cells were killed, while the T6SS$^-$ cells were largely untouched (Basler et al., 2013). The lack of collateral damage associated with activation of *P. aeruginosa* T6SS is perhaps indicative of the prevalence of *P. aeruginosa* in multispecies communities (Ha et al., 2012; Tashiro et al., 2013), where it might stand to gain from coexistence with non-hostile cohabitants.

An interesting and still unanswered question that arises from these results is how *P. aeruginosa* is able to avoid being killed by the T6SS effectors of these heterologous species. The "T6SS effector armor" might be attributable to its notorious outer-membrane impermeability (Nikaido, 1994), but it is hard to imagine how any membrane structure could repel T6SS attacks. Perhaps modifications of peptidoglycan structure or robust repair mechanisms underlie this observed resistance. Thus, immunity to heterologous effectors coupled with T6SS counterattacks may be fueling an arms race in antagonistic bacterial cell-cell interactions.

Based on bioinformatic analysis of the genes needed for dueling, this post-translation T6SS regulation is likely limited to a subset of Fha-containing T6SSs (Figure 1.3A). Specifically, this phenomenon may be restricted to *Pseudomonas* species, as this genus is the only one so far identified to contain all of the requisite regulatory components. Indeed, other organisms such as *S. marcescens* that still require phosphorylation of Fha by PpkA for T6SS activation but lack the TagQRST system do not require cell-cell contact to fully activate their T6SS (Fritsch et al., 2013). This observation suggests that the rapid response associated with post-translational control is not necessarily limited to responding to attacking bacterial neighbors as has been observed in *P. aeruginosa*. Rather, T6SS in each of these bacterial species might be adapted to specifically respond to the threats each species is likely to encounter in nature.

Recently, the T6SS of *E. coli* EAEC strain 17-2 has been observed to exhibit what

appeared to be T6SS dueling behavior (Brunet et al., 2013). However, given that none of the TagQRST system genes required for T6SS dueling in *P. aerugionsa* are found in sequenced *E. coli* strains (Figure 1.3A), it is unlikely that these bacteria are exhibiting the same process observed in *P. aeruginosa*. Indeed, the dueling cells presented in this study do not appear to exhibit the precise geometric orientation observed in *P. aeruginosa* (Basler et al., 2013; Basler and Mekalanos, 2012) and thus may be more a consequence of T6SS organelles coincidentally being aimed at each other in adjacent cells. Another important clarification between the putative dueling observed in the studies by Brunet et al. (2013) described above and the dueling exhibited by *P. aeruginosa* is that since there is little to no collateral damage from these retaliatory T6SS attacks, T6SS activity does not tend to spread through a population of *P. aeruginosa* cells (Basler et al., 2013; Basler and Mekalanos, 2012). The T6SS activity observed in EAEC was reported to propagate within a population of growing cells (Brunet et al., 2013), suggesting that this organism may be responding to other signals associated with growth on a solid surface as a community (e.g., quorum sensing) or some diffusible signal released by cells undergoing T6SS attack. These observations stand as a testament to both the diversity and specialization of T6SS regulation in diverse bacterial species.

Although a precise definition of the signal recognized by *P. aeruginosa* that triggers T6SS assembly remains elusive, we now have some significant new clues. Recently, it was discovered that broad host range conjugation systems can also induce a *P. aeruginosa* T6SS in the form of a "donor-directed counterattack" (Ho et al., 2013). In this report, T4SS associated with the plasmid RP4 was found to render *E. coli* 30-times more sensitive to killing by the *P. aeruginosa* T6SS. Because this RP4-dependent, T6SS-dependent killing involved precise target selection and required both TagT and PppA, the authors concluded that RP4 was

triggering aimed assembly of the *P. aeruginosa* T6SS organelle in a manner perfectly analogous to the T6SS dueling response. Extensive genetic analysis of the RP4 conjugation system revealed that DNA transfer was not required for this response, but genes involved in sex pilus and mating pair formation were (Ho et al., 2013). Furthermore, the antibiotic polymyxin B, a cationic cyclic peptide that binds the outer membrane component lipid A to cause disruption of membrane integrity, also induced rapid TagT-dependent assembly and firing of the *P. aeruginosa* T6SS (Ho et al., 2013). Altogether, these observations suggested that the signal for T6SS assembly is a highly localized, physical or chemical signal associated with membrane perturbation. As such, the T6SS represents a generalized bacterial defense mechanism against foreign attack and acquisition of potentially infectious DNA elements. It remains unclear whether other membrane-penetrating processes such as phage infection, eukaryotic defensin or perforin might also induce similar T6SS counterattacks or if these hypothetical T6SS counterattacks can be used by bacteria to defend against phage or eukaryotic host cell responses.

As noted earlier, T6SS can also deliver effectors that are toxic to eukaryotic cells and indeed, evidence suggest that genes encoding this organelle are induced during infection and have been shown to induce host damage in experimental animals (Kapitein and Mogk, 2013; Ma and Mekalanos, 2010; Mandlik et al., 2011; Miyata et al., 2013; Zheng et al., 2010). The antibacterial activity associated with T6SS may also enhance colonization of the host by targeting heterologous or homologous bacterial cells. Recent evidence for the latter has been obtained in *V. cholerae* where a mutant defective in *tsiV3*, the cognate immunity protein to the bactericidal effector VgrG-3 (Dong et al., 2013), exhibited a defect in intestinal colonization (Yang et al., 2013). This in vivo colonization defect of the *tsiV3* mutant depended on its co-colonization with $T6SS^{+}$ strains carrying an intact VgrG3 gene. These data suggest that

V. cholerae T6SS is functional during infection and that antagonistic sister cell-sister cell interactions occur during the infection process. Such a result predicts that heterologous species may also be subject to T6SS-dependent attacks and that these anti-microbiota interactions might thereby influence the virulence and in vivo fitness of T6SS$^+$ species.

In summary, rapid progress has been made toward understanding the scope of biological activities associated with the bacterial T6SS, but many questions remain unanswered (**Box 1**). Besides acting in many species as virulence factors, T6SS is likely to be important for the ecological fitness of bacteria that live in consortia such as mixed biofilms (Miyata et al., 2013). Bacterial species that activate T6SS organelles and fire them in an unregulated manner (e.g., *Vibrio* and *Acinetobacter* species) are likely using them to kill all susceptible neighbors indiscriminately and thus may attack preformed biofilms efficiently. *P. aeruginosa* may have adapted to establishing beneficial complex biofilm communities (Kolenbrander et al., 2010; Peters et al., 2012), and therefore as a species *P. aeruginosa* would cooperate with other organisms so long as they do not pose a threat. On the other hand, if microbial neighbors threaten *P. aeruginosa* with either T6SS attack or with T4SS-mediated transfer of infectious conjugative elements, *P. aeruginosa* will use its T6SS as a primitive "innate immune system" (Ho et al., 2013) to neutralize these challenges. Understanding whether any of these ecological phenomenon lead to significant changes in the fitness of pathogens in vivo remains a priority for this rapidly moving field.

Chapter 2. Genetic analysis of anti-amoebae and anti-bacterial activities of the type VI secretion system in *Vibrio cholerae*

A type VI secretion system (T6SS) was recently shown to be required for full virulence of *Vibrio cholerae* O37 serogroup strain V52. Here, we systematically mutagenized each gene in the T6SS locus and characterized their functions based on expression and secretion of the hemolysin co-regulated protein (Hcp), virulence towards amoebae of *Dictyostelium discoideum*, and killing of *Escherichia coli* bacterial cells. We grouped the 17 proteins characterized of the T6SS locus into four categories: twelve (VipA, VipB, VCA0109–VCA0115, ClpV, VCA0119, and VasK) are essential for Hcp secretion and bacterial virulence and likely function as structural components of the apparatus; two (VasH and VCA0122) are regulators required for T6SS gene expression and virulence; another two, VCA0121 and valine-glycine repeat protein G 3 (VgrG-3), are not essential for Hcp expression, secretion or bacterial virulence, and their functions are unknown; the last group is represented by VCA0118, which is not required for Hcp expression or secretion but still plays a role in both amoebae and bacterial killing and may be an effector protein. We also showed that the *clpV* gene product is required for *Dictyostelium* virulence but is less important for killing *E. coli*. Additionally, one *vgrG* gene (*vgrG-2*) outside of the T6SS gene cluster was required for bacterial killing, while another (*vgrG-1*) was not. However, a bacterial killing defect was observed when *vgrG-1* and *vgrG-3* were both deleted. Several genes encoded in the same putative operon as *vgrG-1* and *vgrG-2* also contribute to virulence toward *Dictyostelium* but have a smaller effect on bacterial killing. Our results provide new insights into the functional requirements of *V. cholerae*'s T6SS in the context of secretion as well as killing of bacterial and eukaryotic phagocytic cells.

Foreword

A modified version of this chapter was published in *PLoS One* on September 13, 2011. The published version can be found on the web at the following URL:

http://dx.doi.org/10.1371/journal.pone.0023876

The full citation for this article is:

> Zheng, J., Ho, B., and Mekalanos, J.J. (2011). Genetic analysis of anti-amoebae and anti-bacterial activities of the type VI secretion system in Vibrio cholerae. PLoS One *6*, e23876.

This work was a collaborative effort between Dr. Jun Zheng and myself. We split the efforts of making the T6SS gene deletions. While he characterized their T6SS activity through Hcp secretion in and virulence toward *Dictostelium* amoebae (Figure 2.1 and 2.4), I focused on characterizing their antibacterial activity (Figure 2.5). Dr. Zheng also performed experiments characterizing VCA0122 (Figure 2.2) and VCA0118 (Figure 2.3) as well as experiments addressing the role of the Type II secretion system (Figure 2.6), while I performed the bioinformatic analysis of potential effector proteins (Tables 2.1-2.3). I would like to thank Dr. Zheng for writing the initial draft of this chapter and Professor Mekalanos for considerable help in the editing and revision process. Because this work presented in this chapter was published in 2011 and the blistering pace at which the field has advanced, some statements regarding the "current" knowledge of the field are no longer accurate. Furthermore, our understanding of the mechanism by which the T6SS is able to kill bacteria is now significantly better developed. I have elected to retain original the language used so that the reader can gain some insight into what was known at the time the work was completed and direct the reader to Chapter 1 of this dissertation for a comprehensive overview of our understanding of the T6SS.

I would also like to thank Dr. Dominique Schneider from Université Joseph FOURIER for providing the plasmid pDS132. This work was supported by grant AI-018045 to John J.

Mekalanos from the National Institute of Allergy and Infectious Diseases.

Introduction

Pathogenicity of bacteria is often critically dependent on secretion systems to export toxic molecules into the environment or translocate effectors into the host cells. These secreted or injected molecules result in interference with or stimulation of host cellular processes. At least six different secretion systems (type I through type VI) have been found in Gram-negative bacterial pathogens of animals and plants (Cascales, 2008; Economou et al., 2006; Filloux et al., 2008). These secretion systems are distinguished in part by the conserved structural components that define them but also by the characteristics of their substrates and the subcellular paths that their substrates take during the export process. Among these secretion systems, the type VI secretion system (T6SS) has recently emerged as an exciting new topic for experimental exploration (Mougous et al., 2006; Pukatzki et al., 2006).

T6SSs have been described in many bacterial pathogens and have been implicated in a variety of functions ranging from inter-bacterial relationships and biofilm formation, to cytotoxicity and survival in phagocytic cells (Cascales, 2008; Hood et al., 2010; MacIntyre et al., 2010; Pukatzki et al., 2009; Schwarz et al., 2010b). T6SS gene cluster can be found in approximately 25% of all sequenced Proteobacteria and is a virulence factor in many bacteria including *Vibrio cholerae* (Pukatzki et al., 2006), *Edwardsiella tarda* (Zheng and Leung, 2007), *Pseudomonas aeruginosa* (Mougous et al., 2006), and *Burkholderia* species (Aubert et al., 2008; Schell et al., 2007). T6SS gene clusters contain from 15 to more than 20 genes and secrete substrates lacking N-terminal hydrophobic signal sequences (Bingle et al., 2008). Functional assays and protein localization studies suggested that the proteins encoded by T6SS gene clusters are assembled into a multi-component apparatus (Aschtgen et al., 2008; Aschtgen et al., 2010a; Mougous et al., 2007; Zheng and Leung, 2007). Bioinformatic analysis has identified a core of

13 genes that may constitute the minimal number needed to produce a functional apparatus (Boyer et al., 2009). T6SS core components include DotU and IcmF orthologs believed to stabilize the multi-protein complex in the membrane (Ma et al., 2009b; Zheng and Leung, 2007), and an AAA+ family ATPase called ClpV (Bonemann et al., 2009; Mougous et al., 2006). ClpV associates with several other conserved T6SS proteins, and its ATPase activity has been reported to be essential for T6SS function (Cascales, 2008). In most T6SSs, hemolysin co-regulated protein (Hcp) and valine-glycine repeat protein G (VgrG) are exported by T6SS. They are proposed to be the extracellular components of T6SS apparatus, and their secretion is codependent (Hood et al., 2010; Leiman et al., 2009; Pell et al., 2009; Pukatzki et al., 2007; Zheng and Leung, 2007). Multiple distinct T6SS gene clusters have been identified in various bacteria (Mougous et al., 2006; Mougous et al., 2007; Pukatzki et al., 2006; Zheng and Leung, 2007). In *E. tarda*, a systematic mutation of one T6SS cluster has been performed and three categories of proteins have been identified, including 12 genes required for the Hcp secretion (Zheng and Leung, 2007).

V. cholerae is a Gram-negative bacterium that causes a severe, life-threatening diarrheal disease, cholera. Disease occurs when contaminated food or water is ingested, resulting in a voluminous secretory diarrhea that can lead to dehydration and death if untreated (Faruque et al., 1998). Orally ingested bacteria colonize the intestinal epithelium through expression of toxin co-regulated pili (TCP), which in turn is coordinately regulated with cholera toxin (CT), the enterotoxin responsible for the bulk of the secretory diarrhea observed during disease progression (Matson et al., 2007). Besides these classic virulence factors, T6SS was recently implicated as a virulence determinant of *V. cholerae* using *Dictyostelium discoideum*, mouse and rabbit as model systems (Ma and Mekalanos, 2010; Pukatzki et al., 2006; Zheng et al., 2010). In

V. cholerae O37 serogroup strain V52, T6SS is required for full virulence towards *Dictyostelium* amoebae and J774 macrophages (Pukatzki et al., 2006) and for inflammatory diarrhea in infant mice (Ma and Mekalanos, 2010). In the seventh pandemic O1 El Tor strain C6706, T6SS contributes to fecal diarrhea and intestinal inflammation in infant rabbits (Zheng et al., 2010). In addition, the T6SS in *V. cholerae* displays antimicrobial properties and can cause up to a 100,000-fold reduction in Escherichia coli K12 survival when they co-cultivated with *V. cholerae* strain V52 on solid agar media (MacIntyre et al., 2010).

The T6SS in *V. cholerae* is responsible for the secretion of Hcp as well as three VgrG proteins (VgrG-1 to -3) (Pukatzki et al., 2006). VgrG-1, which functions as both a T6SS structural element and an effector protein (Pukatzki et al., 2007), contains a C-terminal domain with strong homology to the actin cross-linking domain (ACD) of *V. cholerae* RtxA or MARTX toxin (Sheahan et al., 2004). VgrG-1 causes actin cross-linking in host cells following its T6SS-dependent translocation during infection (Ma et al., 2009a; Ma and Mekalanos, 2010; Pukatzki et al., 2007). However, the ACD domain of VgrG-1 is not required for killing *E. coli* (MacIntyre et al., 2010). VgrG-1 is the only effector protein demonstrated to be translocated into eukaryotic host cells by a functional T6SS. However, recently several proteins have been identified as being likely translocated into bacterial target cells by the T6SS of *P. aeruginosa* (Hood et al., 2010).

Structural biology has revealed interesting evolutionary relationships between components of the T6SS apparatus and other dynamic structures that penetrate cell membranes (Leiman et al., 2009; Pukatzki et al., 2007). For example, the X-ray crystal structure of an *E. coli* VgrG-related protein predicts that VgrG proteins likely trimerize to form a complex that strongly resembles the bacteriophage T4 tail spike complex (Leiman et al., 2009; Pukatzki et al., 2007). The atomic structure of Hcp-related protein from *Pseudomonas aeruginosa* (Mougous et al.,

2006) revealed its ability to form tube-like structures in crystals that are similar to tubes formed by the N-terminal domain of trimeric VgrG proteins (Leiman et al., 2009; Pell et al., 2009). These data suggest that in the context of a T6SS appratus, Hcp may form a tube-like structure that interacts with VgrG trimers in a complex analogous to phage tail tubes and spikes (Leiman et al., 2009; Pell et al., 2009). Other T6SS proteins also have domains that are similar to phage tail base plate proteins (Leiman et al., 2009).

In the *V. cholerae* V52 T6SS locus, VipA, VipB, VasH, VasF, ClpV, VasK, and VgrG-3 have been characterized by genetic knockout (Bonemann et al., 2009; Pukatzki et al., 2006) and bioinformatic analysis (Shrivastava and Mande, 2008). VasH is a regulator and VipA, VipB, VasF, ClpV and VasK are T6SS structural components essential for Hcp secretion (Bonemann et al., 2009; Pukatzki et al., 2007; Pukatzki et al., 2006). VipA binds to VipB, and together they form tubules in *E. coli* (Bonemann et al., 2009) that Leiman *et al*. (2009) noted to have a striking resemblance to structures corresponding to the contracted tail sheath of bacteriophage T4. Thus, a phage sheath-like contraction mechanism might power the membrane penetration/secretion process of the VgrG-Hcp portion of the T6SS phage tail-like apparatus (Economou et al., 2006; Leiman et al., 2009). ClpV ATPase activity can remodel VipA/VipB tubules in vitro, and the ATPase activity of this protein has been reported to be a critical for substrate secretion in *P. aeruginosa* and *V. cholerae* (Bonemann et al., 2009; Mougous et al., 2006).

Here we report the genetic analysis of the T6SS locus of *V. cholerae* V52 in the context of its role in virulence against both *E. coli* and *Dictyostelium* amoebae. Our results show that deletion of 15 individual genes in T6SS locus result in loss of virulence towards amoebae. Twelve of these 15 individual genes are required for secretion of Hcp but not its expression. Another two, VCA0118 and VCA0122, encode a potential effector protein and a regulator,

respectively. In addition, we show that several genes in the putative operons encoding *vgrG-1* and *vgrG-2* are likely involved in type VI secretion and affect T6SS-dependent virulence toward amoebae. Deletion of any of the genes predicted to encode T6SS structural elements caused significant decreases in the ability of *V. cholerae* to kill *E. coli*. Additionally, the regulatory gene *vasH*, VCA0118 and VCA0020 also contribute to T6SS-dependent killing of bacterial cells.

Results

Systematic mutagenesis of genes in the T6SS locus. The T6SS locus in *V. cholerae* contains 18 open reading frames (Pukatzki et al., 2006). Additionally, VCA0118, VCA0121 and VCA0122 have been found to be restricted to a smaller group of $T6SS^+$ organisms and could have species-specific roles (Shrivastava and Mande, 2008). While some genetic analysis of VipA, VipB, VasF, VasH, ClpV, VasK and VgrG-3 has been performed previously (Bonemann et al., 2009; Pukatzki et al., 2007; Pukatzki et al., 2006), the function of other proteins encoded in this locus have not been explored in terms of their participation in both bacterial and eukaryotic T6SS-dependent killing. Thus, we began by systematically mutating all genes predicted to be in the T6SS locus of *V. cholerae* strain V52 (Figure 2.1A). We generated non-polar mutations by making in-frame deletions of each gene. Thirteen mutants were successfully constructed but we were unable to delete any portion of VCA0124 for unknown reasons. VCA0124 may be essential and could encode an immunity protein for a toxic effector as has been reported for the *P. aeruginosa* T6SS (Hood et al., 2010).

In order to determine the effects of these mutations on T6SS function, standard Hcp expression and secretion assays were performed utilizing western blot analysis and anti-Hcp antibody. Protein fractions were prepared from bacterial cell pellets and cell-free supernatants

from 16 T6SS mutants (Δ*vca0107 to* Δ*vca0122*). As shown in Figure 2.1B, Hcp was detected in the bacterial cell pellet of all the mutants except Δ*vasH*. In addition, Hcp expression was significantly decreased in Δ*vca0122* compared to the wild type and other T6SS mutants (excluding Δ*vasH*), suggesting that VCA0122 may either promote the expression of T6SS substrates as a regulator or their stabilization as a chaperone. Because Ponceau S staining of the western blot membranes showed a similar total protein level among the different mutants analyzed (data not shown), we conclude that the different levels of Hcp observed in the bacterial pellets was not due to sample loading variation during the analysis. Expression of Hcp in the cell

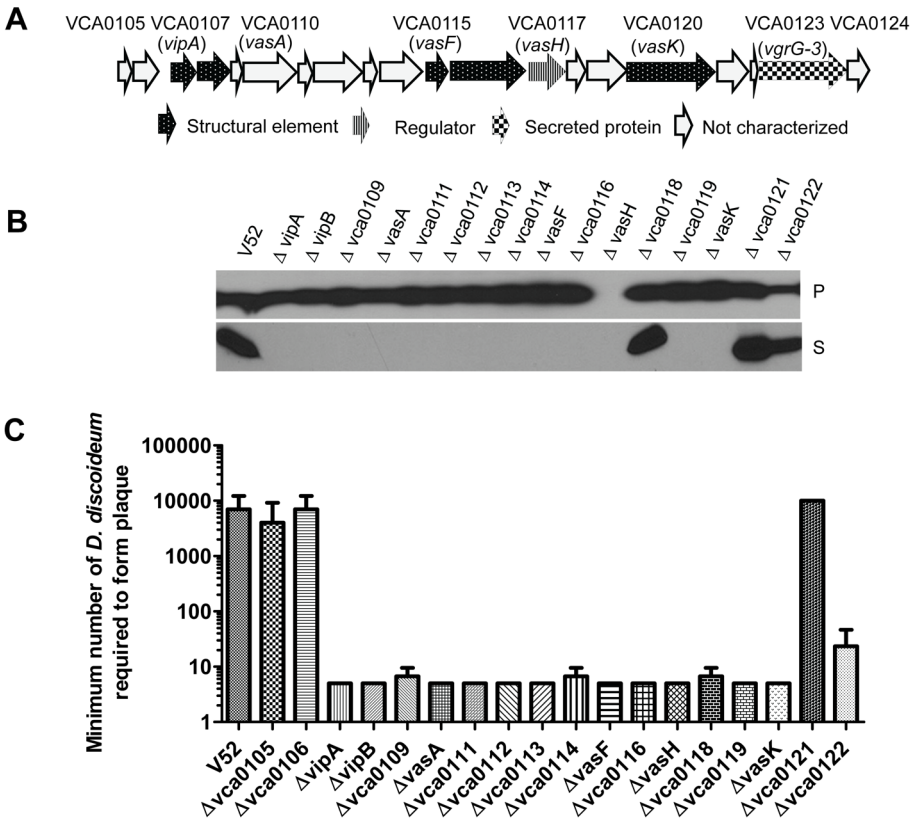

Figure 2.1 T6SS locus genes required for Hcp secretion and amoebae killing. (**A**) Schematic representation of the gene organisation in the *V. cholerae* T6SS locus. Genes that have been characterized are represented by arrows filled the indicated patterns and genes that have not been characterized were shown with empty arrows. (**B**) Hcp expression in bacterial pellet (P) and secretion in culture supernatant (S) in different T6SS deletion mutants were examined by western blot with anti-Hcp serum. (**C**) *D. discoideum* plaque formation assay for individual T6SS deletion mutants. The minimum number of *Dictyostelium* amoebae cells required for plaque formation on the lawns of *V. cholerae* wild-type or mutants was shown.

pellet did not predict whether Hcp would be secreted by a given mutant. Thus, we examined the presence of Hcp in the supernatant of mutants. As shown in Figure 2.1B, Hcp could not be detected in the supernatant of twelve mutants (VCA0107 through VCA0116, VCA0119, and VCA0120) even though deletion of these genes did not affect Hcp expression in the cell pellet. Additionally, the level of Hcp in the Δ*vca0122* mutant supernatant was significantly reduced when compared to the wild type (Figure 2.1B). VCA0118 and VCA0121 were not required for wild-type levels of Hcp secretion (Figure 2.1B).

To further characterize the effects of these non-polar single gene mutations on *V. cholerae* virulence, we examined plaque formation by *Dictyostelium* amoebae on bacterial lawns produced with different mutant strains. We plated wild-type V52 and different individual mutants on SM/5 agar plates. 5 µl of SorC buffer containing different numbers of amoebae was then deposited on each of these bacterial lawns. Plaque formation was examined after 3-5 days of incubation at 22 C, and the minimum number of *Dictyostelium* cells required for plaque formation was recorded. As shown in Figure 2.1C, 10,000 *Dictyostelium* amoebae were required to form plaque on wild-type V52 lawns. However, 5-10 amoebae cells were sufficient to do so on lawns of the 14 mutants carrying deletions in Δ*vca0107* through Δ*vca0120.* The minimum number of *Dictyostelium* cells required to form plaques on a Δ*vca0122* lawn was 10-50 amoebae cells, slightly higher than other mutants. In contrast, VCA0121 was not required for virulence in that it behaved identically to the wild type in these amoebae plaque formation assays. Virulence of the Δ*vca0121* mutant towards *Dictyostelium* is consistent with the observation that this mutant still secretes normal levels of Hcp (Figure 2.1B). Similarly, deletions of two genes (VCA0105 and VCA0106) encoded upstream of VCA0107 did not shown any significant *Dictyostelium*

killing defect (Figure 2.1A, C), suggesting that these genes are outside the boundary of the functional T6SS locus.

VCA0122 controls Hcp expression at the transcriptional level. VCA0122 is a gene found only in *Vibrio* species and encodes an 80 amino acid protein with no recognizable conserved domains. The Δ*vca0122* mutant expressed decreased levels of Hcp in the bacterial pellet as well as in its culture supernatant (Figure 2.1B). To determine whether VCA0122 is required for transcription of T6SS genes, we examined the expression of *hcp-2* in the Δ*vca0122* mutant. We constructed on low copy-number plasmid pTL61T a transcriptional fusion between the promoter region of *hcp-2* gene and a *lacZ* reporter gene. The resulting plasmid (pTL-*hcp*) was then transformed into wild-type V52 and Δ*vca0122* respectively and the β-galactosidase activities of these two strains were examined. As shown in Figure 2.2, strong β-galactosidase activity was detected in the bacterial lysate of V52 with pTL-*hcp*. In contrast, this activity was

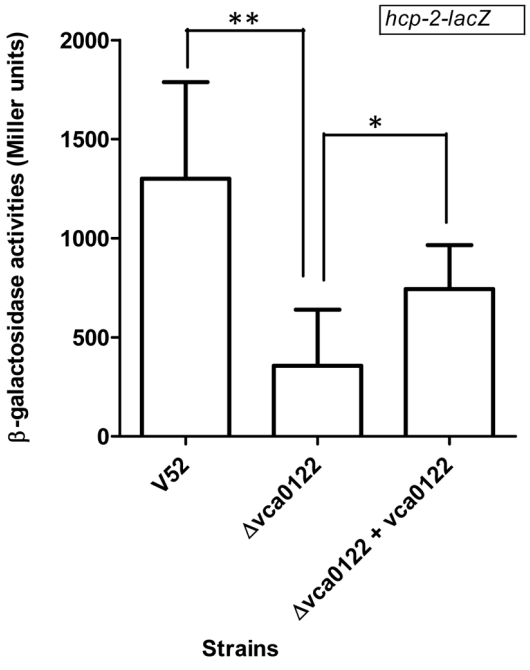

Figure 2.2 VCA0122 is a positive regulator of T6SS. The regulation of VCA0122 on T6SS substrate gene *hcp-2* was examined using *lacZ* reporter plasmid. Bacteria were cultured in LB broth. The values represent the mean ± SD. Data were analyzed with student's *t* test. Double asterisks (**) indicates $p<0.001$ and single asterisk (*) indicates $p<0.05$.

decreased by about 4-fold in the Δ*vca0122* mutant. The decrease in β-galactosidase activity was partially complemented by a copy of VCA0122 provided in trans (Figure 2.2). These results suggest that VCA0122 is a regulator controlling the expression of the *hcp-2* locus.

VCA0118 is not required for VgrG-1 secretion but enhances actin cross-linking activity in a macrophage cell line. VCA0118 encodes a 227 amino acid protein that contains a conserved uncharacterized domain, DUF3121. VCA0118 homologs can be found in various strains of *Vibrio* as well as many other bacterial species, including *E. coli*, *Aeromonas hydrophila*, and *Pseudomonas putida*. However, VCA0118 is absent from many other T6SS$^+$ organisms (Shrivastava and Mande, 2008), suggesting that it does not encode an essential structural component of the T6SS apparatus. The Δ*vca0118* mutant displayed a distinctly different phenotype than the other 15 deletion mutants in terms of its Hcp secretion profile and virulence towards *Dictyostelium* amoebae (Figure 2.1B, C). Deletion of VCA0118 had no significant effect on Hcp expression or its secretion into the supernatant in vitro (Figure 2.1B). However, Δ*vca0118* is avirulent toward *Dictyostelium* amoebae. As shown in Figure 2.3A, 10,000 amoebae cells are required to form plaques on wild-type V52 lawns, while only 5 amoebae are needed to form a plaque on Δ*vca0118* mutant lawns. This defect was partially recovered when VCA0118 was expressed in trans (data not shown).

We also examined whether VCA0118 was required for the secretion of VgrG-1, the only T6SS effector required for *Dictyostelium* and macrophage virulence so far reported for *V. cholerae* (Pukatzki et al., 2007). As shown in Figure 2.3B, Hcp and an epitope-tagged version of VgrG-1 (HA-VgrG-1) were expressed at similar levels in wild-type, Δ*vca0118* and Δ*vasK* V52. Deletion of *vasK* totally abolished Hcp and VgrG-1 secretion into culture supernatant. In contrast, deletion of *vca0118* did not affect secretion of VgrG-1 and Hcp, both of which were

detected in the culture supernatant at similar levels as wild-type V52. Previous reports showed that V52 uses T6SS to translocate VgrG-1 into macrophage J774 cells, where the ACD domain of VgrG-1 causes actin cross-linking (Ma et al., 2009a; Pukatzki et al., 2007). In these studies,

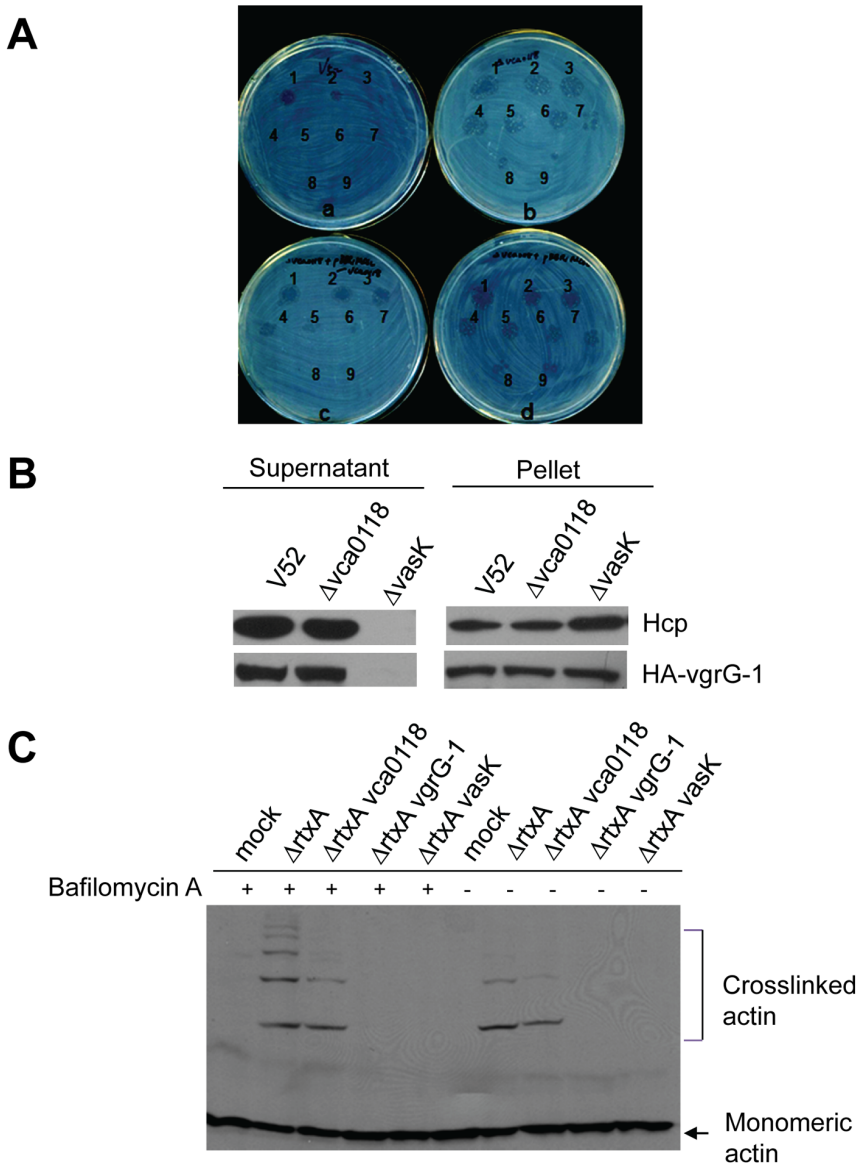

Figure 2.3 VCA0118 is a virulence factor. (**A**) *D. discoideum* plaque formation assay for Δ*vca0118* (plate b) and its complementation strain (plate c). The plaques formed by amoebae on the lawns of *V. cholerae* wild type (plate a) or wild type with empty plasmid (plate d) were also shown as controls. The number of *Dictyostelium* amoebae cells deposited on the plate was 1) 5×10^4; 2) 1×10^4; 3) 5×10^3; 4) 1×10^3; 5) 5×10^2; 6) 1×10^2; 7) 5×10^1; 8) 1×10^1; 9) 5×10^0, respectively. (**B**) Western blot showed that VCA0118 is not required for Hcp and VgrG-1 secretion. (**C**) Mutation of VCA0118 reduced but does not abolish actin cross-linking by VgrG-1 with or without bafilomycin A.

the addition of bafilomycin A, a specific inhibitor of vacuolar acidification, enhanced the VgrG-1-dependent actin cross-linking activity seen in target cells (Ma et al., 2009a). Because VCA0118 is required for virulence of *V. cholerae* towards *Dictyostelium* amoebae but is not essential for the secretion of Hcp or VgrG-1, we tested if the deletion of VCA0118 affected VgrG-1 actin cross-linking activity in infected J774 macrophages. For these experiments, background actin cross-linking activity was eliminated by disrupting *rtxA* for all *V. cholerae* strains tested (Ma et al., 2009a; Pukatzki et al., 2007). Consistent with previous reports (Ma et al., 2009a; Pukatzki et al., 2007), V52 Δ*rtxA* induced cross-linking of cytosolic actin in J774 cells after a 3-hour infection (Figure 2.3C). Interestingly, while the Δ*rtxA vca0118* double mutant could still cause actin cross-linking in the presence or absence of bafilomycin A, the actin cross-linking activity we observed was less pronounced than its V52 Δ*rtxA* parent (Figure 2.3C). As expected, no actin cross-linking was detected in Δ*rtxA vasK* or Δ*rtxA vgrG-1* double mutants (Figure 2.3C). These results suggest that VCA0118 contributes in some way to the delivery or activity of the actin cross-linking domain of VgrG-1 within J774 macrophages and likely within *D. discoideum* amoebae as well.

Other genes in the *vgrG-1* and *vgrG-2* operons contribute to virulence. The *V. cholerae* T6SS substrates Hcp-1, VgrG-1 and Hcp-2, VgrG-2 are encoded outside of T6SS locus. Bioinformatic analysis using Promscan (Studholme and Dixon, 2003) and Transterm (Ermolaeva et al., 2000) suggest that *hcp-1*, *vgrG-1* and the five downstream open reading frames (VC1417 to VC1421) use the same promoter upstream of *hcp-1* and the same terminator downstream of VC1421 (Figure 2.4A). Similarly, *vgrG-2* and the three downstream open reading frames (VCA0019 to VCA0021) are predicted to use the same promoter and terminator (Figure 2.4A). All proteins encoded in these putative *vgrG-1* and *vgrG-2* operons are uncharacterized

proteins, and most of them do not contain conserved domains (Table 2.1). Interestingly, bioinformatic analysis using HHPRED (Soding, 2005) identified very weak structural homology of VCA0020 and VCA0021 to colicins and type 3 secretion system components, respectively (Table 2.2, 2.3).

We deleted all the five genes following *vgrG-1* (VC1417 through VC1421) to get the

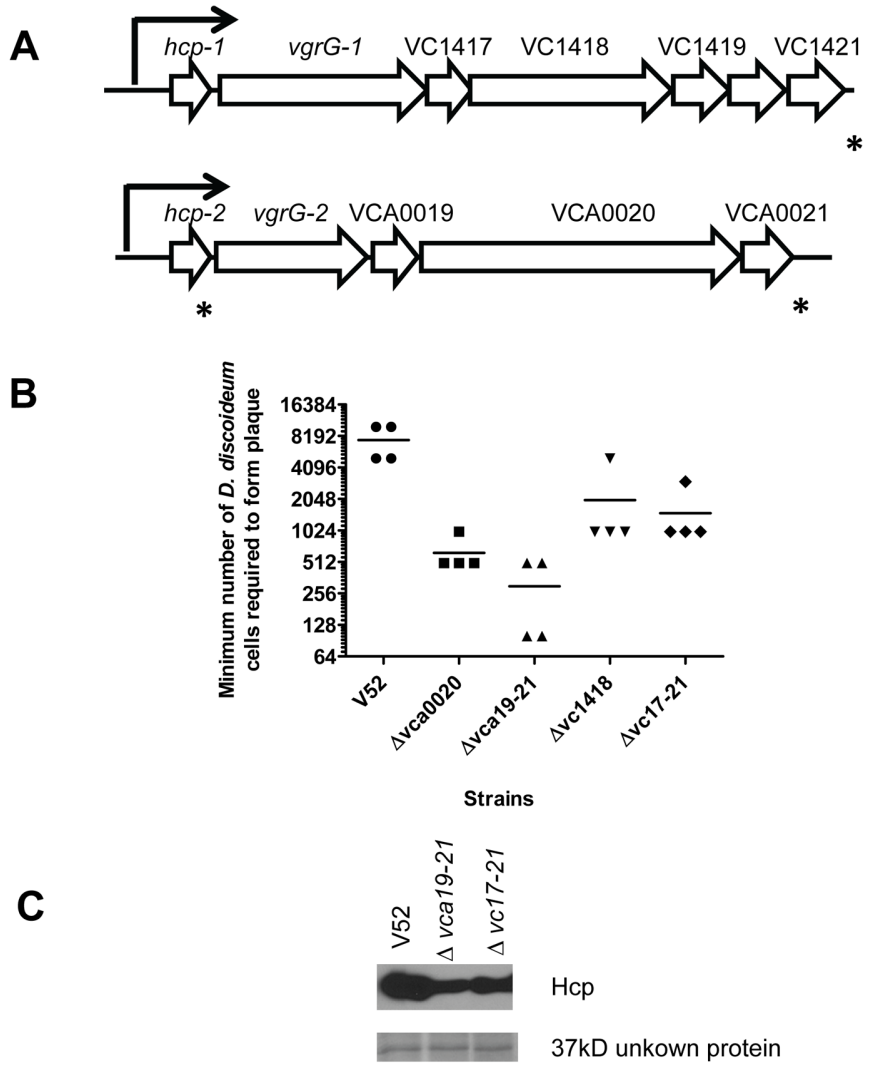

Figure 2.4 Genes encoded in *vgrG-1* and *vgrG-2* operons contribute to *V. cholerae* virulence and Hcp secretion. (A) Schematic representation of genes organization in the putative *vgrG-1* and *vgrG-2* operons. The prompters predicted by PromScan and terminitors predicted by TransTerm are indicated by arrows and stars respectively. (B) The minimum number of *Dictyostelieum* amoebae cells required to form plaque on the lawns of different mutants in *vgrG-1* and *vgrG-2* operons. (C) Deletion of genes in *vgrG-1* and *vgrG-2* operons affected Hcp secretion examined by western blot. A 37 kD unknown protein demonstrated by Ponceau S staining was used as a control to show the equal protein loading.

mutant Δ*vc17-21* and deleted the single gene (VC1418) to get the mutant Δ*vc1418*. Similarly, we deleted all three genes following *vgrG-2* (VCA0019 through VCA0021) to get Δ*vca19-21* and deleted the single gene (VCA0020) to get Δ*vca0020*. We then examined the virulence of each of these mutants towards *Dictyostelium* amoebae. As shown in Figure 2.4B, on average at least

Table 2.1 Properties of proteins encoded in *vgrG-1* and *vgrG-2* putative operons.

Protein	Protein length (amino acids)	Conserved domain	Function
VCA0019	295	No	Uncharacterized
VCA0020	1085	No	Uncharacterized
VCA0021	242	No	Uncharacterized
VC1417	286	No	Uncharacterized
VC1418	641	COG3675; Esterase/Lipase superfamily	Uncharacterized
VC1419	247	No	Uncharacterized
VC1420	245	DUF2931	Uncharacterized
VC1421	212	LysE superfamily	Uncharacterized

Table 2.2 The first ten hits of VCA0020 analyzed by HHPRED.

No.	Hit	Prob.	E-Val.	P-Val.	Query HMM	Template HMM
1	RhoGEF and PH domain containing 6, pleckstrin homology domain	75.1	48	0.00039	75-177	9-109
2	RhoGEF and PH domain containing protein 6	74.5	32	0.00026	74-177	8-109
3	Tapp1	73.9	24	0.00019	75-169	4-98
4	Pleckstrin	67.9	75	0.00061	73-182	4-112
5	Colicin pore forming domain	67.5	270	0.0022	773-915	56-182
6	Variant surface antigen, stevor family	66.8	490	0.0039	797-919	185-311
7	Src-associated adaptor protein Skap2	66.5	53	0.00043	73-167	8-107
8	KIAA0640 protein; PH domain	61.2	73	0.0006	75-169	9-101
9	Src kinase-associated phosphoprotein SKAP55 (SCAP1)	59.3	73	0.00059	75-166	2-98
10	Phosphoinositide phospholipase C	57.4	59	0.00048	74-114	1-43

Table 2.3 The first ten hits of VCA0021 analyzed by HHPRED.

No.	Hit	Prob.	E-Val.	P-Val.	Query HMM	Template HMM
1	SseC Secretion system effector C	89.2	1	$8.3x10^{-6}$	114-147	58-92
2	DUF3040 Protein of unknown function	73.2	9	$7.0x10^{-5}$	3-73	6-76
3	Predicted membrane protein (DUF2208)	68.6	79	$6.3x10^{-4}$	13-108	56-182
4	Aluminum activated malate transporter	62.3	80	$6.5x10^{-4}$	38-135	66-170
5	Bacteriocin AS-48	60.7	41	$3.3x10^{-4}$	103-148	16132
6	EspD	59.4	23	$1.9x10^{-4}$	114-146	178-213
7	Photosystem I P subunit	56.1	70	$5.6x10^{-4}$	24-89	87-149
8	UPF0239: Uncharacterized protein family	56	32	$2.6x10^{-4}$	107-135	14-45
9	DUF2208 Predicted membrane protein	54.4	230	0.0018	13-108	56-182
10	Aminoglycoside/multidrug efflux system	52.7	350	0.0028	5-148	307-468

7,500 amoebae cells were required for plaque formation on wild-type lawns. For each of the mutants, the minimum number of *Dictyostelium* cells required to form plaques decreased significantly. The most notable of these was the Δ*vca19-21* mutant, which supported plaque formation with an average of only 300 amoebae cells (Figure 2.4B). These results suggest that other genes in the *vgrG-1* and *vgrG-2* putative operons might contribute to V52 virulence toward *Dictyostelium* amoebae. Since T6SS is the major *V. cholerae* virulence factor towards *Dictyostelium*, and loss of T6SS activity abolished the virulence to amoebae cells (Pukatzki et al., 2006), we tested whether the Δ*vca19-21* mutation affected T6SS function. Culture supernatants from wild-type V52 and the Δ*vca19-21* and Δ*vc17-21* mutants were examined for Hcp secretion by western blot. As shown in Figure 2.4C, deletion of VCA0019 through VCA0021 or VC1417 through VC1421 decreased Hcp secretion. Ponceau S staining of the western blot membrane showed a similar amount of other unknown secreted proteins had been loaded in each lane, suggesting the differences in Hcp secretion were not due to sample loading variation. A similar reduction in Hcp secretion was also observed in the single deletion mutant Δ*vca0020* (data not shown). These results suggest that genes encoded by the *vgrG-1* and *vgrG-2* putative operons also contribute to secretion by the T6SS and its function in virulence towards *Dictyostelium* amoebae.

Antibacterial properties of different T6SS-related mutants. Recently, T6SS has been implicated in bacterial killing in *P. aeruginosa*, *Burkholderia thailandensis* as well as *V. cholerae* (Hood et al., 2010; MacIntyre et al., 2010; Schwarz et al., 2010b). To test the contribution of each T6SS gene to the antibacterial properties of *V. cholerae*, we examined whether each of these mutants could kill *E. coli* when grown in competition on agar plates. *V. cholerae* and *E. coli* K12 were mixed, spotted onto Luria-Bertani (LB) agar plates and

incubated at 37 C for 3.5 hours. Surviving *E. coli* K12 was then recovered from the plate and enumerated by quantitative plate counts. As previously reported (MacIntyre et al., 2010), *V. cholerae* V52 is highly virulent toward *E. coli* K12 and no viable *E. coli* were recovered from these plates (Figure 2.5A). In contrast, deletion of VCA0107 (*vipA*) through VCA0115 (*vasF*), or deletion of VCA0117 (*vasH*), VCA0119 and VCA0120 (*vasK*) resulted in complete loss of *E. coli* killing. Under the assay conditions used, T6SS-dependent killing was responsible for a 1,000 to 10,000-fold drop in the recovery of viable *E. coli* cells. Furthermore, these results were remarkably consistent with the requirement of these same genes for *Dictyostelium* amoeba

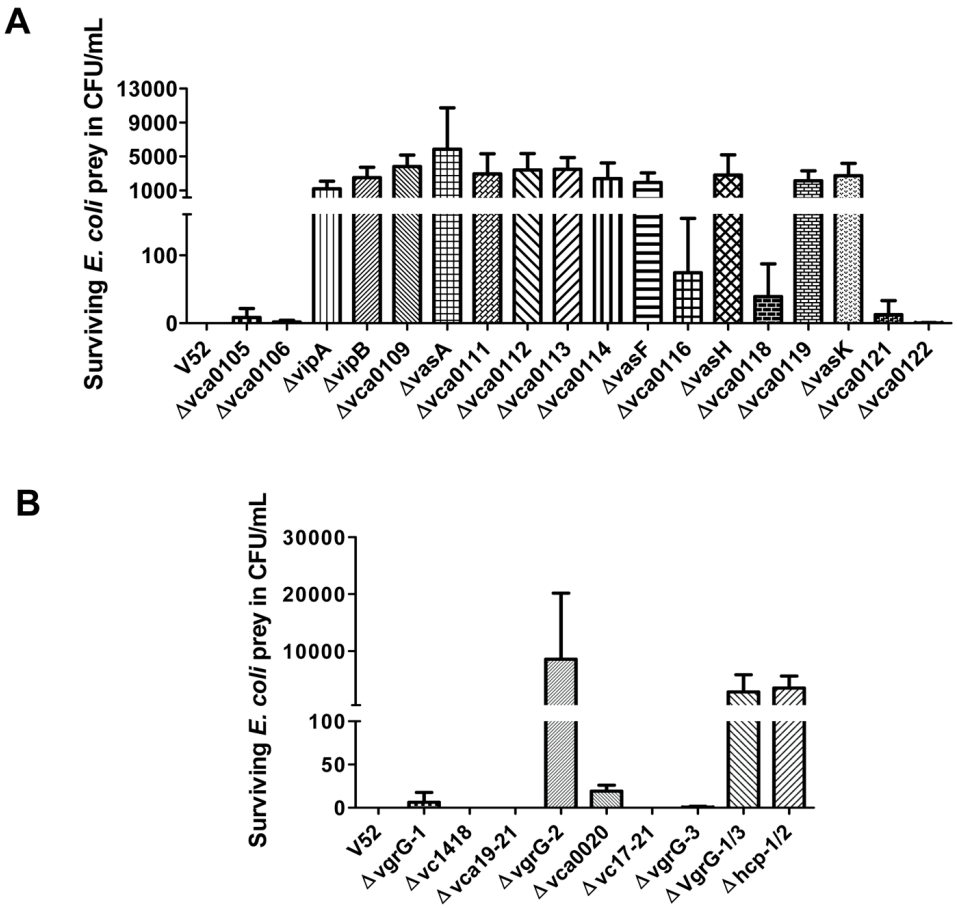

Figure 2.5 Contributions of different T6SS locus genes to *V. cholerae* anti-bacterial properties. Survival of tetracycline-resistant *E. coli* CC114 was determined by measuring cfu following exposure to the streptomycin-resistant *V. cholerae* predator listed on the x-axis. The data represent three independent experiments and values given are means ± SD.

killing (Figure 2.1C). Thus, this group of genes likely consists of genes required for producing a functional T6SS apparatus. Remarkably, deletion of *clpV* (VCA0116) also resulted in a clear attenuation in the bacterial killing, but not to the same degree as seen in mutants defective in VCA0107-VCA0115, VCA0117, VCA0119 and VCA0120. Compared to the T6SS apparatus knockout mutants, approximately 30-fold less *E. coli* was recovered from the competitions with Δ*clpV* mutant, indicating that the Δ*clpV* mutant still displays significant killing activity. Similarly, deletion of VCA0118 caused an attenuation of *E. coli* killing activity in that about 2-fold less *E.coli* was recovered compared to Δ*clpV*. In contrast, loss of VCA0105, VCA0106, VCA0121 and VCA0122 had no significant effect on bacterial killing (Figure 2.5A).

We next examined the antibacterial properties of the three VgrG proteins (VgrG-1 to -3). As shown in Figure 2.5B, deletion of *vgrG-2* resulted in complete loss of killing. Surprisingly, we did not observe a significant bacterial killing defect in the Δ*vgrG-1* and Δ*vgrG-3* mutants. However, simultaneous deletion of both of these genes (Δ*vgrG-1/3*) produced a similar phenotype as Δ*vgrG-2* and other T6SS apparatus knockout mutants. Additionally, deletion of *hcp-1* and *hcp-2* together (Δ*hcp-1/2*) also led to loss of bacterial killing. The genes in the *vgrG-1* and *vgrG-2* putative operon were also evaluated. There is no virulence defect in bacterial killing in Δ*vc1418* or Δ*vc17-21*. However, deletion of VCA0020 caused a slight attenuation in *E. coli* killing. Interestingly, this defect was not observed in Δ*vca19-21,* in which all three genes following *vgrG-2* (VCA0019 through VCA0021) were deleted (Figure 2.5B).

Type 2 secretion system is not required for Hcp secretion. A bioinformatic analysis of proteins in *V. cholerae* T6SS locus did not predict any proteins with trans-membrane domains that might provide an outer membrane channel for secretion of T6SS effectors (Shrivastava and Mande, 2008). We thus asked whether outer membrane proteins from other secretion systems

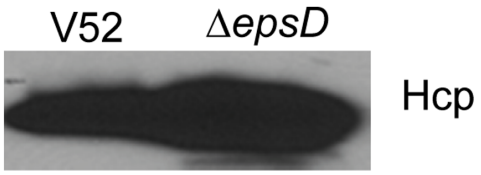

Figure 2.6 Type II secretion system outer membrane protein EpsD is not requited for Hcp secretion. Western blot of Hcp from the cell-free supernatant fluids of *V. cholerae* wild type and Δ*epsD* with anti-Hcp was shown.

might be involved in type VI protein secretion. *V. cholerae* contains a type II secretion system in addition to its T6SS (Sandkvist et al., 1997). We deleted EpsD (VC2733), the outer membrane channel of type II secretion system. The secreted proteins from bacterial culture supernatants were collected and Hcp secretion was examined by western blot. Although EpsD deficiency greatly impaired growth of *V. cholerae* (data not shown), Hcp was still readily detected in the bacterial supernatant (Figure 2.6), suggesting that T6SS in *V. cholerae* does not make use of type II secretion system channel for secretion of its substrates.

Discussion

Using a *D. disoideum* model, the T6SS of *V. cholerae* was identified and designated a virulent determinant of *V. cholerae* O37 strain V52 toward amoebae (Pukatzki et al., 2006). More recently the T6SS of V52 has also been shown to have antibacterial activity (MacIntyre et al., 2010). In this study, to further understand T6SS in V52, we undertook a systematic mutagenesis approach. We characterized each mutant for Hcp expression and secretion, and examined their contributions to virulence toward *Dictyostelium* amoebae and *E. coli*. We identified four groups of proteins encoded in the T6SS locus: structural apparatus components, regulators, proteins of unknown function and a potential effector.

VipA, VipB, VasF, ClpV and VasK have been shown to be essential for Hcp secretion in O37 serogroup strain V52 in previous reports (Bonemann et al., 2009; Pukatzki et al., 2006).

Here we identified another seven genes (VCA0109 through VCA0114, and VCA0119) required for Hcp secretion in V52. Deletion of these genes completely abolished Hcp secretion even though hcp expression levels remained similar to the wild type levels. These mutants were also avirulent towards *Dictyostelium* amoebae and *E. coli* bacteria. Thus, we speculate that collectively these genes constitute important components of the T6SS apparatus (Table 2.4). Deletion of T6SS structural components of the T6SS apparatus might cause defects in either secretion or translocation of T6SS effectors, either of which would likely compromise virulence.

Interestingly, deletion of *clpV* (VCA116) had a similar effect on Hcp secretion and attenuation of *Dictyostelium* virulence as deletion of other T6SS apparatus genes but had a smaller effect on killing activity towards *E. coli*. These data suggest that ClpV is not essential for the process that ultimately allows *V. cholerae* to kill *E. coli,* but rather ClpV simply increases its efficiency. Given the pore-like structure and protein translocation capability of Clp family proteins, there has been speculation that ClpV may provide the energy to translocate T6SS substrates out of bacterial cells and into target cells (Bonemann et al., 2009; Mougous et al., 2006). Indeed, a ClpV ortholog has also been shown to be essential for secretion of Hcp in *P. aeruginosa* (Mougous et al., 2006) and for bacterial killing (Hood et al., 2010). ClpV of *V. cholerae* has previously been shown to be required for remodeling of the tubular complex formed by the products of VCA107 (VipA) and VCA108 (VipB) as well as efficient secretion of Hcp and VgrG-2 proteins (Bonemann et al., 2009). Our results suggest that ClpV may not be required for assembly of a functional T6SS apparatus but rather simply improves the efficiency of its function. Because the tubular structure formed by VipA and VipB resembles contracted tail sheath of bacteriophage T4, Leiman *et al*. (2009) suggested that the T6SS-mediated secretion and membrane insertion process might be powered through conformational changes in VipA and

VipB that mimic those occurring in phage tail contraction (rather than through the energy generated by ClpV ATP hydrolysis). It follows that in the absence of ClpV such a phage tail-like contraction mechanism might also insert the VgrG spike and Hcp tube structure (Leiman et al., 2009; Pukatzki et al., 2007) into closely contacting *E. coli* target cells. The non-essentiality of ClpV for V52 killing of *E. coli* is consistent with the hypothesis that ClpV is not essential for formation of the T6SS apparatus per se. Rather, ClpV might play its role in the disassembly of the contracted sheath (Economou et al., 2006; Leiman et al., 2009) (after a bacterial killing event) and thus likely improves the efficiency of killing by recycling VipA/B out of contracted sheath structures and back into functional non-contracted T6SS phage tail-like assemblies. A few functional T6SS assemblies might be sufficient to kill detectable numbers of *E. coli* cells in our sensitive bioassay, whereas a larger number of T6SS assemblies (or the rapid recycling of contracted assemblies) may be needed to translocate detectable amounts of effector proteins into the supernatant or into amoebae or other types of target cells.

Although *V. cholerae* encodes three VgrG proteins, we found that VgrG-2 is the only VgrG protein individually essential for killing of amoebae and bacteria. VgrG-1 has been reported to be essential for Hcp secretion and amoebae killing (Ma et al., 2009a; Pukatzki et al., 2007; Pukatzki et al., 2006) but is not needed for *E. coli* killing (Figure 2.5B) (MacIntyre et al., 2010). This curious fact suggests that bacterial killing may occur by a process that does not generate a large amount of extracellular Hcp and that the T6SS apparatus mediating this killing can still be assembled in the absence of VgrG-1. It is possible that like ClpV, some T6SS-related proteins are not absolutely required for assembly or function of the apparatus, but rather alter the efficiency of its assembly or reassembly. For example, despite the fact that inactivation of VgrG-1 or VgrG-3 alone does not affect bacterial killing, inactivation of both of these genes does block

killing. Because VgrG-2 interacts with VgrG-1 and VgrG-3 (Pukatzki et al., 2007), we propose that VgrG-2 likely needs to interact with one of these other VgrG proteins to efficiently form a critical component of the T6SS apparatus such as a homo- or heterotrimer of VgrG-2. VgrG-2 is the shortest of the three *V. cholerae* VgrG proteins and carries virtually no C-terminal extension domain. Leiman *et al*. (2009) noted that short VgrG proteins are the most common form found among the hundreds of VgrG proteins encoded by microbial genomes. Thus, the short form of VgrG proteins may be the essential form of the protein needed to form an apparatus with antibacterial activity through its ability to puncture cells using its needle-like β-helix C-terminal domain (Leiman et al., 2009). By analogy to phage tail-like pyocins (Michel-Briand and Baysse, 2002), the T6SS phage tail-like spike and needle penetration would be followed quickly by lethal channel formation via insertion of the phage tube-like Hcp structure through the envelop of the target cell (Leiman et al., 2009). Recently, the T6SS of *P. aeruginosa* has been shown to have antibacterial activity through the delivery of soluble toxic effector proteins (Hood et al., 2010). Other than the anti-eukaryotic ACD effector domain of VgrG-1 (Ma et al., 2009a; Ma and Mekalanos, 2010; Pukatzki et al., 2007; Pukatzki et al., 2006), we have not uncovered a separate antibacterial effector in the present study and thus conclude that a functional T6SS apparatus may be sufficient for *V. cholerae* to kill *E. coli*. However, it is worth emphasizing that killing different bacterial or eukaryotic targets and using different killing mechanisms, such as membrane breaching versus delivering a separate toxic effector protein, might all require different threshold levels of T6SS assemblies. For example, pyocins kill with single hit kinetics (i.e., insertion of one pyocin can kill one bacterial cell) but soluble protein bacteriocins likely require more than one molecule to be translocated into a target cell in order to kill (Michel-Briand and Baysse, 2002).

Four genes in the T6SS cluster of *V. cholerae* are not absolutely required for secretion of Hcp including *vasH,* VCA0118, VCA0121, and VCA0122 (Table 2.4). VCA0121 is also not required for virulence toward amoebae and bacteria. A bioinformatic analysis showed that both VCA0119 and VCA0121 have ImpA-rel-N superfamily domains, a feature found in inner membrane proteins participating in intracellular protein transport (Shrivastava and Mande,

Table 2.4 Functions of genes encoded by the T6SS locus.

		Required for			
Gene	Function	Hcp secretion	Virulence toward amoebae	Bacteria killing	References
VCA0107 (*vipA*)	Structure protein	Yes	Yes	Yes	This study and (Bonemann et al., 2009)
VCA0108 (*vipB*)	Structure protein	Yes	Yes	Yes	This study and (Bonemann et al., 2009)
VCA0109	Structure protein	Yes	Yes	Yes	This study
VCA0110 (*vasA*)	Structure protein	Yes	Yes	Yes	This study
VCA0111	Structure protein	Yes	Yes	Yes	This study
VCA0112	Structure protein	Yes	Yes	Yes	This study
VCA0113	Structure protein	Yes	Yes	Yes	This study
VCA0114	Structure protein	Yes	Yes	Yes	This study
VCA0115 (*vasF*)	Structure protein	Yes	Yes	Yes	This study and (Pukatzki et al., 2006)
VCA0116 (*clpV*)	Structure protein	Yes	Yes	Yes/No[a]	This study and (Bonemann et al., 2009)
VCA0117 (*vasH*)	Regulator	Yes	Yes	Yes	This study and (Pukatzki et al., 2006)
VCA0118	Putative effector	Yes	Yes	Yes/No[a]	This study
VCA0119	Structure protein	Yes	Yes	Yes	This study
VCA0120 (*icmF*)	Structure protein	Yes	Yes	Yes	This study
VCA0121	Unknown	No	No	No	This study
VCA0122	Regulator	No[b]	Yes	No	This study
VC1415 (*hcp-1*), VCA0017 (*hcp-2*[c])	Structure/Secreted protein	Yes	Yes	Yes	This study and (Pukatzki et al., 2006)
VC1416 (*vgrG-1*)	Structure protein/effector	Yes	Yes	Yes/No[d]	This study and (Pukatzki et al., 2007)
VCA0018 (*vgrG-2*)	Structure/Secreted protein	Yes	Yes	Yes	This study and (Pukatzki et al., 2007)
VCA0123 (*vgrG-3*)	Unknown/Secreted protein	No	No	Yes/No[d]	This study and (Pukatzki et al., 2007)

[a] *clpV* and VCA0118 mutants exhibited bacterial killing activity but at a significantly lower level than wild type.
[b] VCA0122 enhances Hcp expression and secretion. The VCA0122 mutant exhibited a slightly lower level of Hcp expression than wild type.
[c] *hcp-1* and *hcp-2* fully complement each other. Their requirement for virulence is only observed in the context of the double knock-out.
[d] *vgrG-1* and *vgrG-3* are able to complement each other for *E. coli* killing activity only. The double mutant is avirulent toward *E. coli*.

2008). VCA0119 is important for T6SS-dependent secretion (Figure 2.1B, C), suggesting that VCA0121 might simply be a non-functional derivative of a VCA0119 duplication. However, given their low sequence similarity (12.7% identity) it is possible that VCA0121 was acquired by horizontal gene transfer from a non-*Vibrio* species and may have some as of yet undetermined function.

The expression of T6SS gene clusters is typically tightly regulated (Cascales, 2008; Economou et al., 2006; Filloux et al., 2008). Before this study, four regulators have been shown to control T6SS in *V. cholerae*, namely, VasH, TsrA, HapR and RopN (Ishikawa et al., 2009; Pukatzki et al., 2006; Zheng et al., 2010). VasH is a sigma-54 dependent regulator encoded in T6SS locus and is required for Hcp expression (Pukatzki et al., 2006). TsrA is a global regulator that represses T6SS and virulence factors (CT and TCP) and activates the gene for the secreted hemagglutinin protease HapA (Zheng et al., 2010). Both HapR and RpoN are positive regulators for T6SS, and RpoN has been shown to directly bind to the *hcp-1*, *hcp-2*, and *vipA* promoter regions (Bernard et al., 2011; Zheng et al., 2010). Here, we found that VCA0122 is an additional regulator for *V. cholerae* T6SS. VCA0122 is an 80 amino acid protein and is not homologous to any characterized protein. Mutation of VCA0122 decreased Hcp expression at the transcriptional level presumably by affecting *hcp-2* promoter activity. Interestingly, VCA0122 plays important role in the *Dictyostelium* killing but seems to have no contribution to T6SS-dependent bacterial killing. Deletion of VCA0122 decreased but did not abolish Hcp expression and secretion (Figure 2.1B). It is likely that the number of functional T6SS assemblies in Δ*vca0122* is sufficient to kill bacteria but not eukaryotic cells.

VCA0118 is a 227 amino acids protein and predicted to be exported (Shrivastava and Mande, 2008). It contains a DUF3121 superfamily domain, which has no characterized function.

In *V. cholerae*, VCA0118 is different from all other proteins encoded in the T6SS locus in that deletion of VCA0118 did not affect the secretion of Hcp or VgrG-1, the only known eukaryotic effector protein of T6SS, but totally abolished virulence in the *Dictyostelium* amoebae model. Further investigation of actin cross-linking showed that the VCA0118 mutant was still able to cause actin cross-linking but at a lower efficiency than its V52 Δ*rtxA* parental strain (Figure 2.3C). These results suggest that VCA0118 might be required for efficient translocation of VgrG-1 into host cells. VCA0118 may represent an extracellular adhesin that promotes binding and phagocytosis of *V. cholerae* by macrophages. VCA0118 might also participate in the translocation of T6SS effectors into target cells after phagocytosis of *V. cholerae*. If VCA0118 protein is also translocated into the host cell, then it is also possible that it might interact with VgrG-1 to promote VgrG-1 actin cross-linking activity within the host cell cytoplasm. However, considering inactivation of VCA0118 causes a total loss of virulence toward Dictyostelium but only slightly decreases actin cross-linking, it seems unlikely that VCA0118 functions only through its interaction with VgrG-1, as deletion of VCA0118 also decreased virulence toward *E. coli*, which does not require VgrG-1 or its ACD domain (Figure 2.5B) (MacIntyre et al., 2010). These data suggest that VCA0118 likely plays some other role besides being an enhancer of VgrG-1 toxicity. Further experiments are needed to define the contribution that VCA0118 makes to the functionality of the T6SS of *V. cholerae*.

In addition to the proteins encoded in T6SS locus, we also determined that the genes encoded downstream of *vgrG-1* and *vgrG-2* contribute to the virulence of V52 toward *Dictyostelium*. Deletion of a single gene (VCA0020) caused attenuation of V52 virulence toward amoebae, possibly by causing a small decrease in Hcp secretion (Figure 2.4C). The attenuation level in this mutant as well as a triple mutant lacking genes VCA0019 through VCA0021 was

relatively small compared to the decreases in virulence caused by deletion of T6SS apparatus genes, suggesting that they do not encode essential structure components of the apparatus. In the bacterial killing assay, deletion of VCA0020 showed a decreased virulence toward *E. coli*. Interestingly, this attenuation was not seen in ΔVCA19-21 in which the genes VCA0019-VCA0021 were deleted simultaneously. This result suggests that VCA0020 may interact with VCA0019 and VCA0021 in a complex way that affects the functionality of the T6SS apparatus in killing assays. Consistent with these results, Miyata *et al*. (2011) have recently reported that mutation of VCA0020 significantly reduces virulence of *V. cholerae* toward *Dictyostelium* without altering secretion of Hcp or VgrG proteins.

In conclusion, we have shown in this study that proteins encoded in *V. cholerae* T6SS locus contribute in different ways to its functionality in Hcp secretion and the killing of amoebae and bacteria. Since T6SS is an important virulence factor in many bacterial pathogens, the characterization of gene products that are absolutely required for the functionality of the T6SS apparatus should benefit the understanding of T6SS mechanism in other bacterial species and may provide new targets for control of bacterial infectious diseases.

Materials and Methods

Strains, plasmids and culture conditions. *V. cholerae* O37 serogroup strain V52 and its derivatives were used in this study. *E. coli* strains DH5α*λpir*, and SM10*λpir* were used for cloning and mating, respectively. The bacterial strains and plasmids used in this study are listed in Table 2.5. All bacterial strains were grown in LB broth supplemented with streptomycin (800 μg/ml), kanamycin (50 μg/ml), and carbenicillin (50 μg/ml) when necessary. Macrophage J774 cells were obtained from the American Type Culture Collection (ATCC). *D. discoideum* strain

AX3 was used for bacterial virulence assay. AX3 was grown in liquid HL5 cultures or SM/5 agar plate as described by Fey et al. (2007).

Table 2.5 Strains and plasmids for this study.

Strain or plasmid	Description	Reference or source
V. cholerae		
V52	Wild type, StrepR	(Pukatzki et al., 2006)
Δvca0105	V52, in frame deletion of amino acid 1 to 61 from VCA0105	This study
Δvca0106	V52, in frame deletion of amino acid 34 to 356 from VCA0106	This study
ΔvipA	V52, in frame deletion of amino acid 8 to 163 from VCA0107	This study
ΔvipB	V52, in frame deletion of amino acid 12 to 486 from VCA0108	This study
Δvca0109	V52, in frame deletion of amino acid 4 to 142 from VCA0109	This study
ΔvasA	V52, in frame deletion of amino acid 5 to 554 from VCA0110	This study
Δvca0111	V52, in frame deletion of amino acid 14 to 313 from VCA0111	This study
Δvca0112	V52, in frame deletion of amino acid 1 to 488 from VCA0112	This study
Δvca0113	V52, in frame deletion of amino acid 1 to 152 from VCA0113	This study
Δvca0114	V52, in frame deletion of amino acid 2 to 413 from VCA0114	This study
ΔvasF	V52, in frame deletion of VCA0115	(Pukatzki et al., 2006)
ΔclpV	V52, in frame deletion of amino acid 3 to 850 from VCA0116	This study
ΔvasH	V52, in frame deletion of VCA0117	This study
Δvca0118	V52, in frame deletion of amino acid 12 to 225 from VCA0118	This study
Δvca0119	V52, in frame deletion of amino acid 3 to 468 from VCA0119	This study
ΔvasK	V52, in frame deletion of VCA0120	(Pukatzki et al., 2006)
Δvca0121	V52, in frame deletion of amino acid 1 to 421 from VCA0121	This study
Δvca0122	V52, in frame deletion of amino acid 10 to 48 from VCA0122	This study
ΔvgrG-3	V52, in frame deletion of VCA0123	(Pukatzki et al., 2007)
ΔvgrG-2	V52, in frame deletion of VCA0018	(Pukatzki et al., 2007)
Δvca0020	V52, in frame deletion of amino acid 3 to 1077 from VCA0020	This study
Δvca19-21	V52, in frame deletion of genes from VCA0019 to VCA0021	This study
ΔvgrG-1	V52, in frame deletion of VC1416	(Pukatzki et al., 2007)
Δvc1418	V52, in frame deletion of amino acid 2 to 626 from VC1418	This study
Δvc1417-21	V52, in frame deletion of genes from VC1417 to VC1421	This study
Δhcp-1/2	V52, in frame deletion of VCA0017 and VC1415	(Pukatzki et al., 2006)
ΔvgrG-1/3	V52, in frame deletion of VCA0123 and VC1416	This study
ΔepsD	V52, in frame deletion of amino acid 49 to 670 from VC2733	This study
ΔrtxA	V52, in frame deletion of rtxA	This study
ΔrtxAvca0118	V52, in frame deletion of rtxA and VCA0118	This study
ΔrtxAvgrG-1	V52, in frame deletion of rtxA and vgrG-1	This study
ΔrtxAvasK	V52, in frame deletion of rtxA and vasK	This study
E. coli		
DH5α pir	*fhuA2 Δ(argF-lacZ)U169 phoA glnV44 Φ80 Δ(lacZ)M15 gyrA96 recA1 relA1 endA1 thi-1 hsdR17 pir*	(Miller and Mekalanos, 1988)
SM10 pir	*thi thr leu tonA lacY supE recA-RP4-2-Tc-Mu pir*	(Rubires et al., 1997)
Plasmids		
pDS132	pCVD442 derivative, pir dependent, sacB, CmR	(Philippe et al., 2004)
pTL61T	AmpR, lacZ reporter vector	(Linn and St Pierre, 1990)
pBBR1MCS2	KmR, broad host range	(Kovach et al., 1995)

Non-polar deletion mutants and LacZ reporter plasmid construction. Overlap extension PCR was used to generate in-frame deletion of individual genes as described previously (Zheng et al., 2005). Briefly, for construction of a gene X deletion mutant, two PCR fragments were generated from V52 genomic DNA with the primer pair of X-for plus X-int-rev, and X-rev plus X-int-for. The resulting products generated about 1kb fragment containing the upstream of gene X and a 1kb fragment containing the downstream of gene X, respectively. A 20-bp overlap sequences in the primers permitted amplification of an about 2 kb product during a second PCR with the primers X-for and X-rev. The resulting PCR product contained a deletion of the internal fragment of gene X. This PCR product was then sub-cloned into plasmid pDS132 (Linn and St Pierre, 1990) to result in a suicide plasmid construct. Non-polar deletion mutants were generated by *sacB*-based allelic exchange. Mutants were verified by PCR. For construction of LacZ reporter plasmid, *hcp-2* putative promoter region was amplified from *V. cholerae* V52 genomic DNA and the PCR products were subcloned into *Xho*I and *Xba*I digested pTL61T plasmid (Linn and St Pierre, 1990).

Protein assay. Secreted proteins were isolated from mid-log cultured *V. cholerae* (OD_{600} = ~0.4 – 0.5) in LB broth. Briefly, various overnight bacterial cultures were diluted at 1:1,000, and were grown for about 3 to 4-hour at 37ºC with shaking. The bacteria were collected by centrifuge, and the bacterial pellet was resuspended in 2 × loading buffer. The bacterial culture supernatants were sterilized by passing through a 0.2 μm filter, and proteins were precipitated with trichloroacidic acid (TCA) and subjected to 10-20% gradient SDS/PAGE. The Hcp polyclonal antibodies were generated by New England Peptide (Gardner, MA).

Plaque formation assay. Two millilitre bacteria grown in LB broth for 16-hour were pelleted by centrifugation at 7600 rpm for 5 min, washed once, and resuspended in the same

volume of SorC buffer. One hundred microliters of the bacteria were plated on SM/5 agar plate. *Dictyostelium* amoebae cells from mid-logarithmic cultures were collected by centrifugation, washed once with SorC buffer, and different number of amoebae cells (5×10^4; 1×10^4; 5×10^3; 3×10^3; 1×10^3; 5×10^2; 1×10^2; 5×10^1; 1×10^1; 5×10^0, respectively) in 5 µl SorC buffer were deposited on the top of the agar plates with wild-type *V. cholerae* and different mutants. The plates were allowed to dry under a sterile flow of air and then were incubated at 22ºC for 3–5 days. The plaques formed by *Dictyostelium* amoebae were recorded. The least number of *Dictyostelium* amoebae cells deposited above that was able to form plaque on the bacterial lawns was defined as the minimum number of *Dictostelium* cells required for plaque formation in this study.

Bacterial killing assay. The bacterial killing experiment was performed as described (MacIntyre et al., 2010). Briefly, *V. cholerae* and *E. coli* K12 CC114 were mixed at a multiplicity of infection (MOI) of 10. Twenty microliters of the mixture was spotted on LB agar plate and was incubated at 37 C for 3.5 hours. Bacterial spots were harvested and resuspended in 1 ml of LB broth. The colony-forming unit (cfu) per milliliter of surviving *V. cholerae* and *E. coli* were measured by a serial dilution and selective growth on LB agar plates containing 100 µg/ml streptomycin (for *V. cholerae*) and 12 µg/ml tetracycline (for *E.coli*) respectively.

Actin cross-linking assay. Actin cross-linking assay was performed as described previously (Pukatzki et al., 2006). Briefly, J774 cells were seeded into six-well tissue culture plates at a density of 10^6 cells per well. After 16-hour incubation at 37 ºC, cells were infected with various *V. cholerae* strains. The infections were performed at a MOI of 10 for 3-hour. Cells were harvested and resuspended in 50 µl of 2 × loading buffer, and 10 µl each sample was analyzed by western blot using actin antiserum with the dilution at 1:1,000.

β-galactosidase assays. Bacteria were grown in LB broth overnight at 37 C. Beta-galactosidase activities were determined with cells permeabilized with SDS and chloroform as described by Miller (Miller, 1972).

Chapter 3. PAAR-repeat proteins sharpen and diversify the type VI secretion system spike

The bacterial type VI secretion system (T6SS) is a large multicomponent, dynamic macromolecular machine that has an important role in the ecology of many Gram-negative bacteria. T6SS is responsible for translocation of a wide range of toxic effector molecules, allowing predatory cells to kill both prokaryotic as well as eukaryotic prey cells. The T6SS organelle is functionally analogous to contractile tails of bacteriophages and is thought to attack cells by initially penetrating them with a trimeric protein complex called the VgrG spike. Neither the exact protein composition of the T6SS organelle nor the mechanisms of effector selection and delivery are known. Here we report that proteins from the PAAR (proline-alanine-alanine-arginine) repeat superfamily form a sharp conical extension on the VgrG spike, which is further involved in attaching effector domains to the spike. The crystal structures of two PAAR-repeat proteins bound to VgrG-like partners show that these proteins sharpen the tip of the T6SS spike complex. We demonstrate that PAAR proteins are essential for T6SS-mediated secretion and target cell killing by *Vibrio cholerae* and *Acinetobacter baylyi*. Our results indicate a new model of the T6SS organelle in which the VgrG–PAAR spike complex is decorated with multiple effectors that are delivered simultaneously into target cells in a single contraction-driven translocation event.

Foreword

A version of this chapter was published in *Nature* on August 15, 2013. The article can be found on the web at the following URL:

http://dx.doi.org/10.1038/nature12453

The full citation for this article is:

> *Shneider, M.M., *Buth, S.A., Ho, B.T., Basler, M., Mekalanos, J.J., and Leiman, P.G. (2013). PAAR-repeat proteins sharpen and diversify the type VI secretion system spike. Nature *500*, 350-353. (*authors contributed equally)

This work was a collaborative effort between the Mekalanos Lab and the laboratory of Petr G. Leiman at the École Polytechnique Fédérale de Lausanne (EPFL). Initial bioinformatic identification of the PAAR-motif proteins and all crystallographic work (Figures 3.1-3.7) was performed by members of the Leiman laboratory. *Acinetobacter baylyi* mutants were made by Dr. Marek Basler while I made the equivalent mutants in *Vibrio cholerae*. All of the characterization of the PAAR-motif proteins and their effect on T6SS activity (Figure 3.8 and 3.10) as well as bioinformatic analysis of the extension domains of PAAR-motif proteins (3.9) was performed by me. I would like to acknowledge Professor Leiman and Professor Mekalanos for writing the original draft of this manuscript an Professor Leiman for preparation of the crystallography and structure figures presented.

I would like to thank the entire staff of the Swiss Light Source PX beamlines and V. Olieric in particular for support related to crystallographic data collection. The project was made possible by the Swiss National Science Foundation (grant 31003A_127092) and EPFL funding to Petr G. Leiman and grants AI-026289 and AI-01845 from the National Institute of Allergy and Infectious Diseases to John J. Mekalanos. The atomic coordinates and the structure factors of the refined atomic models of gp5(VCA0018)–VCA0105 and gp5(c1883)–c1882 complexes were deposited to the Protein Data Bank (http://www.rcsb.org) under the accession numbers 4JIV and

4JIW, respectively.

Results and Discussion

The type 6 secretion system (T6SS) (Mougous et al., 2006; Pukatzki et al., 2006) organelle is a 1,000-nm long tubular structure consisting of an inner tube made of multiple copies of the Hcp protein and an external contractile sheath composed of VipA and VipB proteins (also known as TssB/TssC) (Basler et al., 2012). It has been visualized in two conformations (extended and contracted), which are both attached to the cell envelope by means of a baseplate complex (Basler et al., 2012). Rapid contraction of the sheath results in translocation of the inner tube out of the predator cell and into the prey cell (Basler et al., 2012). The trimeric VgrG spike protein is positioned at the end of the tube (Leiman et al., 2009). It is believed to penetrate the prey cell with its needle- shaped carboxy-terminal β-helical domain. VgrG proteins can contain additional C-terminal domains that act as effectors (Pukatzki et al., 2007) and may also bind effectors through undefined mechanisms (Dong et al., 2013).

Because VgrG proteins are orthologous to the central baseplate spikes of bacteriophages with contractile tails, we reasoned that additional structural components present in certain phage spikes might have corresponding orthologous components in T6SS. The cryoEM reconstruction of phage T4 baseplate shows that an unknown protein with a molecular weight between 7 and 23 kilodaltons (kDa) binds to the tip of the β-helical domain of the central spike protein gp5 (Kostyuchenko et al., 2003). We analysed all known genes encoding small proteins in phage genomes with gp5-like spikes and compared them to T6SS genes. Proteins containing the PAAR-repeat motif were strongly represented in this group with gp5.4 being the corresponding protein of T4 phage. Furthermore, genes encoding proteins with PAAR motifs were frequently found immediately downstream of vgrG-like genes suggesting that the two are genetically linked (Leiman et al., 2009). Therefore, we devised a strategy to test the hypothesis that these PAAR

proteins were binding to the tip of gp5 and VgrG proteins.

Careful examination of VgrG sequences showed that a β-structural repeat, which is presumed to be responsible for β-helix formation (Kanamaru et al., 2002; Pukatzki et al., 2007), either extends to the very C terminus of the protein or terminates with a glycine/serine-rich stretch (Figure 3.1A). We surmised that the glycine/serine-rich stretch bends the polypeptide chain away from the β-helix without disturbing its tip, and that all VgrG β-helices have blunt ends resembling that of T4 gp5 β-helix. Thus, we further speculated that the binding site for a PAAR protein was the blunt end of the β-helix and designed experiments to test this idea.

A

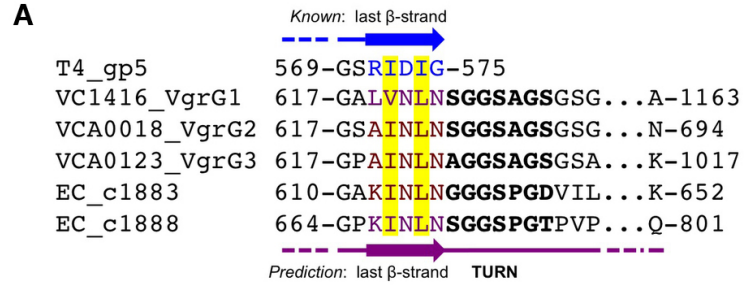

B

gp5 C-terminal residues	VgrG source	VgrG residue range	PAAR protein	Expression system type
...DIKGAKINLN	c1883	607...616	c1882	*cis*
...HIVGSAINLN	VCA0018 (VgrG-2)	614...623	VCA0105	*trans*
...HIVGSAINLN	VCA0018 (VgrG-2)	614...623	VCA0284	*trans*
...HLVGPAINLN	VCA0123 (VgrG-3)	614...623	VCA0284	*trans*
...**TIDGSRIDIG**	**gp5 wild type**		**gp5.4**	***cis***
...**TIDGSRIDIG**	**gp5 wild type**		**c1882***	***cis***
...**TIDGSRIDIG**	**gp5 wild type**		**VCA0105**	***trans***
...KIKSGNVEIG	c3393	726...735	c3396	*cis*
...TLKGGNIELG	PA1511	732...741	PA1508	*cis*

Figure 3.1 Design of gp5–VgrG chimaeras and analysis of their interaction with selected PAAR proteins. (**A**) Identification of the blunt ends of selected VgrG β-helices. The last β-strand of the known T4 gp5 structure is shown in blue. Putative β-strands terminating VgrG β-helices are in purple. The glycine/serine-rich motif is bold highlighted. The residue number for the first amino acid of the shown fragment and that for the C-terminal amino acid of the protein are given. Abbreviations used EC, *E. coli* CTF073; VC, *V. cholerae* O1 biovar El Tor str. N16961. (**B**) Binding of several PAAR proteins to gp5-based VgrG-like β-helices. Two complexes for which the crystal structures are reported in this paper are highlighted with green background. Entries showing gp5 modifications that did not result in PAAR binding have a grey background. c1882* contains three mutations T28K, T64K and T90K that were made to mimic T4 gp5.4. Note that VCA0105 and VCA0284 contain threonines and serines in these positions and they bind wild-type gp5.

Because of the solubility problems of most tested VgrG and PAAR proteins, we used a soluble fragment of T4 gp5 β-helix (residues 484– 575), which is known to fold into a stable native-like trimeric structure (Kanamaru et al., 2002), as a platform for creating β-helices mimicking the blunt end of various VgrG spikes. We replaced the tip of gp5 β-helix (the last two β-strands) with an equivalent fragment from several putative β-helices of VgrGs from *Escherichia coli*, *Vibrio cholerae* and *Pseudomonas aeruginosa* (Figure 3.1B). These gp5–VgrG chimaeras (hereafter referred to as gp5(VgrG)) were then co-expressed with various PAAR proteins, in *cis* and in *trans*, in different combinations (Figure 3.1B). Surprisingly, the *V. cholerae* VCA0105 and *E. coli* c1882 PAAR proteins were found to bind not only to the ends of their endogenous VgrG proteins but also to the non-mutated wild-type end of the gp5 β-helix as well.

The gp5(c1883)–c1882 and gp5(VCA0018)–VCA0105 complexes were purified to

	gp5(VCA0018)–VCA0105	gp5(c1883)–c1882
Data collection		
Space group	$P4_222$	$P6_122$
Cell dimensions		
a, *b*, *c* (Å)	113.7, 113.7, 76.9	187.16, 187.16, 238.89
α, *β*, *γ* (°)	90.0, 90.0, 90.0	90.0, 90.0, 120.0
Resolution (Å)	80.4 – 1.9 (2.0 – 1.9)*	48.6 – 3.4 (3.6 – 3.4)*
R_{meas}	0.06 (0.37)	0.15 (1.01)
$I/\sigma I$	20.0 (4.9)	12.6 (2.1)
Completeness (%)	99.9 (99.3)	99.8 (98.9)
Redundancy	6.9 (7.0)	7.0 (6.7)
Refinement		
Resolution (Å)	80.4 – 1.9	48.6 – 3.4
No. reflections	40054	33366
R_{work} / R_{free}	0.16 / 0.21	0.18 / 0.24
No. atoms		
Protein	2880	10848
Ligand/ion	60	11
Water	453	49
B-factors		
Protein	39.4	163.1
Ligand/ion	63.3	173.7
Water	49.3	122.4
R.m.s deviations		
Bond lengths (Å)	0.007	0.002
Bond angles (°)	0.995	1.039

Figure 3.2 Crystallographic data collection and refinement statistics. Both data sets were collected using a single crystal. *Highest resolution shell is shown in parentheses.

homogeneity and crystallized (Figure 3.2). The structures were solved by molecular replacement (Rossmann and Blow, 1962) using the corresponding gp5 β-helix fragment as a search model (Kanamaru et al., 2002). In both complexes, a single chain of the PAAR protein folds into a symmetrical cone-shaped structure with a sharp tip and a triangular base fully occupying the blunt end of the β-helix (Figure 3.3). The cone contains nine short β-strands, three of which

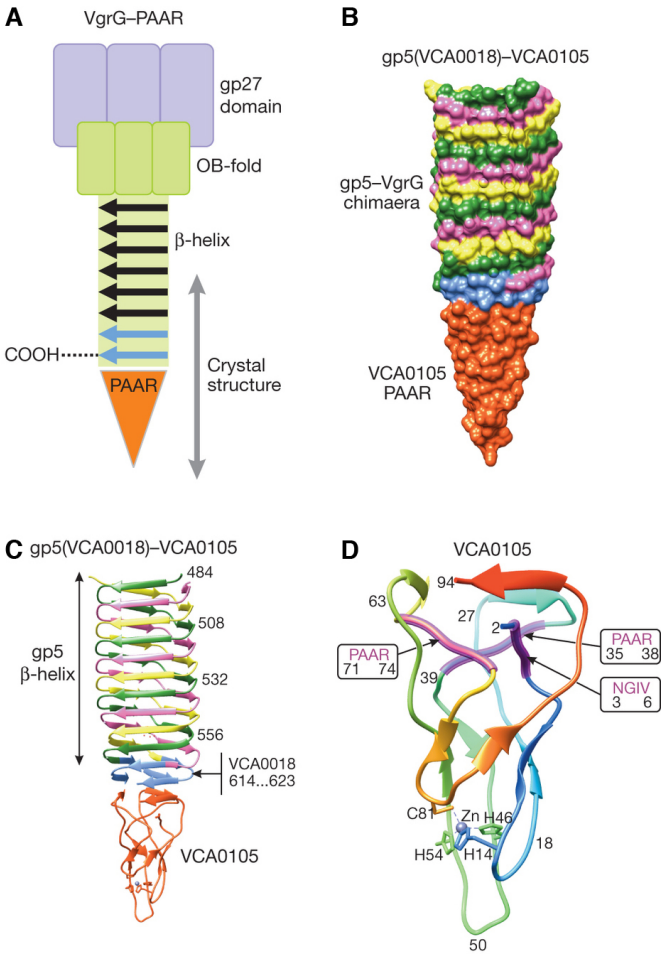

Figure 3.3 Crystal structure of the VCA0105 PAAR-repeat protein bound to its VgrG-like partner. (**A**) Schematic representation of the conserved domains comprising the VgrG–PAAR complex. The last strands of the β-helix that form the PAAR binding site are in light blue. The grey arrow shows the fragment roughly corresponding to the crystal structure. (**B**) Molecular surface representation of the gp5(VCA0018)–VCA0105 complex crystal structure. Each protein chain is labeled with its own color. (**C**) Ribbon diagram of the gp5(VCA0018)–VCA0105 complex. (**D**) The polypeptide chain of the VCA0105 PAAR protein is colored in rainbow colors with the N terminus in blue and C terminus in red. Residues responsible for Zn binding are labeled. PAAR motifs are highlighted with thick purple coils. The sequence and residue numbers of the starting and ending position for each of the three PAAR motifs are boxed.

create its base and participate in binding to the VgrG β-helix and six others form three β-hairpins that point towards the vertex of the cone, but have different lengths. The PAAR proteins interact with the VgrG β-helix by means of a virtually flat hydrophobic patch and 14 or 16 hydrogen bonds for c1882 or VCA0105, respectively (Figure 3.4). In both proteins, 12 hydrogen bonds between the main chain atoms of the VgrG β-helix and those of the PAAR domain form a perfect

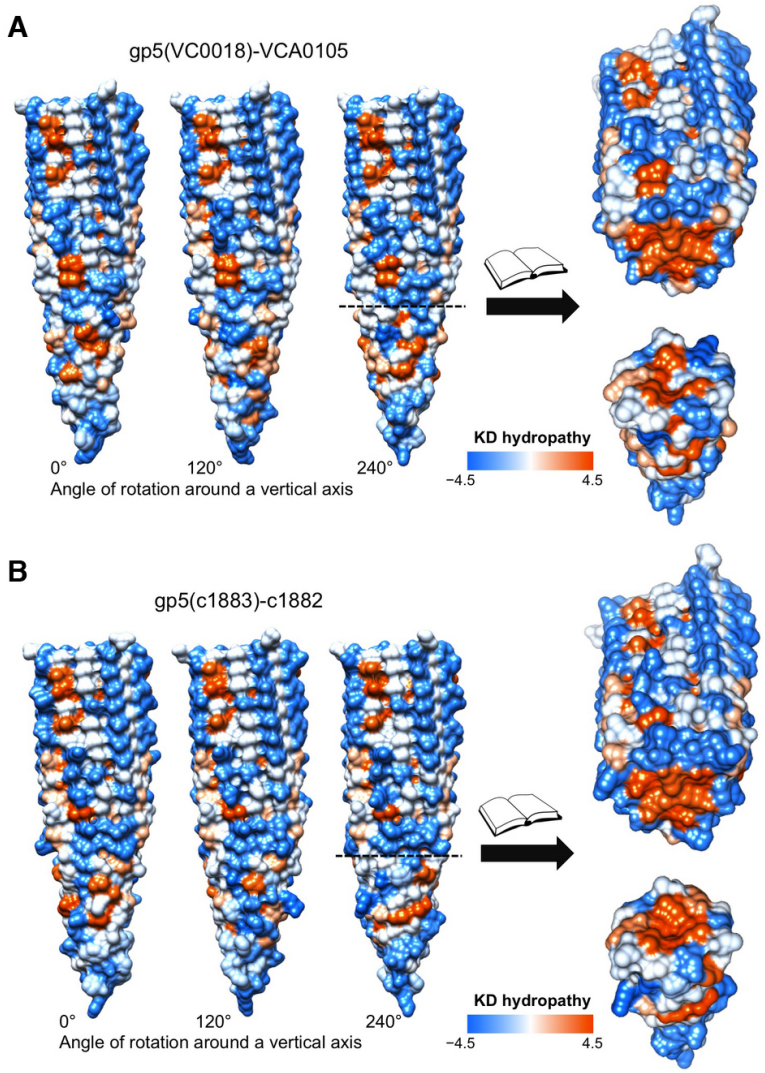

Figure 3.4 Surface features of gp5(VgrG)–PAAR complexes and VgrG–PAAR interface. (**A** and **B**) Molecular surfaces are colored according to their hydrophobicity with sky blue, white, and orange corresponding to the most hydrophilic, neutral and hydrophobic patches, respectively. Residue hydrophobicity values are according to the Kyte-Doolittle scale (Kyte and Doolittle, 1982), which is given as a colored bar labeled 'KD hydropathy'. Three orientations of the gp5(VgrG)–PAAR complex and an 'open book' view of the VgrG–PAAR interface are shown for both PAAR proteins.

triangle surrounding the central hydrophobic patch creating a unique binding platform (Figure 3.5). PISA software (Krissinel and Henrick, 2007) shows that ~16.5% of the PAAR protein surface is buried in this interface and the free energy of interaction between the VgrG tip and c1882 or VCA0105 PAAR proteins is -5.5 kcal/mol or -3.4 kcal/mol, respectively.

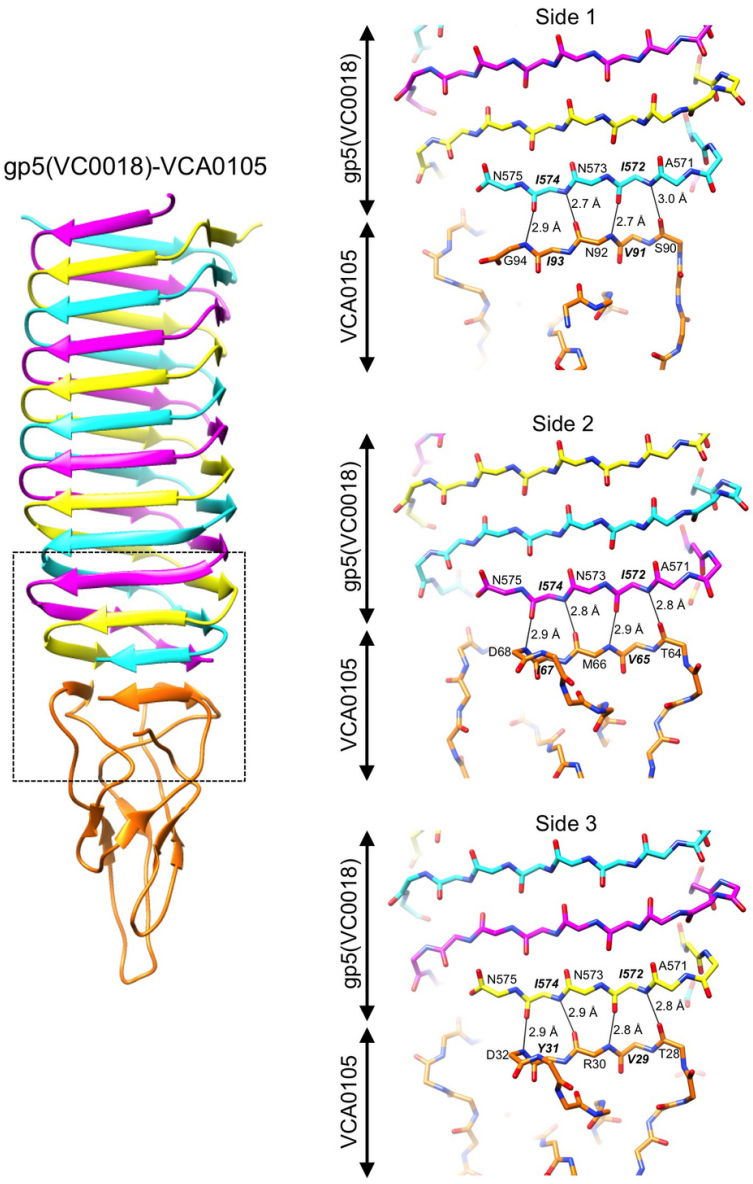

Figure 3.5 Main chain hydrogen-bonding network of VgrG–PAAR interface. The dashed line rectangle in the left panel indicates the area shown enlarged in the panels on the right. The three right panels show the main chain hydrogen bonds between VgrG and PAAR proteins for three different sides of the gp5(VgrG)–PAAR complex. Residues with side chains pointing inwards and forming the VgrG–PAAR hydrophobic interface are in bold italic. Side chains are not shown for clarity. The carbon atoms of the PAAR protein are colored orange.

The fold of the PAAR protein is stabilized by a zinc atom positioned close to the vertex of the cone (Figure 3.3D). The Zn binding site consists of three histidines and one cysteine – H14, H46, H54 and C81 in VCA0105 — that are well conserved in close homologues (Figure 3.6A). These residues are replaced with similar or complementary metal-binding residues (arginines, lysines and glutamines) in more distant homologues suggesting that they also carry a metal ion at roughly the same position. The metal ion, being a natural ligand for this site,

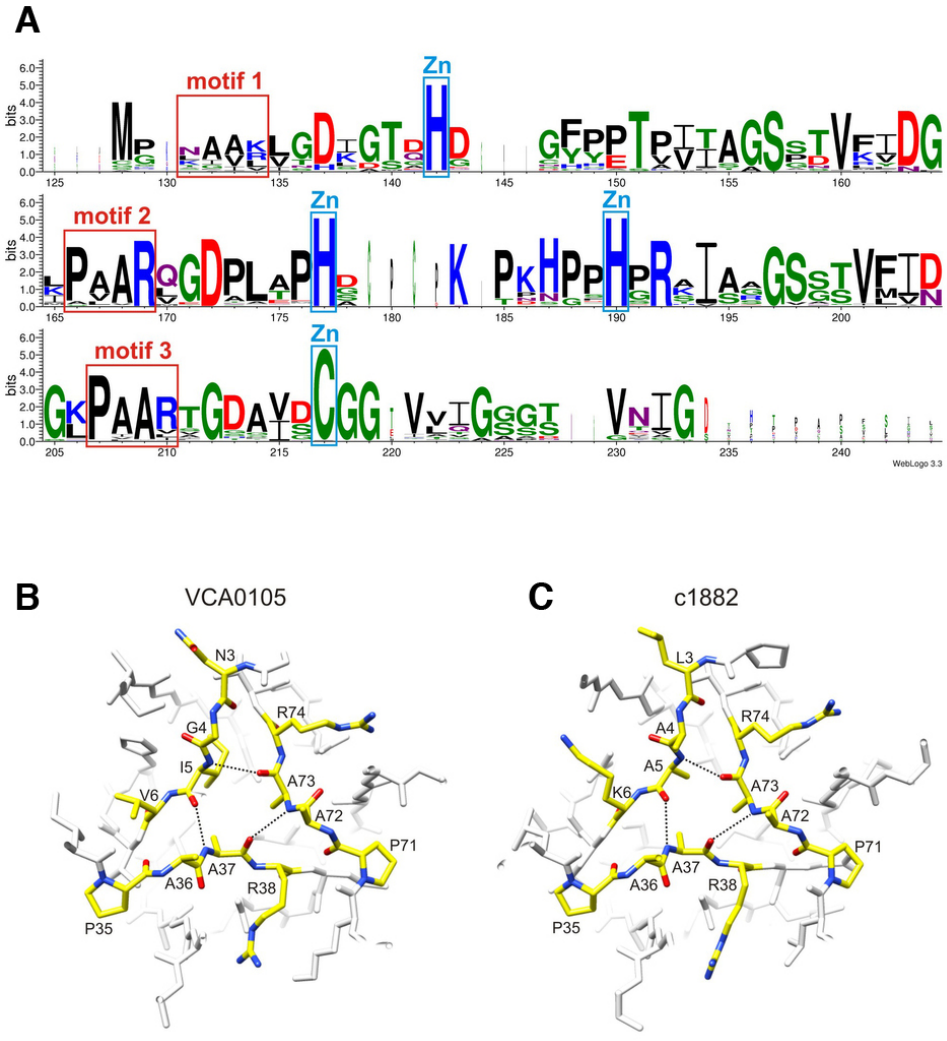

Figure 3.6 Conserved features of PAAR proteins. (**A**) WebLogo (Crooks et al., 2004) sequence alignment of VCA0105 homologues identified with BLAST (Altschul et al., 1990). The conserved PAAR motif and residues forming the Zn binding site are labeled. (**B** and **C**) Pseudotrimeric organization of the three interacting PAAR motifs in VCA0105 and c1882, respectively. The buried hydrogen bonds stabilizing the fold are shown with dashed lines.

stabilizes the pointed tip of the PAAR domain and is likely to be important for its integrity during penetration of the target cell envelope.

The PAAR motif sequence is also conserved, albeit to a lower degree than the Zn binding site (Figure 3.6A). The PAAR motifs function to stabilize the fold by forming the central part of the structure where the three regions of the polypeptide chain containing the PAAR motif meet and intertwine (Figure 3.3, 3.6B, C). Hydrophobic interactions and buried main chain hydrogen bonds mediate the interaction of the three PAAR motifs. (Figure 3.6B, C). The distance between the C_α atoms of the third residue of the three PAAR motifs in both proteins is only 5.3 ± 0.1 Å (Figure 3.6B, C). c1882 and VCA0105 show 61.3% sequence identity and as a consequence the two structures are very similar with a root mean square deviation (r.m.s.d.) of 0.53 Å between all 94 C_α atoms comprising the backbone (Figure 3.7).

Given such a critical location of PAAR proteins within the T6SS organelle and their high structural conservation, we speculated that inactivation of PAAR genes would likely interfere

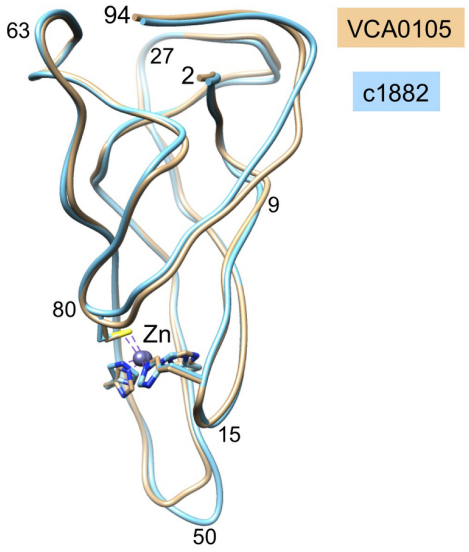

Figure 3.7 Superposition of VCA0105 and c1882 PAAR structures. Residue numbers are given at strategic positions. Note that the N- and C-termini are exposed and can be extended without disrupting the PAAR-VgrG interaction surface or the overall sharp conical structure.

with T6SS functions including protein secretion and prey cell killing. Because some T6SS$^+$ organisms have many gene products predicted to carry the PAAR motif, we focused on *Vibrio cholerae* strain 2740-80 and *Acinetobacter baylyi* ADP1, which each encode only two and three PAAR proteins, respectively. In *A. baylyi* inactivation of all three PAAR genes (*aciad0051*, *aciad0052*, *aciad2681*) led to an ~90% reduction in Hcp secretion (Figure 3.8C, D) and at least a 10,000-fold decrease in T6SS-dependent killing of E. coli (Figure 3.8A). Similarly, inactivation of both genes encoding PAAR proteins in *V. cholerae* 2740-80 (*vca0105* and *vca0284*) resulted in a ~100-fold decrease in T6SS-dependent killing of *E. coli* (Figure 3.8B) and ~70% reduction in Hcp secretion (Figure 3.8C, D). Notably, in both bacterial species, mutants inactivated in single PAAR genes showed no or only a modest defect in the functionality of their respective T6SS apparatuses indicating that PAAR proteins within a species are interchangeable.

The dramatic reduction in Hcp secretion in the triple PAAR gene knockout mutant of *A. baylyi* suggests that PAAR proteins participate in the assembly of the T6SS complex by either nucleating the folding of VgrG trimers or regulating their incorporation into the T6SS organelle. Similar to the T4 phage system in which mutants lacking gp5 (VgrG orthologue) are tailless (Kikuchi and King, 1975), any disruption in VgrG trimeric assembly probably blocks the assembly of the T6SS organelle. Alternatively, PAAR proteins may be important for another function of the apparatus such as translocation of the VgrG spike through the predator outer membrane during the sheath contraction event.

The PAAR-repeat proteins form a diverse superfamily called CL15808 in the conserved domains (CDD) database (Marchler-Bauer et al., 2013) that contains three families PF05488, COG4104 and PF13665 (or DUF4150). The first two families are similar and describe PAAR domains that are on average ~95 residues long, whereas the PF13665 family is somewhat more

distant and its members typically contain ~130 amino acids. The crystal structures reported here include representatives of the PF05488 family. Hundreds of hypothetical proteins in the database contain PAAR domains that are extended both N- and C-terminally by domains with various

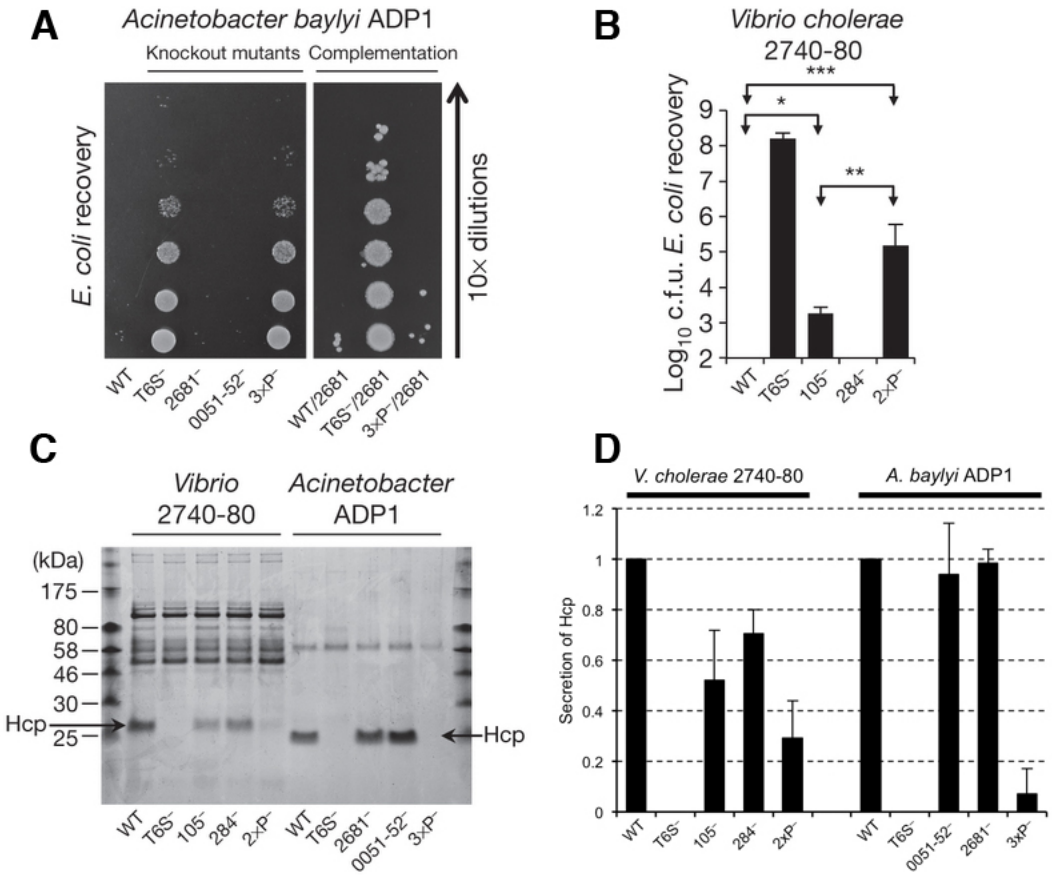

Figure 3.8 PAAR proteins are required for full functionality of the T6SS in *V. cholerae* and *A. baylyi*. (**A**) Recovery of viable *E. coli* MG1655 after co-incubation with *A. baylyi* ADP1 (wild-type, WT) and its T6SS and PAAR genes knockout mutants. The following genes were inactivated in the mutants shown: T6S^{-}, *aciad2688* to *aciad2694*; 2681^{-}, *aciad2681*; 0051-52^{-}, both *aciad0051* and *aciad0052*; 3 × P^{-}, all three PAAR genes *aciad0051*, *aciad0052* and *aciad2681*. Uninduced, basal expression of the *aciad2681* PAAR gene from plasmid pMMB67EH (Furste et al., 1986), labelled as p2681, restores the killing defect in the triple PAAR mutant (right panel). (**B**) Recovery of *E. coli* MG1655 colony forming units (c.f.u.) after co-incubation with *V. cholerae* 2740-80 and its T6SS and PAAR gene knockout mutants, which are labelled as follows: T6S^{-}, *vipA*; 105^{-}, *vca0105*; 284^{-}, *vca0284*; 2 × P^{-}, *vca0105* and *vca0284*. Symbols *, ** and *** indicate deviations from the wild-type with *P* values of 6×10^{-3}, 8×10^{-3} and 5×10^{-7}, respectively, for a sample size of 8. Error bars represent one standard deviation. (**C**) SDS–PAGE for T6SS-dependent secretion of Hcp proteins by the parental strains and T6SS and PAAR genes knockout mutants. Panels **A** and **C** show one out of three experiments with similar outcomes. (**D**) Hcp secretion was evaluated by quantifying the intensity of the Hcp bands in **C** using the Fiji (Schindelin et al., 2012) software and normalizing it to the wild-type. The presented data are the average of three experiments. Error bars correspond to one standard deviation.

predicted functions (Figure 3.9). The crystal structure shows that the termini of the PAAR domain are open to solution and thus can be extended without distorting the VgrG binding site (Figure 3.3, 3.7).

The C-terminal domains of many hypothetical PAAR proteins are predicted to have various enzymatic activities that are toxic for prokaryotic and eukaryotic cells (Figure 3.9). Very similar putative effector domains can be found fused to the C termini of VgrG proteins (for example, VIP2 ADP-ribosyl transferase). Binding of these larger PAAR proteins to the tip of

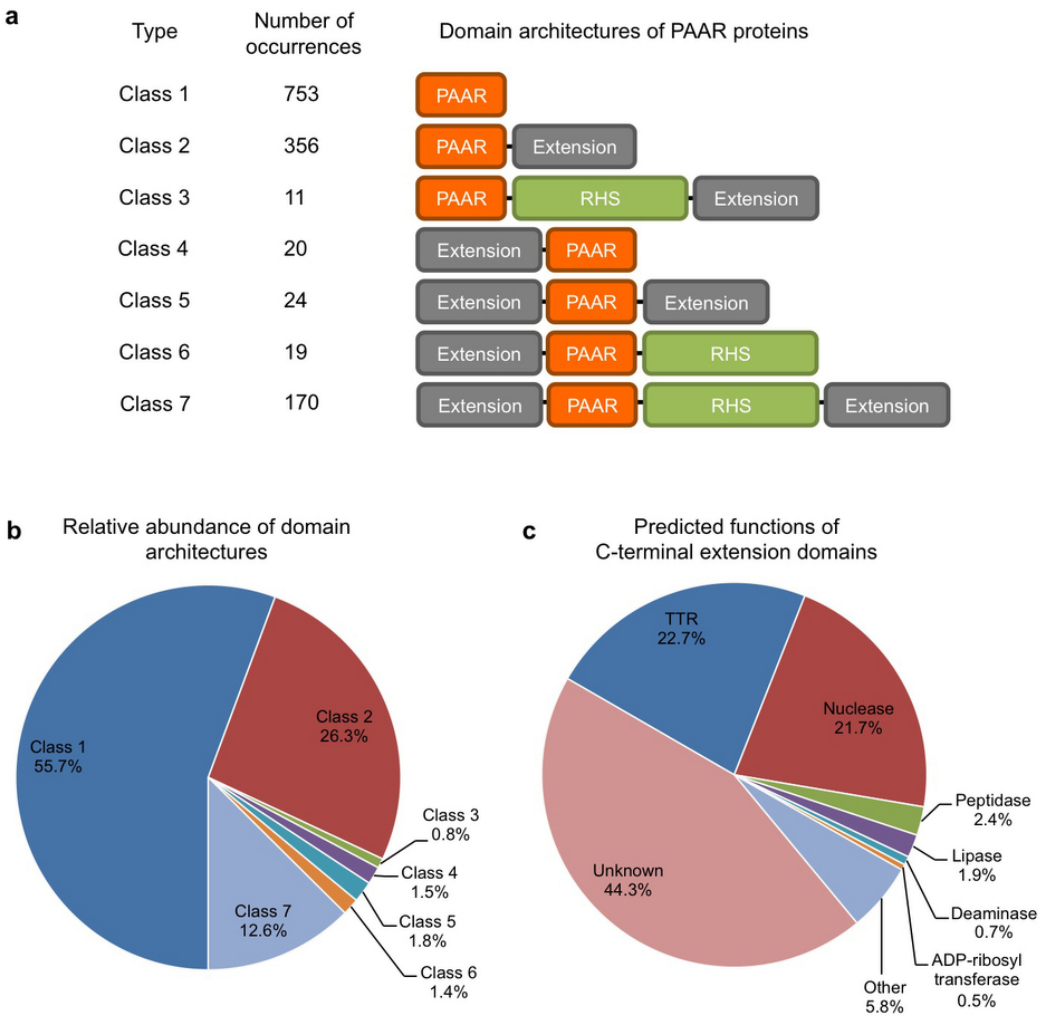

Figure 3.9 Bioinformatic analysis of PAAR proteins. (**A**) Domain organization of all identifiable bacterial (non-phage) PAAR proteins present in sequenced genomes. Extension domains are defined as sequences of 50 or more residues beyond the PAAR motif. (**B**) Relative abundance of the seven distinct domain organizations. (**C**) Predicted functions of the C-terminal domains. TTR stands for transthyretin-like domains.

VgrG spikes would decorate the T6SS spike with a great variety of effector domains. To test this hypothesis, we expressed a VSV-G epitope-tagged version of the ACIAD2681 PAAR protein in the wild-type *A. baylyi* ADP1 and in its triple PAAR gene knockout mutant (Figure 3.10). The epitope-tagged protein was secreted by T6SS and fully restored T6SS-mediated killing of E. coli in the triple PAAR gene knockout strain (Figure 3.8A, 3.10), suggesting that other effector proteins fused to PAAR domains will probably also be targeted for secretion by binding the tip of VgrG trimers.

VCA0284, the larger of the two *V. cholerae* V52 PAAR proteins, carries a partial transthyretin domain (TTR) at its C terminus, which is a very common architecture of PAAR proteins (Figure 3.9). TTR is an immunoglobulin-like domain that is known to form oligomeric structures in which these domains interact with each other or with other partners (Hamburger et al., 1999). Thus, PAAR-associated TTR domains may act as adapters to further decorate the VgrG tip with effectors displaying TTR domains or serve to bind the spike to other TTR domain-containing proteins such as the TssJ/SciN lipoprotein (Felisberto-Rodrigues et al., 2011), an

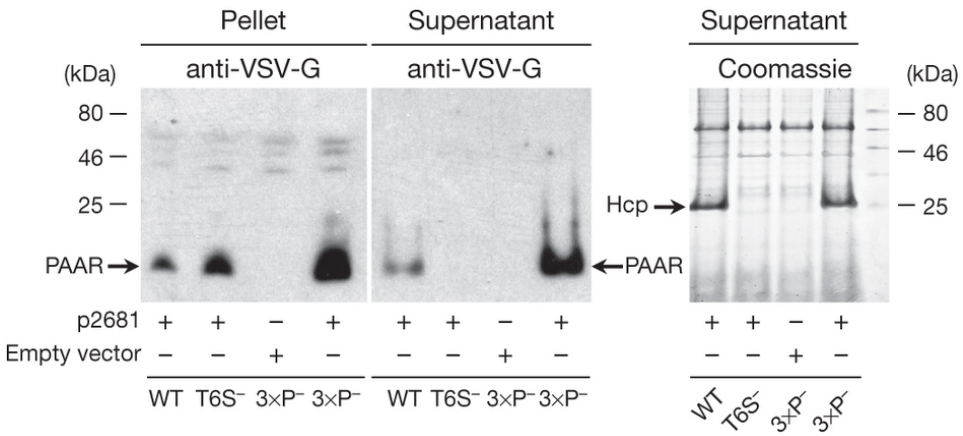

Figure 3.10 The VSV-G epitope-tagged PAAR protein ACIAD2681 is secreted by *A. baylyi* ADP1. T6SS-dependent secretion of VSV-G epitope-tagged ACIAD2681 expressed from plasmid pMMB67EH (left panels). VSV-G epitope-tagged ACIAD2681 fully restores the Hcp secretion defect of the triple knockout PAAR mutant of *A. baylyi* ADP1 (right panel). The mutants are labeled as in Figure 3.8. A representative of three identical experiments was chosen for each panel.

outer membrane structural component of the T6SS 'baseplate' (Basler et al., 2012).

Besides being in T6SS gene clusters, many PAAR genes are frequently found downstream of vgrG genes (Pukatzki et al., 2007), which in turn, often encode Rhs elements (accessory sequences that have the hallmarks of horizontally acquired DNA, Figure 3.9). A recent report (Koskiniemi et al., 2013) shows that two different nucleases encoded by the *rhsA* and *rhsB* genes of *Dickeya dadantii* are delivered into target cells in a VgrG-dependent process, suggesting that the T6SS locus of this organism mediates translocation of these effectors. Interestingly, both RhsA and RhsB proteins contain PAAR repeat regions and other features that categorize them as Class 7 PAAR domain architecture proteins (Figure 3.9A). Thus, our working model (Figure 3.11) predicts that these T6SS nuclease effectors should bind to the tip of VgrG trimers through their PAAR repeat domains and in this way be targeted for secretion and translocation into prey cells.

The structural, functional and bioinformatic findings summarized above allow us to make several conclusions and predictions. Because a PAAR-repeat protein caps the end of the β-helix of a VgrG spike, it is in fact the piercing tip that is responsible for the initial event of creating an opening in the target cell envelope. Furthermore, because the crystal structure demonstrates that the canonical PAAR-repeat domain can be extended N- or C-terminally without distorting its structure or its VgrG β-helix binding site, we predict that large PAAR proteins carrying effector domains will probably also bind to VgrG spikes and be translocated into target cells by the T6SS organelle. Considering the findings reported here and other published data, we propose that there are five mechanisms by which effectors can be incorporated into the T6SS spike complex (Figure 3.11). Three of them are supported by direct or indirect experimental evidence: 1) C-terminal extensions of the VgrG spike (Pukatzki et al., 2007), 2) binding surface features on the

VgrG protein (Dong et al., 2013; Hachani et al., 2011), and 3) N- or C-terminal extensions of the PAAR protein (Koskiniemi et al., 2013). Two others remain speculative: 4) binding surface features or additional domains (for example, the TTR domain) on PAAR proteins and 5) incorporation into the cavity formed by the gp27 domain of VgrG. Thus, the T6SS machine may be capable of delivering a multifunctional 'cargo' or multiple effector translocation VgrG (MERV) spike into the target prey cell in a single molecular translocation event driven by T6SS sheath contraction.

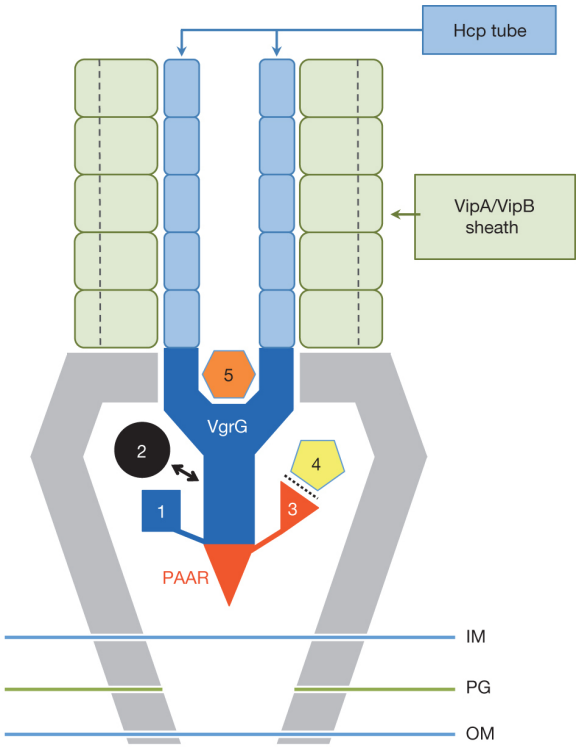

Figure 3.11 Multiple effector translocation VgrG (MERV) model for the organization of the T6SS central spike/baseplate. Effectors are predicted to be loaded onto the spike complex by five distinct mechanisms: 1) C-terminal extensions of the VgrG spike; 2) non-covalent binding to the VgrG spike; 3) N- or C-terminal extensions of the PAAR protein; 4) non-covalent binding to the PAAR protein or its extension domains; 5) incorporation into the cavity formed by the gp27 domain of VgrG. A single T6SS sheath contraction event translocates the VgrG spike with all of its cargo proteins into a nearby target cell. Other proteins making up the T6SS 'baseplate' (grey colour) are not labelled but presumably reside within or attached to the inner and outer membranes and peptidoglycan layer (IM, OM, and PG, respectively).

Materials and Methods

Structure determination of gp5(VgrG)–PAAR complexes. The gp5 fragment containing residues 484–575 and its variants with modified C termini mimicking VgrG were cloned into a derivative of the pET-23a expression vector (Novagen) with a TEV-cleavable N-terminal polyhistidine tag. For expression in cis, PAAR genes were cloned downstream from the gp5 fragment with a spacer containing the AGGAGG ribosome-binding site. For expression in trans, PAAR genes were cloned into a modified pACYCDuet-1 expression vector (Novagen), retaining its wild-type N- and C-termini. The complexes were purified by metal-affinity, ion exchange and size exclusion chromatographies. Conditions yielding diffraction quality crystals were refined from the initial hits obtained with the help of commercial crystallization screens (Jena Bioscience). The structures were solved by molecular replacement with the help of PHASER19 using the corresponding fragment of the gp5 β-helix as a search model (Protein Data Bank (PDB) accession ID number 1K28) (Kanamaru et al., 2002). Crystallographic refinement was performed with PHENIX (Adams et al., 2011), REFMAC5 (Murshudov et al., 2011) and COOT (Emsley et al., 2010).

Bioinformatics. Putative orthologs of PAAR repeat proteins were identified with the help of HMMER (Finn et al., 2011). A search for high confidence hits to PFAM (Punta et al., 2012) domains PF05488 or PF13665 that describe the two distinct PAAR repeat domains resulted in 1353 PAAR domain-containing proteins. Phage proteins and orphan genes were excluded from this analysis. Functional assignment of extension domains was based on high confidence hits obtained with the help HHpred (Soding et al., 2005), HMMER (Finn et al., 2011), CDD (Marchler-Bauer et al., 2013) and CDART (Geer et al., 2002) web services.

Bacterial killing assays. Bacterial competitions and statistical analysis involving

V. cholerae 2740-80, *A. baylyi* ADP1 and *E. coli* MG1655 were performed as described previously (Basler et al., 2013). The plasmid pMMB67EH was used for VSV-G-tagging and expression of ACIAD2681 (Furste et al., 1986). Two-tailed Student's t-test was used to interpret the statistical significance of the number of the colony forming units.

Protein secretion. Protein supernatants were analyzed as described previously (Basler et al., 2012). Overnight cultures of *V. cholerae* 2740-80 and *A. baylyi* ADP1 were washed in LB and diluted 200 fold into fresh LB and cultivated for 5 h at 37 C. One ml of culture supernatant was passed through a 0.2-mM filter, precipitated with TCA, subjected to 12% SDS-PAGE and stained with Coomassie blue. The recombinantly expressed ACIAD2681 PAAR protein carried a C-terminal VSV-G epitope tag. Western blots were performed on the TCA precipitated samples following standard methodology using anti-VSV-G primary antibodies (Sigma). Band intensities were quantified using Fiji software (Schindelin et al., 2012).

Molecular graphics. UCSF Chimera (Pettersen et al., 2004) was used to prepare Figures 3.3-3.7.

Chapter 4. Tit-for-tat: type VI secretion system counterattack during bacterial cell-cell interactions

The bacterial type VI secretion system (T6SS) is a dynamic organelle that bacteria use to target prey cells for inhibition via translocation of effector proteins. Time-lapse fluorescence microscopy has documented striking dynamics of opposed T6SS organelles in adjacent sister cells of *Pseudomonas aeruginosa*. Such cell-cell interactions have been termed ‘‘T6SS dueling’’ and likely reflect a biological process that is driven by T6SS antibacterial attack. Here, we show that T6SS dueling behavior strongly influences the ability of *P. aeruginosa* to prey upon heterologous bacterial species. We show that, in the case of *P. aeruginosa*, T6SS- dependent killing of either *Vibrio cholerae* or *Acinetobacter baylyi* is greatly stimulated by T6SS activity occurring in those prey species. Our data suggest that, in *P. aeruginosa*, T6SS organelle assembly and lethal counterattack are regulated by a signal that corresponds to the point of attack of the T6SS apparatus elaborated by a second aggressive $T6SS^{+}$ bacterial cell.

Foreword

A version of this chapter was published in *Cell* on February 14, 2013. The article can be found on the web at the following URL:

http://dx.doi.org/10.1016/j.cell.2013.01.042

The full citation for this work is:

> Basler, M., Ho, B.T., and Mekalanos, J.J. (2013). Tit-for-Tat: Type VI Secretion System Counterattack during Bacterial Cell-Cell Interactions. Cell *152*, 884-894.

This work was a collaborative effort between Dr. Marek Basler and myself. Dr. Basler made the initial observation of T6SS dueling and performed the microscopy analysis (Figures 4.1, 4.3, and 4.4) with help from me with the quantification presented (Tables 4.1, 4.2 and Figure 4.4) that revealed T6SS counterattacks, while my efforts were focused on the quantitative bacterial killing assays (Figure 4.2, 4.3, 4.5, and 4.6) with Dr. Basler helping with some of the experimental replicates. Dr. Basler generated the *Pseudomonas aeruginosa* mutants used in this study that did not already exist in the laboratory collection. Data figures were organized and formatted by Dr. Basler, while I generated the model figure. I would like to thank Professor Mekalanos for considerable help in the editing and revision process.

I would also like to thank Casey Gifford for constructing pEXG2-ΔtagT plasmid used to make the *tagT* mutants used in this work. I would like to also thank Russell Vance and Stephen Lory for helpful discussions and Tom Bernhardt and David Rudner for access to microscopic resources and tips for optimal use. This work was supported by NIAID grants AI-018045 and AI-26289 to John J. Mekalanos.

Introduction

The ecological interactions between bacterial species range from cooperative (e.g., mutualism and commensalism) to competitive (e.g., parasitism and predation). Contact-dependent, cooperative interactions involving adherence and nutrient scavenging within biofilms have been demonstrated (Kolenbrander et al., 2010; Peters et al., 2012). Several types of contact-dependent, antagonistic interactions have also been described. For example, contact-dependent growth inhibition (CDI) in *Escherichia coli* involves the interaction of outer-membrane protein CdiA on cdi^+ cells with BamA receptors on cdi^- target cells, a process that triggers growth inhibition when cdi^- cells lack the cognate immunity protein CdiI (Aoki et al., 2008; Aoki et al., 2005; Aoki et al., 2009). *Proteus mirabilis* strains display a self- versus nonself- discrimination that has been recently genetically defined but is not well understood mechanistically (Gibbs et al., 2008; Gibbs et al., 2011).

One of the most widely distributed examples of contact-dependent antagonistic behavior involves the type VI secretion system (T6SS) (Pukatzki et al., 2006). This secretion system is functionally analogous to a bacteriophage tail and corresponds to a dynamic organelle located in the cytosol and attached to the cell envelope by a base plate structure (Basler et al., 2012; Leiman et al., 2009; Pukatzki et al., 2007). The T6SS apparatus can power secretion of proteins between cells by utilizing a contractile phage sheath-like structure (Basler et al., 2012; Bonemann et al., 2009; Leiman et al., 2009). "T6SS activity" (i.e., T6SS sheath extension, contraction, and disassembly cycles) can be readily visualized by time-lapse microscopy utilizing fluorescent fusion proteins to orthologs of either of two *Vibrio cholerae* T6SS gene products, VipA or ClpV (Basler and Mekalanos, 2012; Basler et al., 2012). This dynamic activity leads to the translocation of proteins that comprise the T6SS spike/tube complex, VgrG and Hcp, out of

the cell (Basler et al., 2012; Leiman et al., 2009).

Approximately 25% of all sequenced Gram-negative bacteria, including members of the genera *Vibrio*, *Pseudomonas*, and *Acinetobacter*, encode T6SS gene clusters (Boyer et al., 2009). In several of these species, T6SS has been associated with either antagonistic (Hood et al., 2010; Schwarz et al., 2010b) or outright bacteriocidal (Chou et al., 2012; MacIntyre et al., 2010; Murdoch et al., 2011; Zheng et al., 2011) activity toward heterologous bacterial species. For example, *Pseudomonas aeruginosa* can outcompete *Pseudomonas putida* in mixed culture through the translocation of one or more of three different T6SS effector proteins termed Tse1, Tse2, and Tse3 (Russell et al., 2011). *P. aeruginosa* sister cells avoid inhibiting each other by encoding three immunity proteins, Tsi1, Tsi2, and Tsi3, which bind to and presumably neutralize the activity of their cognate effectors (Ding et al., 2012; Li et al., 2012). However, despite having this immunity, P. aeruginosa cells respond to T6SS activity directed at them by adjacent sister cells with their own T6SS activity (Basler and Mekalanos, 2012). The spatial and temporal coincidence of T6SS activity between adjacent *P. aeruginosa* sister cells suggests that contact-dependent protein translocation produces a signal that triggers T6SS activity in the adjacent cell. The dynamic T6SS activity that occurs between pairs of interacting cells was termed "T6SS dueling" and was proposed to reflect a biologically significant process that occurred between heterologous T6SS$^+$ species (Basler and Mekalanos, 2012).

In order to characterize the contact-dependent signal that triggers T6SS dueling behavior, we have explored the ability of P. aeruginosa to prey upon T6SS$^+$ and T6SS$^-$ *V. cholerae* and *Acinetobacter baylyi*. We found that *P. aeruginosa* does not efficiently kill T6SS$^-$ *V. cholerae* or T6SS$^-$ *A. baylyi* but readily attacks these species if they express a functional T6SS. The TagQRST-PpkA-Fha1-PppA regulatory system is essential for *P. aeruginosa* T6SS dueling and

prey selection, indicating that it is likely responsible for sensing a T6SS-mediated attack on *P. aeruginosa* cells by heterologous T6SS$^+$ predatory species. These results provide evidence for a bacterial "tit-for-tat" evolutionary strategy that controls the social interaction among different bacterial species (Axelrod and Hamilton, 1981).

Results

***P. aeruginosa* specifically targets T6SS$^+$ *V. cholerae* cells for T6SS-mediated counterattack.** Previously, we proposed that T6SS dueling behavior specifically marks the location of T6SS effector delivery between sister cells of *P. aeruginosa* (Basler and Mekalanos, 2012). We first considered the possibility that the penetration of the outer membrane by the T6SS spike/tube complex injected by sister cells triggers the T6SS dueling response. Because the VgrG and Hcp proteins that comprise this complex are highly conserved among different bacterial species (Leiman et al., 2009), we hypothesized that the T6SS spike/tube complex of heterologous organisms might also induce a T6SS dueling response in *P. aeruginosa*. *V. cholerae* has been reported to effectively kill *E. coli* using its T6SS (MacIntyre et al., 2010; Zheng et al., 2011), and its T6SS apparatus has been structurally characterized (Basler et al., 2012). Thus, the T6SS from *V. cholerae* was a logical candidate for testing this hypothesis.

To determine whether *V. cholerae* T6SS could induce T6SS activity in *P. aeruginosa*, we observed mixtures of *P. aeruginosa* PAO1 with *V. cholerae* 2740-80 by time-lapse fluorescence microscopy. As in previous studies, we used *retS* derivatives of *P. aeruginosa* that are known to overexpress the H1-T6SS locus at the transcriptional level (Basler and Mekalanos, 2012; Mougous et al., 2006). T6SS activity was monitored with ClpV1-GFP and ClpV-mCherry2 fusion proteins in *P. aeruginosa* and *V. cholerae*, respectively. This experiment revealed that

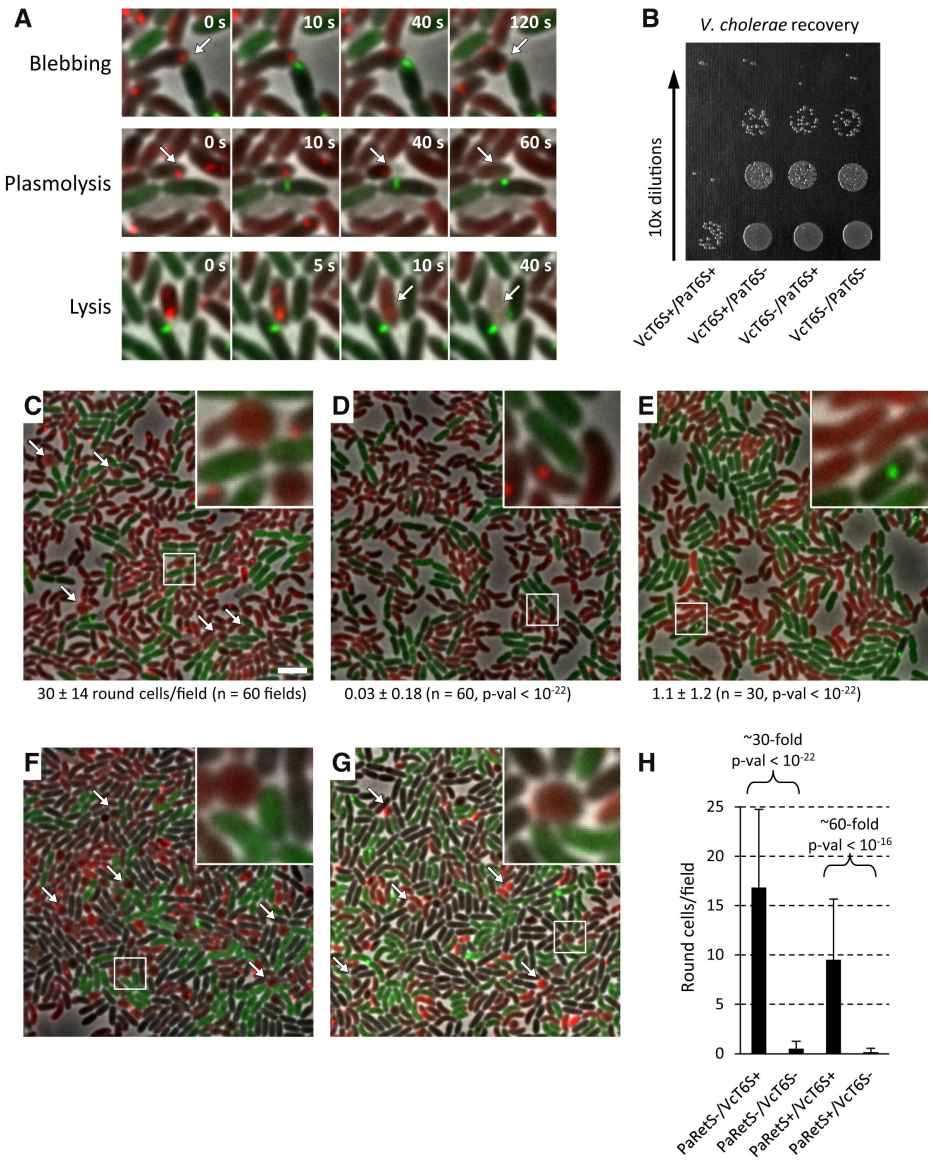

Figure 4.1 *P. aeruginosa* T6SS preferentially targets T6SS$^+$ *V. cholerae*. VcT6S$^+$ indicates *V. cholerae clpV-mCherry2*, VcT6S$^-$ indicates *V. cholerae ΔvipA clpV-mCherry2*, PaT6S$^+$ indicates *P. aeruginosa ΔretS clpV1-gfp*, and PaT6S$^-$ indicates *P. aeruginosa ΔretS ΔvipA1 clpV1-gfp*. PaRetS$^-$ indicates *P. aeruginosa ΔretS*, and PaRetS$^+$ indicates *P. aeruginosa*. (**A**) Examples of morphological changes of *V. cholerae* seen in mixtures of *P. aeruginosa ΔretS clpV1-gfp* (T6SS$^+$, green) and *V. cholerae clpV-mCherry2* (T6SS$^+$, red). 4.5 × 4.5 μm fields are shown. (**B**) Example of a dilution series used to enumerate *V. cholerae* recovery from a competition with *P. aeruginosa*. (**C**–**G**) 30 × 30 μm representative field of cells with a 4× magnified 3 × 3 μm inset (marked by box). Bar in (**C**) is 3 μm and applies to (**C**)–(**G**). Arrows point to examples of round *V. cholerae* cells. (**C**–**E**) Average number of round *V. cholerae* cells per 30 × 30 μm field (±SD) is shown for each mixture (n fields were analyzed); p value compared to mixture in (**C**). (**C**) *P. aeruginosa ΔretS clpV1-gfp* (T6SS$^+$, green) mixed with *V. cholerae clpV-mCherry2* (T6SS$^+$, red). (**D**) *P. aeruginosa ΔretS ΔvipA1 clpV1-gfp* (T6SS$^-$, green) mixed with *V. cholerae clpV-mCherry2* (T6SS$^+$, red). (**E**) *P. aeruginosa ΔretS clpV1-gfp* (T6SS$^+$, green) mixed with *V. cholerae ΔvipA clpV-mCherry2* (T6SS$^-$, red). (**F** and **G**) *V. cholerae clpV-mCherry2* (T6SS$^+$, red) and *V. cholerae ΔvipA clpV-gfp* (T6SS$^-$, green) strains were mixed at equal ratios with (**F**) *P. aeruginosa ΔretS* (T6SS$^+$, unlabeled) and (**G**) *P. aeruginosa* (T6SS$^+$, unlabeled). (**H**) Quantification of number of round *V. cholerae* cells detected per 30 × 30 μm field (n = 60) for mixtures shown in (**F**) and (**G**). See also Movies S4.1 and S4.2 and Tables 4.1 and 4.2.

P. aeruginosa induced striking morphological changes in *V. cholerae* cells that could be differentiated into categories that include cell rounding, cell blebbing, plasmolysis, and overt lysis (Figure 4.1A and Movies S4.1, S4.2). Rounding of *V. cholerae* cells in these mixtures was dependent on the functionality of H1-T6SS locus of *P. aeruginosa* (Figures 4.1C, D and Table 4.1) and occurred predominantly in *V. cholerae* cells directly contacting *P. aeruginosa* cells. Remarkably, in accordance with our hypothesis that the activity of the T6SS of a heterologous organism might trigger the dueling response of *P. aeruginosa*, rounding of *V. cholerae* cells was virtually absent in mixtures containing T6SS$^-$ *V. cholerae* (Figure 4.1E, Table 4.1, and Movie S4.1).

To ascertain whether preferential rounding of T6SS$^+$ *V. cholerae* under microscopic conditions also reflected preferential killing of T6SS$^+$ cells by *P. aeruginosa*, we performed quantitative competition assays. In agreement with the observed microscopy data, when competed against T6SS$^+$ *P. aeruginosa*, we recovered ~100-fold fewer surviving T6SS$^+$ *V. cholerae* cells than T6SS$^-$ *V. cholerae* cells (Figure 4.1B). T6SS$^+$ and T6SS$^-$ *P. aeruginosa*

Table 4.1 Counting of round cells in mixtures of *P. aeruginosa* and *V. cholerae*.

P. aeruginosa [a]	*V. cholerae* [b]	Fields [c]	Total round cells	Round cells / field (SD [d])
-	-	60	1795	30 (14)
Δ*vipA1*	-	60	2	0.03 (0.18)
-	Δ*vipA*	30	34	1.1 (1.2)
Δ*pppA*	-	30	79	2.6 (3.4)
Δ*pppA*	Δ*vipA*	30	78	2.6 (2.6)
Δ*ppkA*	-	30	5	0.17 (0.46)
Δ*ppkA*	Δ*vipA*	30	0	0.0 (0.0)
Δ*tagT*	-	30	78	2.6 (2.4)
Δ*tagT*	Δ*vipA*	30	72	2.4 (2.4)
Δ*tse1*	-	30	1	0.03 (0.18)
Δ*tse2*	-	30	1010	34 (15)
Δ*tse3*	-	30	811	27 (11)
Δ*tse1-3*	-	30	1	0.03 (0.18)
-	Tsi1	45	102	2.3 (1.7)

[a] Parental strain is *P. aeruginosa* Δ*retS clpV1-gfp*, additional mutations are indicated.
[b] Parental strain is *V. cholerae clpV-mCherry2*, additional mutations are indicated;"Tsi1" represents *V. cholerae*/pBAD24-Tsi1-mCherry2.
[c] Number of 30 x 30 μm fields of cells (similar to fields shown in Figure 4.1C-E) that were analyzed.
[d] SD – standard deviation

were only marginally inhibited by T6SS$^+$ *V. cholerae*, and thus, the difference seen in prey sensitivity does not reflect a difference in *P. aeruginosa* survival in these quantitative assays (Figure 4.2A). These data suggest that an antibacterial *P. aeruginosa* T6SS dueling response was likely directed specifically at T6SS$^+$ *V. cholerae* cells that had attacked *P. aeruginosa* cells first.

We sought to confirm the target specificity of the *P. aeruginosa* heterologous dueling/antibacterial response and that this induced response did not cause collateral damage to nearby cells that had not attacked the retaliating *P. aeruginosa* cell. Accordingly, we designed a mixture experiment involving three strains that would allow the specificity of the *P. aeruginosa* dueling/antibacterial response to be assessed at the microscopic level. We mixed *P. aeruginosa* with differentially fluorescently labeled T6SS$^+$ (red) and T6SS$^-$ *V. cholerae* (green) and scored the relative proportion of red or green cells that showed rounding in the assay. Strikingly,

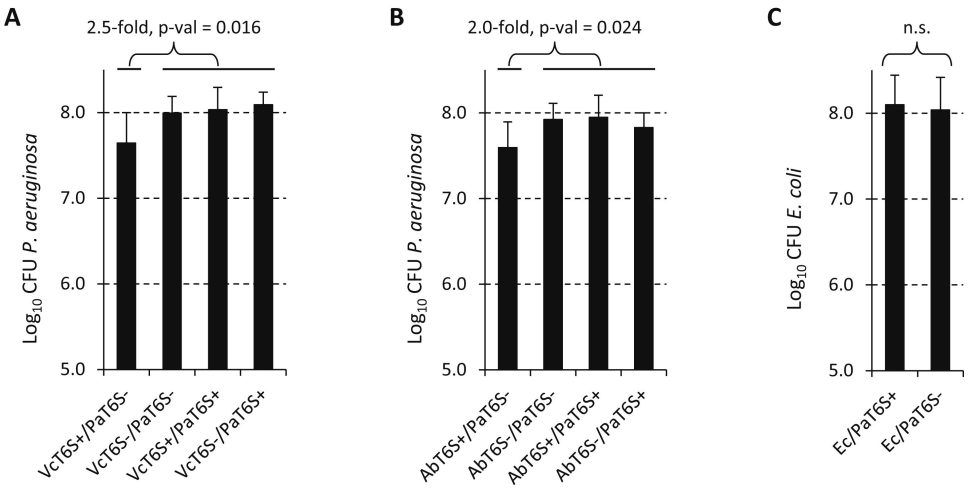

Figure 4.2 *P. aeruginosa* is resistant to T6SS of *V. cholerae* and *A. baylyi* and does not target *E. coli*. PaT6S$^+$ indicates *P. aeruginosa ΔretS clpV1-gfp*, PaT6S$^-$ indicates *P. aeruginosa ΔretS ΔvipA1 clpV1-gfp*. (**A**) Summary of competition assays for *P. aeruginosa* and *V. cholerae* mixtures. Data are presented as mean of Log_{10} CFU of recovered *P. aeruginosa* with error bar representing standard deviation (n = 8). VcT6S$^+$ indicates *V. cholerae clpV-mCherry2*, VcT6S$^-$ indicates *V. cholerae ΔvipA clpV-mCherry2*. (**B**) Summary of competition assays for *P. aeruginosa* and *A. baylyi* mixtures. Data are presented as mean of Log_{10} CFU of recovered *A. baylyi* with error bar representing standard deviation (n = 8). AbT6S$^+$ indicates *A. baylyi* parental strain, AbT6S$^-$ indicates *A. baylyi ΔT6SS*. (**C**) Summary of competition assays for *P. aeruginosa* and *E. coli* mixtures. Data are presented as mean of Log_{10} CFU of recovered *E. coli* with error bar representing standard deviation (n = 15).

Table 4.2 Counting of round cells in three strain mixtures of *P. aeruginosa* and T6SS$^+$/T6SS$^-$ *V. cholerae.*

P. aeruginosa	*V. cholerae*	Fields [a]	Total round cells	Round cells / field (standard deviation)
Δ*retS*	*clpV-mCherry2*	60	1010	16.8 (7.9)
	Δ*vipA clpV-gfp*	60	30	0.50 (0.75)
wild type	*clpV-mCherry2*	60	571	9.5 (6.1)
	Δ*vipA clpV-gfp*	60	9	0.15 (0.40)

[a] Number of 30 x 30 μm fields of cells (similar to fields shown in Figure 4.1F, G) that were analyzed.

V. cholerae cells exhibiting rounded morphologies were predominantly T6SS$^+$, whereas T6SS$^-$ *V. cholerae* cells remained largely unaffected (Figures 4.1F, H, Table 4.2, and Movie S4.1). This selective targeting of T6SS$^+$ *V. cholerae* was also observed in wild-type *P. aeruginosa* PAO1 (Figures 4.1G, H and Table 4.2) and is thus independent of H1-T6SS transcriptional expression level. Collectively, these data suggest that *P. aeruginosa* cells were precisely directing their T6SS-dependent antibacterial activity to specifically target only *V. cholerae* prey cells that had attacked first with their own heterologous T6SS apparatus.

***P. aeruginosa* T6SS delivers Tse1 effector into *V. cholerae* cells, but Tse effectors are dispensable for dueling and *V. cholerae* killing.** When mixed with T6SS$^+$ *P. aeruginosa*, the cell-rounding morphological response of T6SS$^+$ *V. cholerae* was reminiscent of one observed in *E. coli* cells engineered to express the *P. aeruginosa* T6SS effector Tse1 in their periplasm in the absence of the cognate immunity protein Tsi1 (Russell et al., 2011). Therefore, we next asked whether the rounding morphology exhibited by *V. cholerae* could be specifically attributed to Tse1 activity. Although knockouts of tse2 and tse3 in *P. aeruginosa* still caused *V. cholerae* cell rounding, knocking out all three effectors or just *tse1* alone eliminated the cell-rounding activity (Figures 4.3A-D and Table 4.1). Furthermore, expression of Tsi1 (the cognate immunity protein of Tse1) in the periplasm of *V. cholerae* significantly decreased cell rounding when mixed with *P. aeruginosa* (Figure 4.3E and Table 4.1). These data provide clear visual evidence

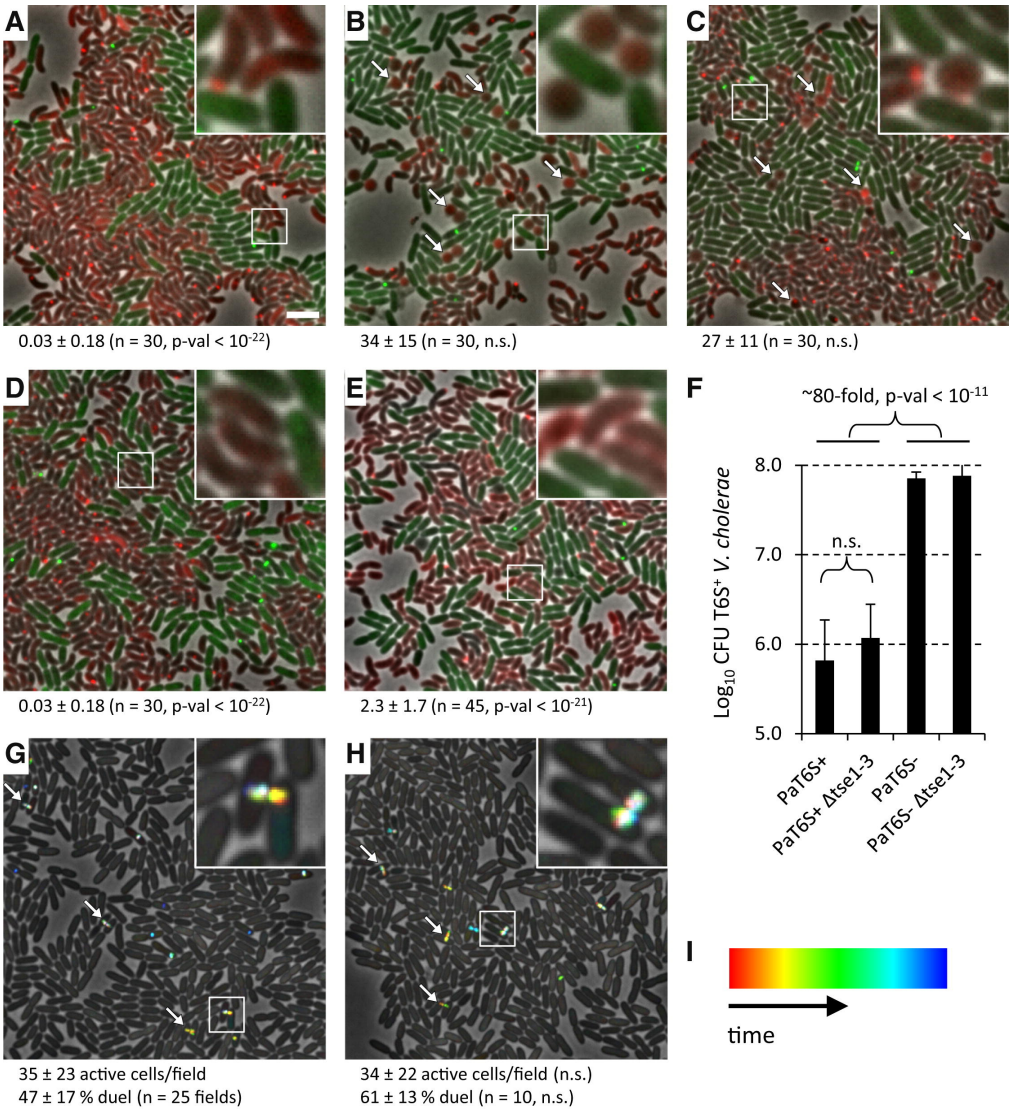

Figure 4.3 *P. aeruginosa* T6SS effector Tse1 is responsible for *V. cholerae* cell rounding, but Tse effectors are dispensable for dueling and *V. cholerae* growth inhibition. 30 × 30 μm representative field of cells with a 4× magnified 3 × 3 μm inset (marked by box) is shown for (**A**)–(**E**), (**G**), and (**H**). Bar in (**A**) is 3 μm and applies to (**A**)–(**E**), (**G**), and (**H**). Strain abbreviations were as used in Figure 4.1. n.s., not statistically significant ($p > 0.01$). (**A**–**E**) Arrows point to examples of round *V. cholerae* cells. Average number of round *V. cholerae* cells per 30 × 30 μm field (±SD) is shown for each mixture (n fields were analyzed); p value is compared to mixture in Figure 1C. For (**A**)–(**D**), *V. cholerae clpV-mCherry2* strain was mixed with (**A**) *P. aeruginosa ΔretS Δtse1 clpV1-gfp*, (**B**) *P. aeruginosa ΔretS Δtse2 clpV1-gfp*, (**C**) *P. aeruginosa ΔretS Δtse3 clpV1-gfp*, and (**D**) *P. aeruginosa ΔretS Δtse1-3 clpV1-gfp*. (**E**) *P. aeruginosa ΔretS clpV1-gfp* was mixed with *V. cholerae*/pBAD24-Tsi1-mCherry2 strain. (**F**) Summary of competition assays for *P. aeruginosa* and *V. cholerae* mixtures. Data are presented as mean of $\log_{10}$ CFU of recovered *V. cholerae* with error bar representing SD (n = 8-19). (**G** and **H**) ClpV1-GFP localization was followed for 3 min and was temporally color-coded. Arrows point to examples of dueling *P. aeruginosa* cells. Average number of active cells and dueling cells per 30 × 30 μm field (±SD) is shown (n fields were analyzed); p-value is compared to strain in (**G**). (**G**) *P. aeruginosa ΔretS clpV1-gfp* and (**H**) *P. aeruginosa ΔretS Δtse1-3 clpV1-gfp*. (**I**) Color scale used to temporally color-code ClpV1-GFP signal. See also Movie S4.3 and Tables 4.1 and 4.3.

(*P. aeruginosa* T6SS-dependent *V. cholerae* cell rounding) of the delivery of a specific T6SS effector (Tse1) into a bacterial target cell by a functional T6SS organelle.

Interestingly, when a competition experiment was performed using a *tse1-3* triple knockout of *P. aeruginosa*, wild-type levels of T6SS-dependent killing were observed (Figure 4.3F). Thus, in the case of *V. cholerae*, even though T6SS-dependent delivery of Tse1 is detected by microscopy, prey cell killing occurs independent of the three known Tse effector proteins of *P. aeruginosa*. Additionally, the *tse1-3* effector knockout strain exhibited dueling activity between sister cells similar to the wild type (Figures 4.3G, H, Movie S4.3, and Table 4.3), indicating that T6SS-mediated translocation of these three Tse effectors into target cells is also not required for the T6SS dueling response.

Inactivation of signaling cascade results in loss of *P. aeruginosa* T6SS dueling. We next sought to define the signaling pathway regulating T6SS dueling and the recognition of homologous or heterologous T6SS attack. The kinase PpkA is known to be required for T6SS function (Mougous et al., 2007). It phosphorylates the essential T6SS apparatus component Fha1, which then associates with the T6SS apparatus visualized with ClpV1-GFP (Mougous et al., 2007). PpkA activity is counteracted by phosphatase PppA, which deactivates the *P. aeruginosa* T6SS apparatus by dephosphorylating Fha1 (Mougous et al., 2007). Moreover, the cell-envelope-associated TagQRST regulatory system controls PpkA phosphorylation of Fha1 (Casabona et al., 2012). Thus, TagQRST-PpkA-Fha1-PppA has been proposed to control assembly or function of the T6SS apparatus posttranscriptionally in response to undefined environmental signals (Casabona et al., 2012; Hsu et al., 2009; Mougous et al., 2007; Silverman et al., 2011). However, this posttranslational regulatory loop has not been previously evaluated for its effect on the dynamics of T6SS organelles.

Accordingly, we tested whether inactivation of PpkA (kinase), PppA (phosphatase), or TagT (ATP-binding cassette transporter) affects the level of T6SS activity and dueling behavior as measured by ClpV1-GFP dynamics (Basler and Mekalanos, 2012). Inactivation of *ppkA* resulted in a complete block of T6SS dynamics (Figure 4.4A, Table 4.3, and Movie S4.3), whereas inactivation of *pppA* resulted in a dramatic increase in the number of cells showing T6SS activity compared to the PppA^{+} parental strain (Figure 4.4B, Table 4.3, and Movie S4.3). Like *V. cholerae*, this T6SS activity occurred spontaneously in most cells and irrespective of neighboring cell T6SS activity. However, unlike *V. cholerae* (Basler and Mekalanos, 2012), the T6SS activity visualized with ClpV1-GFP remained localized to a given subcellular site in each *P. aeruginosa* pppA mutant cell (Figure 4.4B and Movie S4.3). T6SS activity of this sort has been previously hypothesized to reflect either the recycling of the T6SS baseplate complex through multiple rounds of T6SS organelle sheath extension/contraction/disassembly cycles or clustering of multiple dynamic T6SS organelles in close proximity to each other (Basler and

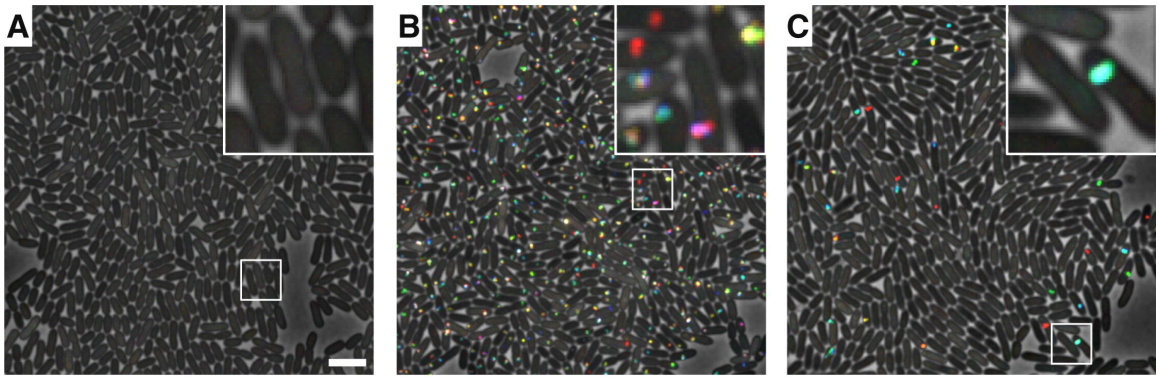

Figure 4.4 T6SS dueling depends on PpkA, PppA, and TagT. (**A**–**C**) ClpV1-GFP localization was followed for 3 min and temporally color-coded (color scale in Figure 4.3I). 30 × 30 μm representative field of cells with a 4× magnified 3 × 3 μm inset (marked by box) is shown for (**A**)–(**C**). Bar in (A) is 3 μm and applies to (**A**)–(**C**). Average number of active cells and dueling cells per 30 × 30 μm field (±SD) is shown (n fields were analyzed); p value is compared to parental strain in Figure 4.3G. (**A**) *P. aeruginosa ΔretS ΔppkA clpV1-gfp*, (**B**) *P. aeruginosa ΔretS ΔpppA ΔclpV1-gfp*, and (**C**) *P. aeruginosa ΔretS ΔtagT clpV1-gfp*. See also Movie S4.3 and Table 4.3.

Mekalanos, 2012). For simplicity, we refer to such cycles of T6SS activity as "firing" in that such activity likely also marks the location of extracellular secretion events that could attack a correctly positioned neighboring prey cell. This positional restriction of T6SS organelle firing was characteristic of a majority of the T6SS activity observed in the *pppA* knockout mutant. Thus, despite its overall increase in T6SS organelle assembly and firing activity, the *pppA* mutant is defective in the T6SS dueling response (Figure 4.4B, Table 4.3, and Movie S4.3). This result suggests that the PppA phosphatase is required to dephosphorylate Fha1 and allow the T6SS organelle to be targeted for disassembly rather than recycling in the same location. Lastly, knocking out *tagT* resulted in loss of dueling activity without loss of T6SS activity in that cells continue to fire their T6SS organelles at the same location, but not in temporal or spatial register with an active sister cell (Figure 4.4C, Table 4.3, and Movie S4.3). This result indicates that the TagQRST signaling cascade is required for sensing the attack of adjacent sister cells. This conclusion is also consistent with the observed stimulation of T6SS organelle formation by the TagQRST system on solid medium compared to liquid medium, where such interactions are more likely to occur (Casabona et al., 2012).

Loss of T6SS dueling behavior blocks targeting of T6SS$^+$ prey cells. We further tested whether mutations in the TagQRST-PpkA-Fha1-PppA regulatory cascade affected *P. aeruginosa* targeting of *V. cholerae* cells by counting round *V. cholerae* cells and measuring inhibition of *V. cholerae* growth. *P. aeruginosa ppkA* mutant cells, which exhibited no T6SS firing activity, did not target V. cholerae for either cell rounding or growth inhibition (Figures 4.5A, B and Table 4.1). Similarly, the dueling-defective *tagT* mutant did not target *V. cholerae* for cell rounding and growth inhibition (Figures 4.5A, B and Table 4.1), which is consistent with the notion that the TagQRST signaling cascade is required for detecting the *V. cholerae* T6SS attack.

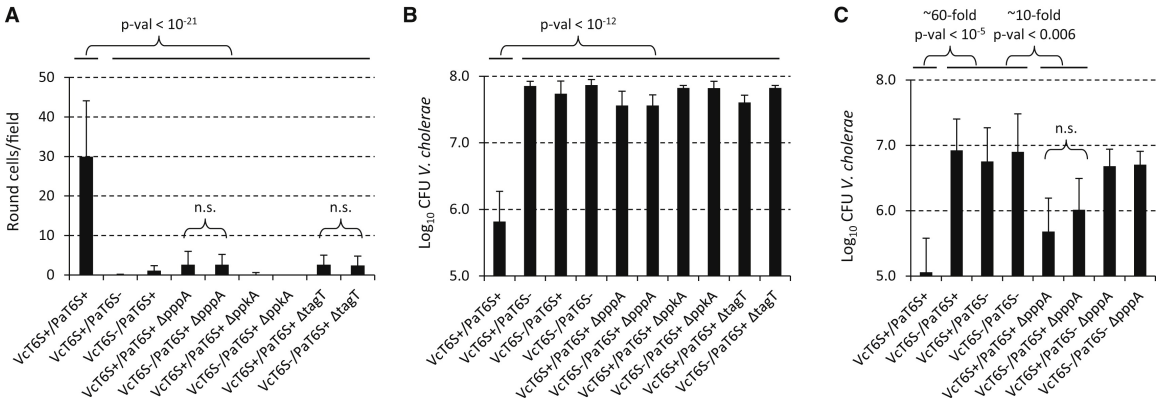

Figure 4.5 PpkA, PppA, and TagT are important for *P. aeruginosa* targeting of prey. Strain abbreviations were as used in Figure 4.1. n.s., not statistically significant ($p > 0.01$). (**A**) Quantification of number of round *V. cholerae* cells per 30 × 30 μm field for indicated mixtures (n = 60 for $VcT6S^+/PaT6S^+$ and $VcT6S^+/PaT6S^-$ mixtures, and n = 30 for all other indicated mixtures). (**B**) Summary of competition assays for *P. aeruginosa* and *V. cholerae* mixtures. Data are presented as mean of $\log_{10}$ CFU of recovered *V. cholerae* with error bars representing SD (n = 6–19). (**C**) Competition assays for *P. aeruginosa* and *V. cholerae* mixtures at 10:1 ratio. Data are presented as mean of $\log_{10}$ CFU of recovered *V. cholerae* with error bars representing SD (n = 5–10). See also Table 4.1.

Given that the *P. aeruginosa pppA* mutant cells fire their T6SS apparatus repeatedly in a specific arbitrary direction but are unable to respond to external T6SS assault (i.e., they are T6SS dueling defective), we made three predictions regarding how effectively the *pppA* knockout mutant would target *V. cholerae* in competition assays. First, because the T6SS of the *pppA* knockout continually fires in a single unchanging direction, these bacteria should be limited in targeting prey cells in a majority of the surrounding space over a unit of time. Thus, a *pppA* mutant cell should attack a target cell only if its T6SS apparatus happened to be in the proper orientation relative to the point of contact between predator and prey cells, which would lead to a decreased frequency of *V. cholerae* prey cell rounding in mixtures with the *pppA* mutant relative to its $PppA^+$ parent. Second, we should be able to compensate for this targeting restriction of *pppA* mutant cells by increasing the ratio of *P. aeruginosa* predator cells to *V. cholerae* prey cells. Increasing the number of *P. aeruginosa* to *V. cholerae* contacts would increase the likelihood that a *P. aeruginosa* T6SS apparatus would happen to be in the correct orientation to

fire directly at the *V. cholerae* cell. Third, if dueling behavior reflects an "aiming" process for directing T6SS firing at aggressive T6SS$^+$ prey, any residual killing activity displayed by the *pppA* mutant should not be selective for killing T6SS$^+$ prey cells compared to T6SS$^-$ prey. Indeed, all three of the above predictions were supported by microscopic and quantitative competition analysis. When the *pppA* knockout mutant was mixed with T6SS$^+$ *V. cholerae* in a 1:1 ratio, there were very few rounded cells (Figure 4.5A and Table 4.1) and virtually no detectable killing of *V. cholerae* in competition assays (Figure 4.5B); however, increasing the relative number of *P. aeruginosa* to *V. cholerae* by 10-fold partially restored the observable killing activity of the *pppA* mutant (Figure 4.5C). This killing activity by the *pppA* mutant was still dependent on *P. aeruginosa* T6SS, and the observable cell rounding and killing activity of the *pppA* mutant exhibited no preference for T6SS$^+$ prey *V. cholerae* cells versus T6SS$^-$ prey cells (Figure 4.5 and Table 4.1). Additionally, the absence of target specificity by the *pppA* mutant also confirms that T6SS$^+$ *V. cholerae* are not inherently more sensitive to *P. aeruginosa* T6SS attack.

Altogether, these results suggest that exogenous T6SS attack on a *P. aeruginosa* cell produces a signal that is perceived by the TagQRST system, which then promotes local, anatomically correct phosphorylation of Fha1 and thus the assembly of a T6SS organelle at the site of the attack followed by its firing in a T6SS "counterattack" directed precisely at the contact point of the attacker.

***Acinetobacter baylyi* T6SS also induces *P. aeruginosa* T6SS-dependent killing, whereas T6SS$^-$ *E. coli* does not.** Given that *P. aeruginosa* can respond to T6SS attack by *V. cholerae*, we wondered whether other heterologous T6SS systems could also induce *P. aeruginosa* T6SS attack. *A. baylyi* has been shown to have a T6SS-dependent growth

phenotype on solid media, suggesting that it has active T6SS (de Berardinis et al., 2008). We confirmed that its T6SS is functional and could effectively target and kill *E. coli* at least as efficiently as *V. cholerae* (Figure 4.6A). When mixed with *P. aeruginosa* in competition, ~1,000-fold fewer *A. baylyi* T6SS$^+$ cells were recovered compared to T6SS$^-$ cells (Figures 4.6B, C). Neither T6SS$^+$ nor T6SS$^-$ *P. aeruginosa* were killed by *A. baylyi* T6SS (Figure 4.2B). Like *V. cholerae*, T6SS$^+$ *A. baylyi* was still killed by *P. aeruginosa tse1-3* null mutant (Figure 4.6C). Furthermore, the TagQRST-PpkA-Fha1-PppA regulatory cascade was required for sensing *A. baylyi* T6SS attack, as mutants altered in PpkA, PppA, or TagT no longer killed T6SS$^+$ *A. baylyi* (Figure 4.6C). These data suggest that the regulatory cascade activating *P. aeruginosa* T6SS can be triggered in response to attack by any arbitrary T6SS$^+$ organism.

If the dueling response of *P. aeruginosa* is indeed an evolutionary adaption to counterattack aggressive T6SS$^+$ heterologous species, we reasoned that *P. aeruginosa* should have little or no ability to kill T6SS$^-$ species such as *E. coli* K12. Indeed, *retS* mutants of

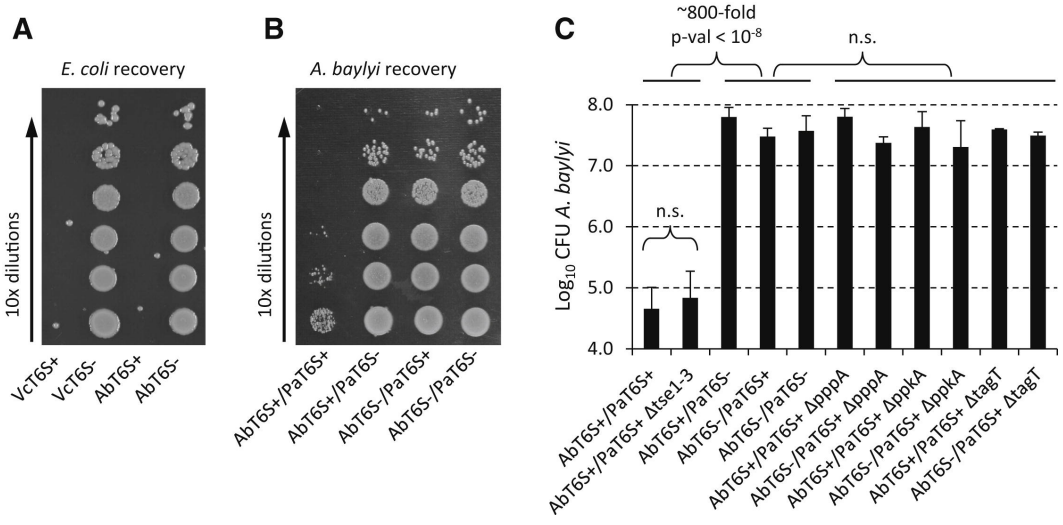

Figure 4.6 *A. baylyi* has a functional T6SS and is targeted by *P. aeruginosa*. Strain abbreviations are as used in Figure 4.1. AbT6S$^+$ indicates *A. baylyi* parental strain, and AbT6S$^-$ indicates *A. baylyi ΔT6SS*. (**A**) Example of a dilution series used to enumerate E. coli survival in mixtures with *A. baylyi* or *V. cholerae*. (**B**) Example of a dilution series used to enumerate *A. baylyi* survival in mixtures with *P. aeruginosa*. (**C**) Summary of competition assays for *P. aeruginosa* and *A. baylyi* mixtures. Data are presented as mean of $\log_{10}$ CFU of recovered *A. baylyi* with error bars representing SD (n = 3–8).

P. aeruginosa cannot kill this species efficiently under conditions that lead to two to three orders of magnitude more efficient killing or inhibition of T6SS$^+$ species (Figure 4.2C).

Discussion

In this study, we explored the biological activity of the bacterial T6SS when four different bacterial species (*P. aeruginosa*, *V. cholerae*, *A. baylyi*, and *E. coli*) interact on solid culture media. In addition to quantitative killing/growth inhibition assays, we utilized time-lapse fluorescence microscopy to reveal cellular and subcellular morphological changes that specifically correlated with the genetic phenotypes of the interacting heterologous species. Our logic for performing these studies stemmed in part from our recent discovery that T6SS$^+$ *P. aeruginosa* cells respond to the T6SS activity of adjacent sister cells with a dramatic increase in their own spatial and temporal T6SS activity (Basler and Mekalanos, 2012). We termed this phenomenon "T6SS dueling" and reasoned that it might reflect a natural process occurring between heterologous T6SS$^+$ species that coexist in the same ecological niche.

The results presented here document the striking ability of T6SS$^+$ *P. aeruginosa* to attack heterologous T6SS$^+$ organisms much more efficiently than T6SS$^-$ organisms. We observed that T6SS$^+$ *V. cholerae* were typically killed ~100-fold more efficiently than isogenic T6SS$^-$ *V. cholerae* (Figures 4.1B and 4.5B). We also observed a statistically significant difference in the ability of T6SS$^+$ *P. aeruginosa* to cause rounding of *V. cholerae* cells, a morphological change attributable to the peptidoglycan degrading T6SS effector Tse1 (Figures 4.1C–H, 4.3A–E and Table 4.1). Furthermore, in mixtures of T6SS$^+$ *P. aeruginosa*, T6SS$^-$ *V. cholerae*, and isogenic T6SS$^+$ *V. cholerae*, only the latter were targeted for attack (Figures 4.1F, G, Table 4.2, and Movie S4.1). The T6SS-dependent morphological changes could not be directly correlated with

killing activity under microscopic conditions because these conditions are not optimal for detecting T6SS-mediated killing; the latter typically requires longer time periods of cellular interaction and aerobic conditions. Nonetheless, both assays yielded the same conclusion that T6SS-dependent events (i.e., killing or morphological changes in prey cells) were strikingly dependent on the T6SS$^+$ activity displayed by *V. cholerae* prey cells. The T6SS of *V. cholerae* was not unique in this regard, as the T6SS of *A. baylyi* induced a similar counterattack by *P. aeruginosa* (Figures 4.6B, C). In contrast, *P. aeruginosa* did not efficiently kill T6SS$^-$ *E. coli* (Figure 4.2C), despite the fact that this species is sensitive to Tse1, Tse-2, and Tse-3 effectors when expressed inside intact cells (Hood et al., 2010; Russell et al., 2011). Although T6SS$^+$ *P. aeruginosa* have been reported to cause the release of about 4-fold more β-galactosidase from *E. coli* than Tse1-negative *P. aeruginosa* (Chou et al., 2012), we view such activity as modest given that *P. aeruginosa* T6SS antibacterial activity directed against either T6SS$^+$ *V. cholerae* or T6SS$^+$ *A. baylyi* appears to be two to three orders of magnitude greater under the conditions we employed in our analysis.

The data presented in this report provide an understanding of prey selection by *P. aeruginosa*. Our results suggest that, in *P. aeruginosa*, T6SS-mediated killing activity is regulated by a signal that corresponds to detection of the point of attack of the T6SS apparatus elaborated by a T6SS$^+$ cell, be it *V. cholerae*, *A. baylyi*, *P. aeruginosa*, or likely other T6SS$^+$ species. The *P. aeruginosa* T6SS counterattack is finely directed with spatial and temporal accuracy so as to engage the T6SS$^+$ attacker within moments of its initial attack. In this way, precise killing of aggressive neighboring T6SS$^+$ cells can be efficiently achieved by *P. aeruginosa* while sparing "peaceful bystanders" despite their close proximity. This strategy makes ecological sense in that biofilms composed of communities of diverse but cooperative

bacterial species likely have more biodegradative (and thus growth) potential than biofilms composed of single bacterial species (Flemming and Wingender, 2010; Wintermute and Silver, 2010). Thus, regulation of T6SS activity by *P. aeruginosa* may be an evolutionary reflection of the old adage "don't bite the hand that feeds you" and that *P. aeruginosa* might prefer to coexist and cooperate with other bacterial species as long as they are not aggressive predators. On the other hand, the ability of *P. aeruginosa* to counterattack an aggressive T6SS$^+$ species provides a bacterial example of a "tit-for-tat" evolutionary strategy predicted by Axelrod and Hamilton in their quantitative analysis of gaming strategies that win the "Prisoner's Dilemma" challenge (Axelrod and Hamilton, 1981). Our results on induced aggressive behavior between competing bacterial species should be of interest to evolutionary biologists in this context.

In this report, we describe a genetic analysis to provide mechanistic detail and biological context for T6SS dueling between heterologous bacterial species. We showed that a null mutation in *pppA* dramatically increases *P. aeruginosa* T6SS dynamic activity on a per cell basis but cause the loss of T6SS dueling behavior and failure to selectively kill or induce rounding of T6SS$^+$ *V. cholerae* (Figures 4.4B and 4.5B and Tables 4.1, 4.3). The observed increase in T6SS activity is consistent with the known activities of PppA, a phosphatase that regulates T6SS secretion through the dephosphorylation of Fha1, a scaffold protein that promotes T6SS apparatus assembly in *P. aeruginosa* specifically after its phosphorylation by the kinase PpkA (Mougous et al., 2007). Our results suggest that the PpkA-Fha1-PppA cycle may well play a role in 1) suppressing random formation of T6SS organelles within the cell, 2) inducing their formation precisely at the point of exogenous T6SS attack, and 3) targeting the disassembly of T6SS organelles once exogenous attack signals are no longer perceived.

Recently, Casabona et al. (2012) have reported that an outer-membrane lipoprotein (TagQ) and a set of periplasmic and inner-membrane proteins (TagR, TagT, and TagS) control the activation of PpkA and thus phosphorylation of Fha1 and assembly of the T6SS apparatus. The fact that TagQRST acts upstream of the PpkA-Fha1-PppA (Casabona et al., 2012; Hsu et al., 2009), together with our new data, suggests that this protein complex may play a direct role in sensing envelope perturbations (e.g., outer-membrane breach, peptidoglycan disruption, inner-membrane perforation) caused by exogenous T6SS attack. Thus, T6SS dueling may be the manifestation of a signal transduction cascade that starts with recognition by the TagQRST system of a subcellularly localized signal associated with exogenous T6SS attack, dimerization, autophosphorylation of PpkA, trans-phosphorylation of Fha1, and, finally, phosphorylated Fha1-directed assembly of a T6SS organelle precisely at the point corresponding to the initial exogenous T6SS attack (Figure 4.7). Repeated firing of the newly assembled T6SS organelle results in a counterattack aimed precisely at the point of initial attack by the heterologous T6SS$^+$ cell. If no further attacks are sensed, then dephosphorylation of Fha1 would allow the T6SS organelle to be disassembled and thus primed (by establishing a pool of T6SS organelle precursors) for a quick response (i.e., de novo organelle assembly) to a new attack at a different anatomical site within the cell (Figure 4.7). It is also worth noting that phosphorylated Fha1 might promote the formation of multiple, clustered T6SS organelles in the vicinity of the initial T6SS exogenous attack as well.

In contrast, the T6SS$^+$ *V. cholerae* strains studied here are able to kill *E. coli* at least 100,000-fold more efficiently than *P. aeruginosa*. We propose that the difference observed in killing activity reflects the dynamics of the *V. cholerae* T6SS apparatus, which forms, fires, and reforms constantly and in different locations within the cell (Basler et al., 2012). In this way,

V. cholerae cells protect their surrounding space and attack all encroaching invaders. However, this strategy is not without an energy cost, as most *V. cholerae* cells show high levels of T6SS activity with no benefit gained, whereas *P. aeruginosa* displays only minor levels until it encounters a T6SS^{+} threat. These two different strategies may also reflect the key underlying evolutionary adaption that is characteristic of two distinct uses for the T6SS organelle:

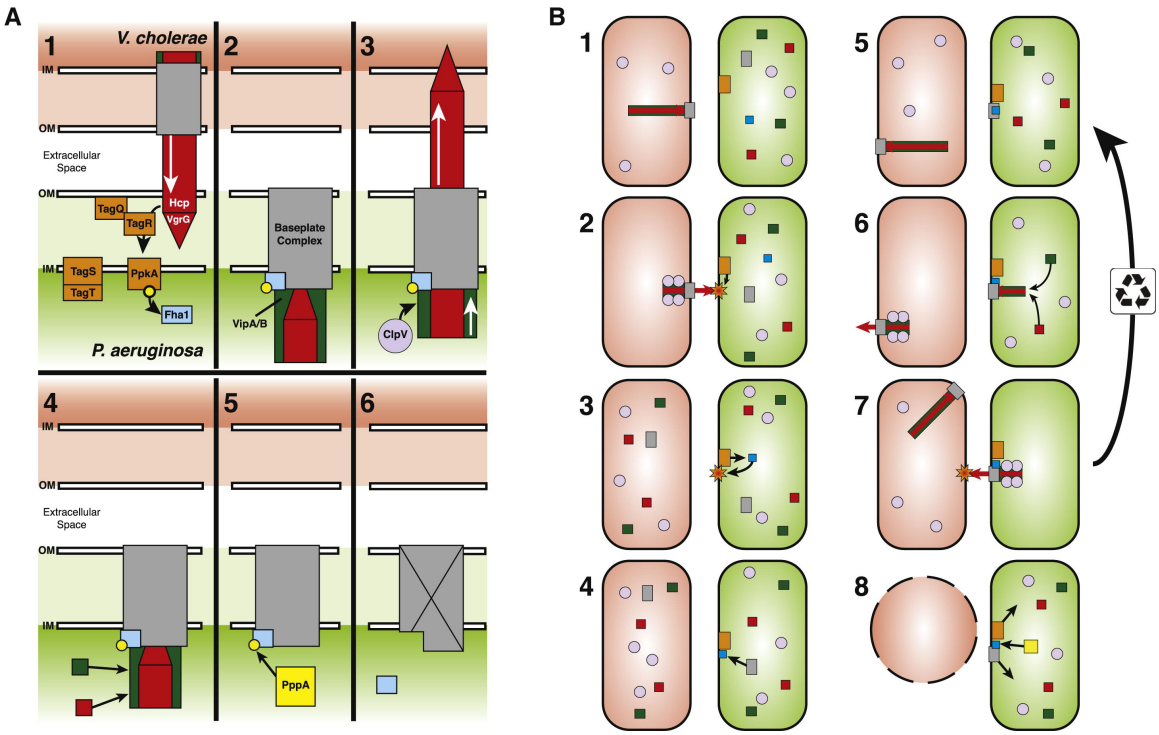

Figure 4.7 Model for TagQRST-mediated T6SS aiming. (**A**) Regulation of the T6SS response in *P. aeruginosa*. (**A1**) T6SS assault from *V. cholerae* is sensed by the TagQRST/ PpkA signal cascade (orange) to phosphorylate Fha1 (blue). (**A2**) Phosphorylated Fha1 interacts with the baseplate complex (gray), locking it in place and allowing assembly of the Hcp/VgrG tube/spike (red) and VipA/B sheath (green). (**A3**) Sheath contraction fires the retaliatory *P. aeruginosa* tube/spike complex at *V. cholerae*. ClpV (light purple) then disassembles the contracted sheath. (**A4**) The baseplate can then be reused to assemble an additional tube/spike/sheath complex, or (**A5**) PppA (yellow) can dephosphorylate Fha1, (**A6**) inactivating or disassembling the baseplate complex. The *P. aeruginosa* T6SS is now ready to respond to new T6SS assaults. (**B**) T6SS interactions between *P. aeruginosa* and *V. cholerae*. (**B1**) *V. cholerae* T6SS will spontaneously fire, occasionally hitting a nearby *P. aeruginosa* cell. (**B2**–**B6**) *P. aeruginosa* senses the assault and builds its T6SS organelle at the location of the assault. (**B7**) *P. aeruginosa* fires its T6SS organelle back at the *V. cholerae* cell. The baseplate is then recycled to allow for multiple firing events, or (**B8**) the Fha1 complex is dephosphorylated by PppA and the baseplate complex is disassembled and free to reform at a new location. (**B5**) Meanwhile, *V. cholerae* continues to fire its T6SS organelle arbitrarily in a different location and direction. (**B8**) After the retaliatory attack from *P. aeruginosa*, the *V. cholerae* cell dies.

V. cholerae uses the apparatus as an offensive weapon, whereas *P. aeruginosa* uses the organelle as a defensive weapon. The ability of *P. aeruginosa* to detect the attack of another T6SS$^+$ cell and to respond with its own T6SS counterattack represents a fascinating example of highly selective, antagonistic bacterial interactions.

In this study, we also show that, although T6SS$^-$ *E. coli* were efficiently killed by T6SS$^+$ *V. cholerae* or *A. baylyi* T6SS$^+$ strains, neither T6SS$^+$ nor T6SS$^-$ *P. aeruginosa* were killed by the *V. cholerae* T6SS$^+$ or *A. baylyi* T6SS$^+$ strains (Figures 4.2A, B). Because *P. aeruginosa* is sensitive to its own T6SS effectors in the absence of its cognate immunity proteins (Hood et al., 2010), it seems highly likely that the resistance of *P. aeruginosa* to T6SS$^+$ *V. cholerae* may be more intrinsic than specific. The "T6SS armor" that *P. aeruginosa* deploys against the killing activity of the *V. cholerae* T6SS may be related to its notorious outer-membrane impermeability (Nikaido, 1994) or perhaps alterations in its peptidoglycan structure. However, because T6SS$^+$ *P. aeruginosa* detect both T6SS$^+$ sister cells (Basler and Mekalanos, 2012) as well as the T6SS$^+$ heterologous species *V. cholerae* and *A. baylyi*, it is clear that *P. aeruginosa* detects T6SS-associated attack signals even if they have no lethal consequence. Understanding in more detail the parameters involved in T6SS$^+$ prey detection as well as prey sensitivity and resistance to T6SS-mediated attacks will be a fruitful area for future investigations. Given that the *P. aeruginosa* T6SS is likely also a mammalian virulence factor (Mougous et al., 2006; Schwarz et al., 2010a), it will also be of interest to determine whether eukaryotic cell-derived signals can induce a *P. aeruginosa* T6SS counterattack.

A key question was how important the best-characterized non-VgrG-related antibacterial effectors, the Tse proteins of *P. aeruginosa* (Hood et al., 2010; Russell et al., 2011), were to the T6SS-dependent killing of sensitive heterologous target cells. Here, we show that this category

of T6SS effector is of little importance to the ability of *P. aeruginosa* to kill T6SS$^+$ *V. cholerae* (Figure 4.3F) or T6SS$^+$ *A. baylyi* (Figure 4.6C). Thus, other yet-to-be-discovered *P. aeruginosa* antibacterial effectors may play a role in killing these T6SS$^+$ prey species. Alternatively, Tse-independent T6SS-dependent killing could be attributed to the dynamic activity of the T6SS apparatus alone. Our data support the hypothesis that the T6SS phage tail-like spike/tube complex of *P. aeruginosa* may kill some target cells after T6SS-mediated envelope insertion without the need for enzymatically active accessory effector delivery. The breech of the outer membrane and/or peptidoglycan and inner membrane of susceptible prey cells with the T6SS VgrG spike/Hcp tube complex might be sufficient to initiate a lethal event in prey cell targets due to, for example, depolarization of the inner membrane, activation of autolytic pathways, or other secondary metabolic responses to this damage (Kohanski et al., 2007; Lewis, 2000; Uratani and Hoshino, 1984).

In this report, we also presented microscopic evidence for delivery of an antibacterial effector to a target prey cell by a native T6SS apparatus. Previous evidence presented for such delivery included the observation that Tsi immunity proteins protect cells from antibacterial Tse effectors secreted by sister cells (Russell et al., 2011) and that Tse effectors are toxic when expressed in heterologous bacterial cells such as *E. coli* (Russell et al., 2011). In our studies, T6SS$^+$ *V. cholerae* cells exposed to T6SS$^+$ *P. aeruginosa* exhibited a rounded morphology that could be specifically attributed to Tse1 activity. Although a Tse1-dependent morphological change in T6SS$^+$ *V. cholerae* could be clearly demonstrated in our studies, as noted earlier, we were unable to attribute a significant contribution of this effector (or indeed any of the known Tse effectors) to the total T6SS-dependent bacteriocidal activity of *P. aeruginosa* directed against T6SS$^+$ *V. cholerae* or T6SS$^+$ *A. baylyi*. We are currently exploring the hypothesis that

Tse effectors may be more important to lysing some target species and thus releasing cytoplasmic contents that could serve as growth substrates than for killing target cells per se. Because there are T6SS$^+$ bacterial species that utilize other bacteria as growth substrates (i.e., *Myxococcus xanthus*), the concept that T6SS effectors may play a role in nutrient scavenging rather than simply being the mediators of lethality is an interesting insight that has emerged from the studies presented here.

Description of Supplemental Movies

Movie S4.1 *P. aeruginosa* T6SS causes morphological changes in T6SS$^+$ *V. cholera*. This movie contains data that are represented in Figure 4.1. Nine individual 3-min-long time-lapse movies were obtained with a frame rate of 5 sec per frame. The movie shows a 48 × 36 μm region and plays 50× faster than real time. Segments: 1–3, *P. aeruginosa ΔretS clpV1-gfp* (T6SS$^+$, green)/*V. cholerae clpV-mCherry2* (T6SS$^+$, red), notice *V. cholerae* cell rounding and lysis; 4–6, *P. aeruginosa ΔretS clpV1-gfp* (T6SS$^+$, green)/*V. cholerae ΔvipA clpV-mCherry2* (T6SS$^-$, red), almost no *V. cholerae* cell rounding; 7–9, *P. aeruginosa ΔretS* (T6SS$^+$, unlabeled)/*V. cholerae clpV-mCherry2* (T6SS$^+$, red) + *V. cholerae ΔvipA clpV-gfp* (T6SS$^-$, green), only T6SS$^+$ (red) *V. cholerae* cells round and lyse.

Movie S4.2. *P. aeruginosa* T6SS causes morphological changes in T6SS$^+$ *V. cholerae* – higher magnification. This movie contains data that are represented in Figure 4.1. Thirty individual 3-min-long time-lapse movies were obtained with a frame rate of 5 s per frame. Movie shows 4.5 × 4.5 μm region and plays 50× faster than real time. Movie was scaled up 4× with no interpolation. *P. aeruginosa ΔretS clpV1-gfp* (T6SS+, green) + *V. cholerae clpV-mCherry2*

(T6SS+, red). Segments: 1–10, morphological changes in *V. cholerae* cells; 11–20, inner-membrane shrinking (plasmolysis); 21–30, *V. cholerae* cell lysis.

Movie S4.3. T6SS dueling depends on PpkA, PppA, and TagT, but not on Tse1-3. This movie contains data that are represented in Figures 4.3 and 4.4. Ten individual 3-min-long time-lapse movies were obtained with a frame rate of 5 sec per frame. Movie shows 48 × 36 μm region and plays 50× faster than real time. Segments: 1–2, *P. aeruginosa ΔretS clpV1-gfp*, T6SS dueling; 3–4, *P. aeruginosa ΔretS ΔppkA clpV1-gfp*, no T6SS activity; 5–6, *P. aeruginosa ΔretS ΔpppA clpV1-gfp*, increased T6SS activity, decreased proportion of dueling; 7–8, *P. aeruginosa ΔretS ΔtagT clpV1-gfp*, no dueling; 9–10, *P. aeruginosa ΔretS Δtse1-3 clpV1-gfp*, T6SS dueling.

Materials and Methods

Bacterial Strains. *V. cholerae* 2740-80 and *P. aeruginosa* PAO1 strains used in this study were described previously (Basler and Mekalanos, 2012; Basler et al., 2012; Mougous et al., 2006). Gentamicin-resistant *E. coli* MG1655 strain was used for bacterial competition assays. *A. baylyi* ADP1 was obtained from ATCC (33305), and spontaneous streptomycin resistant mutant was used as a parental strain. Antibiotic concentrations were streptomycin, 100 μg/ml; gentamicin, 15 μg/ml; and irgasan, 20 μg/ml. Luria-Bertani (LB) broth (5 g/l NaCl) was used for all growth conditions. Liquid cultures were grown aerobically at 37 C.

DNA Manipulations. Genes pa1844, pa2702, and pa3484 (tse1, tse2, and tse3) in *P. aeruginosa* were replaced using the pEXG2 suicide plasmid (Rietsch et al., 2005) by in-frame-deleted genes encoding the following peptides: pa1844, MDSLDQCPRAS; pa2702, MSYDGL; and pa3484, MTTFLDPGMRFP. In-frame deletions of pa0073, pa0074, pa0075, and pa0083 (tagT1, ppkA, pppA, and vipA1) in *P. aeruginosa* were described previously or prepared

by the same approach (Basler and Mekalanos, 2012; Mougous et al., 2006; Mougous et al., 2007). Gene pa1845 (tsi1) was cloned in-frame with mcherry2 (separated by DNA linker encoding 3Ala-3Gly) to pBAD24 plasmid as described previously (Basler et al., 2012) to allow for arabinose-inducible expression of Tsi1-mCherry2 fusion protein in *V. cholerae*. *A. baylyi* T6SS genes aciad2688 to aciad2694 (including homologs of *V. cholerae* T6SS genes: gp25-like, hcp, vipA, vipB, and clpV) were replaced with KanR cassette from pRSFDuet-1 plasmid (Novagen) as described previously (Metzgar et al., 2004). All cloning products were sequence verified. Chromosomal mutations were verified by PCR using primers outside of the replaced region.

Fluorescence Microscopy. Procedures similar to procedures described previously (Basler and Mekalanos, 2012; Basler et al., 2012) were used to detect fluorescence signal in *V. cholerae and P. aeruginosa*. Overnight cultures of *V. cholerae* or *P. aeruginosa* were washed by LB and diluted 50–200× into fresh LB and cultivated for 2.5-3.5 hr to optical density (OD) ~0.5-1.0. For V. cholerae 2740-80 + pBAD24-Tsi1-mCherry2, expression of Tsi1-mCherry2 in V. cholerae was induced by 0.01% arabinose. Cells from 100 µl of the culture were resuspended in 5-10 µl of fresh LB (to OD ~10), mixed as indicated, spotted on a thin pad of 1% agarose in 0.5x PBS (pH 7.4, Invitrogen), and covered with a glass coverslip. Cells were imaged at 25-30 C after 20 to 60 min (for 3 min for detection of morphological changes or dueling) or after 40 to 90 min (for detection of round cells). Cells close to the edge of the agarose pad were imaged. Multiple 30 x 30 µm fields of cells (30-60 for detection of round cells and 10-25 for detection of dueling, indicated as n in figures) were analyzed for at least four biological replicates. Microscope configuration was described previously (Basler and Mekalanos, 2012) – Nikon Ti-E inverted motorized microscope with Perfect Focus System and Plan Apo 100× Oil Ph3 DM (NA

1.4) objective lens. SPECTRA X light engine (Lumencore), ET-GFP (Chroma 49002), and ET-mCherry (Chroma 49008) filter sets were used to excite and filter fluorescence. Photometrics CoolSNAP HQ2 camera (pixel size was 60 nm) and NIS Elements 4.0 were used to record images.

Image Analysis. Fiji was used for all image analysis and manipulations (Schindelin et al., 2012). The individual fluorescence images from a time series were corrected for photobleaching by normalizing the intensity of a region containing mostly cells to the same mean intensity. Image contrast was set to clearly show localization of signal within cells and is set to the same level when direct comparison between strains is presented. Small movement of whole field in time was corrected by registering individual frames using StackReg plugin for Fiji ("Rigid Body" transformation). Fiji macro "Temporal-Color Code" was used to visualize localization of fluorescent foci in time. Merged image of the phase contrast and fluorescence images are presented.

Bacterial Competition Assay. Cells were prepared as for fluorescence microscopy analysis. Cells were mixed at OD ~10 in 1:1 or 10:1 ratio as specified, and 5 µl of the mixture was spotted on a dry LB agar plate. After 2 hr at 37 C, bacterial spots were cut out and the cells were resuspended in 1 ml LB. The cellular suspension was serially diluted in LB, and 5 µl of the suspensions was spotted on selective plates (irgasan for *P. aeruginosa*, streptomycin for *V. cholerae* and *A. baylyi*, and gentamicin for *E. coli*). Colonies were counted after ~16 hr of incubation at 30 C. At least three biological replicates were analyzed.

Statistics. Student's t test was used to determine significance between indicated groups of numbers.

Chapter 5. Type 6 secretion system-mediated immunity to type 4 secretion system-mediated gene transfer

Gram-negative bacteria use the type VI secretion system (T6SS) to translocate toxic effector proteins into adjacent cells. The *Pseudomonas aeruginosa* H1-locus T6SS assembles in response to exogenous T6SS attack by other bacteria. We found that this lethal T6SS counterattack also occurs in response to the mating pair formation (Mpf) system encoded by broad-host-range IncPα conjugative plasmid RP4 present in adjacent donor cells. This T6SS response was eliminated by disruption of Mpf structural genes but not components required only for DNA transfer. Because T6SS activity was also strongly induced by membrane-disrupting natural product polymyxin B, we conclude that RP4 induces "donor-directed T6SS attacks" at sites corresponding to Mpf-mediated membrane perturbations in recipient *P. aeruginosa* cells to potentially block acquisition of parasitic foreign DNA.

Foreword

A modified version of this chapter has been published in *Science* on October 11, 2013. The published version can be found on the web at the following URL:

http://dx.doi.org/10.1126/science.1243745

The full citation for this work is:

> Ho, B.T., Basler, M., and Mekalanos, J.J. (2013). Type 6 Secretion System-Mediated Immunity to Type 4 Secretion System-Mediated Horizontal Gene Transfer. Science 342, 250-253.

I performed all experimental data presented in this chapter. I would like to thank Dr. Marek Basler for contributing preliminary data regarding the effect of polymyxin B on *Pseudomonas aeruginosa* T6SS. I would also like to thank Professor Mekalanos for considerable help in the editing and revising of this chapter. This work was supported by grants AI-018045 and AI-26289 to John J. Mekalanos from the National Institute of Allergy and Infectious Diseases.

Results and Discussion

Bacteria often exhibit antagonistic behaviors toward each other in microbial communities (Hibbing et al., 2010). One molecular mechanism mediating such behavior is the type VI secretion system (T6SS) (Pukatzki et al., 2006). The T6SS is a widely conserved (Boyer et al., 2009) dynamic multicomponent nanomachine structurally related to contractile phage tails (Basler et al., 2012; Leiman et al., 2009). Gram-negative bacteria use the T6SS to kill prokaryotic and eukaryotic prey cells through contact-dependent delivery of toxic effectors (Dong et al., 2013; Hood et al., 2010). In *P. aeruginosa*, T6SS encoded by the H1-T6SS cluster (Mougous et al., 2006) selectively targets $T6SS^+$ bacteria that attack it by sensing these exogenous attacks and post-translationally activating its own T6SS at the precise location of the initial assaults (Basler et al., 2013; Basler and Mekalanos, 2012). We previously hypothesized that the signal triggering the T6SS counterattack was the perturbation of the cell envelope (Basler et al., 2013). Thus, we wondered whether other systems capable of breeching the cell envelope would trigger a similar T6SS response. One system capable of delivering macromolecules across the envelopes of other Gram-negative cells is the type IV secretion system (T4SS) (Luo and Isberg, 2004). This secretion system is associated with conjugative elements such as the broad-host-range, IncPα plasmid RP4 (Pansegrau et al., 1994) as well as virulence elements in several bacterial species (Christie and Vogel, 2000). T4SS-mediated DNA conjugation involves three sets of proteins: (i) the core structure and pilus components comprising the mating pair formation (Mpf) complex, (ii) the relaxosome complex, which initiates DNA transfer by binding to and nicking the origin of transfer, and (iii) a coupling protein that bridges the relaxosome and Mpf complexes (Schroder and Lanka, 2005). During conjugation, the pilus extends from donor cells to mediate close cell-cell contact with recipients,

which allows transfer of the DNA-bound relaxosome components to occur (Schroder and Lanka, 2005).

If T4SS-mediated cell-cell interactions could trigger T6SS attack, donor cells of a heterologous conjugation-proficient T6SS$^-$ species should be sensitive to killing by T6SS$^+$ *P. aeruginosa*. Therefore, we determined whether carrying the RP4 plasmid affected survival of *E. coli* K12 strain MC1061 when grown in competition with *P. aeruginosa*. For consistency with previous studies (Basler et al., 2013; Basler and Mekalanos, 2012), a *retS* mutant with a transcriptionally up-regulated H1-T6SS locus was used. When mixed with *P. aeruginosa*, we recovered ~96% fewer viable *E. coli* cells carrying RP4 as compared with those lacking it (Figure 5.1A). This difference was not observed for *P. aeruginosa* mutants that were T6SS$^-$ (*vipA*) but was still observed in a triple mutant lacking the three known *P. aeruginosa* T6SS effectors Tse1, Tse2, and Tse3 (Figure 5.1A) (Hood et al., 2010). Although a *pppA* mutant with a hyperactive but unregulated T6SS could slightly inhibit *E. coli* growth, there was no enhanced killing of *E. coli* cells carrying RP4 compared with those without it (Figure 5.1A), and deletion of *tagT*, a gene critical for sensing exogenous T6SS attack (Basler et al., 2013), completely abolished *E. coli* killing (Figure 5.1A). Furthermore, in three-strain mixture containing RP4$^+$ and RP4$^-$ *E. coli* with *P. aeruginosa*, only RP4$^+$ *E. coli* were killed (Figure 5.1B). Thus, T6SS-dependent killing of RP4$^+$ *E. coli* involves the same attack-sensing mechanism implicated in the T6SS counterattack responses (Basler et al., 2013).

We next determined the genetic requirements for the RP4-dependent induction of the *P. aeruginosa* T6SS donor-directed attack. RP4 was subjected to transposon mutagenesis and transformed into *E. coli* strain MC1061. Individual mutants were sequenced to determine transposon insertion sites (Figure 5.1C). Conjugation efficiency into recipient *E. coli* strain

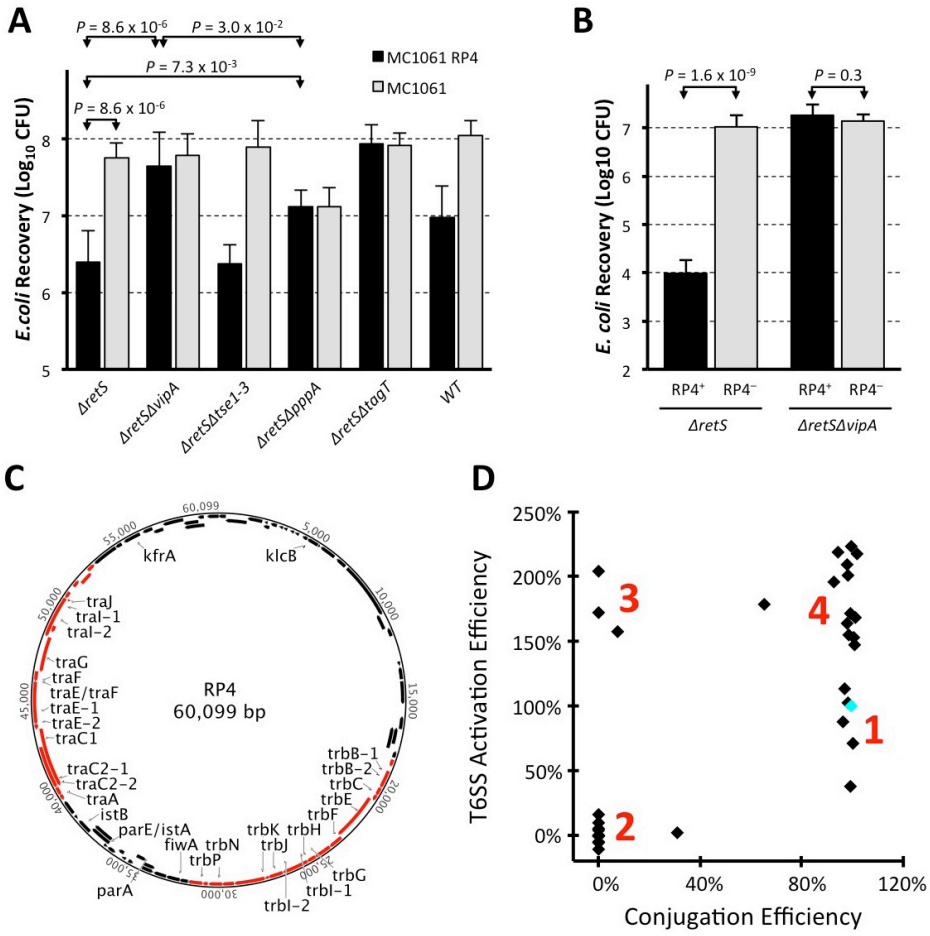

Figure 5.1 Mpf induces a donor-directed T6SS attack in *P. aeruginosa*. (**A**) Summary of competition assays between either MC1061 (gray) or MC1061 RP4 (black) and the indicated strains of *P. aeruginosa*. Reported are the numbers of colony forming units (CFU) of surviving *E. coli*. Data are mean ± SD with $n = 4$ to 8 independent replicates. (**B**) Summary of 3-strain competitions between MC1061, MC1061 RP4 Δ*traG* (Tra$^-$, but Mpf$^+$), and *P. aeruginosa*. Surviving CFUs of each *E. coli* strain determined by plating on media selective for each strain. $n = 6$ independent replicates. (**C**) Map of the RP4 plasmid indicating positions of transposon insertions. Labels with two genes separated by a slash (for example, *traE/traF*) represent insertions into the intergenic region between the two genes. (**D**) Plot of T6SS activation efficiency versus conjugation efficiency for each transposon mutant. See text and Table 5.1 for details on the indicated clusters. Efficiencies are scaled so that values for wild-type RP4 are 100% and the RP4$^-$ parent strain are 0%. The cyan dot represents wild-type RP4. The lower limit of detection for our assay was ~200 conjugants; mutants for which the conjugation efficiency was below this number are reported as 0% in the graph.

MG1655 was then determined for each of these RP4 mutants, and T6SS activation efficiency was calculated from the survival rate of MC1061 *E. coli* with these mutant plasmids grown in competition with T6SS$^+$ *P. aeruginosa* (Table 5.1). Plotting the data for each mutant revealed several different phenotype clusters (Figure 5.1D). Mutants in cluster 1 maintained wild-type

Table 5.1 Conjugation and T6SS activation efficiency for tested RP4 transposon mutants.

Cluster 1	Ins. Site [a]	Conj eff. (*N*) [b]	T6SS act. (*N*) [c]	p-val vs. WT [d]	p-val vs. NP [e]
RP4 WT	n/a	7.72 ± 0.12 (2)	6.34 ± 0.33 (8)	n/a	5.85×10^{-7}
trbK	27628	7.53 ± 0.08 (4)	6.51 ± 0.66 (5)	6.07×10^{-1}	1.27×10^{-2}
parE/istA	36229	7.66 ± 0.18 (3)	6.31 ± 0.20 (3)	8.63×10^{-1}	1.39×10^{-3}
traC2-2	40455	7.75 ± 0.19 (3)	6.75 ± 0.23 (3)	6.21×10^{-2}	6.85×10^{-3}
kfrA	55596	7.57 ± 0.43 (3)	6.15 ± 0.44 (4)	4.94×10^{-1}	3.62×10^{-3}

Cluster 2	Ins. Site [a]	Conj eff. (*N*) [b]	T6SS act. (*N*) [c]	p-val vs. WT [d]	p-val vs. NP [e]
trbB-1	18852	< 2.30 (3)	7.76 ± 0.39 (4)	1.18×10^{-3}	9.75×10^{-1}
trbB-2	19196	< 2.30 (3)	7.84 ± 0.32 (3)	2.95×10^{-3}	6.94×10^{-1}
trbE	21496	< 2.30 (3)	7.76 ± 0.29 (3)	1.80×10^{-3}	9.59×10^{-1}
trbF	23232	< 2.30 (3)	7.91 ± 0.35 (4)	3.86×10^{-4}	4.53×10^{-1}
trbG	24755	< 2.30 (3)	7.68 ± 0.39 (4)	1.57×10^{-3}	7.32×10^{-1}
trbI-1	25418	< 2.30 (3)	7.83 ± 0.38 (3)	7.76×10^{-3}	7.68×10^{-1}
trbI-2	26307	< 2.30 (3)	7.53 ± 0.25 (3)	1.40×10^{-3}	2.47×10^{-1}
traE/traF	46057	< 2.30 (3)	7.62 ± 0.34 (4)	8.14×10^{-4}	5.10×10^{-1}
traF	46198	< 2.30 (3)	7.70 ± 0.29 (3)	2.29×10^{-3}	7.80×10^{-1}
No Plasmid	n/a	n/a	7.75 ± 0.16 (7)	5.85×10^{-7}	n/a

Outliers	Ins. Site [a]	Conj eff. (*N*) [b]	T6SS act. (*N*) [c]	p-val vs. WT [d]	p-val vs. NP [e]
trbH	25212	3.98 ± 0.23 (3)	7.72 ± 0.22 (3)	2.41 x 10-4	8.47 x 10-1
trbN	30035	7.69 ± 0.12 (4)	7.22 ± 0.15 (4)	8.15 x 10-5	8.90 x 10-4

Cluster 3	Ins. Site [a]	Conj eff. (*N*) [b]	T6SS act. (*N*) [c]	p-val vs. WT [d]	p-val vs. NP [e]
klcB	4840	7.77 ± 0.07 (3)	5.59 ± 0.18 (3)	2.23×10^{-3}	1.80×10^{-4}
trbC	20101	7.70 ± 0.15 (3)	5.32 ± 0.67 (4)	4.92×10^{-2}	4.53×10^{-3}
trbJ	27022	7.72 ± 0.14 (5)	4.60 ± 0.43 (5)	1.18×10^{-4}	2.66×10^{-5}
trbP	30956	7.84 ± 0.15 (5)	4.68 ± 0.56 (6)	2.47×10^{-4}	1.88×10^{-5}
fiwA	32160	7.64 ± 0.18 (3)	5.43 ± 0.16 (3)	3.78×10^{-4}	5.15×10^{-5}
parA	34130	7.66 ± 0.17 (5)	4.91 ± 0.66 (5)	5.66×10^{-3}	4.77×10^{-4}
istB	37891	7.62 ± 0.14 (4)	4.80 ± 0.56 (4)	6.76×10^{-3}	1.30×10^{-3}
traA	39820	7.81 ± 0.29 (3)	5.37 ± 0.12 (3)	5.70×10^{-5}	1.05×10^{-6}
traC2-1	40725	7.34 ± 0.29 (3)	4.98 ± 0.28 (3)	2.06×10^{-3}	1.24×10^{-3}
traC1	43045	7.43 ± 0.21 (5)	4.66 ± 0.68 (5)	3.12×10^{-3}	3.74×10^{-4}
traE-2	43952	7.78 ± 0.27 (3)	5.67 ± 0.24 (3)	1.37×10^{-2}	1.16×10^{-3}
traE-1	44529	7.67 ± 0.23 (3)	5.56 ± 0.26 (3)	1.05×10^{-2}	1.47×10^{-3}

Cluster 4	Ins. Site [a]	Conj eff. (*N*) [b]	T6SS act. (*N*) [c]	p-val vs. WT [d]	p-val vs. NP [e]
traG	47386	< 2.30 (4)	4.86 ± 0.54 (8)	2.80×10^{-5}	3.00×10^{-7}
traI-2	49596	2.72 ± 0.32 (5)	5.53 ± 0.68 (6)	3.23×10^{-2}	3.65×10^{-4}
traI-1	50448	< 2.30 (3)	5.31 ± 0.17 (3)	1.83×10^{-4}	4.90×10^{-5}
traJ	50755	5.85 ± 0.10 (5)	5.23 ± 0.69 (6)	9.24×10^{-3}	2.10×10^{-4}

[a] Insertion site is given using NC_001621 as the reference sequence.

[b] Conjugation efficiency (Conj eff.) is the average number of CFU of successful conjugants from an MC1061 donor into an MG1655 recipient during standard mating assays ±SD. Number of independent replicates (*N*) is indicated in parentheses.

[c] T6SS activation efficiency (T6SS act.) is the number of surviving CFU of MC1061 carrying the indicated RP4 mutant after competition with *P. aeruginosa* +/- SD. Number of independent replicates (*N*) is indicated in parentheses.

[d] Significance of the T6SS activation calculated relative to the wild-type plasmid.

[e] Significance of the T6SS activation calculated relative to the parent strain (NP = No Plasmid).

levels of conjugation efficiency and induced T6SS killing at levels comparable with the wild-type plasmid. Most of these mutants were insertions in genes outside of the *tra1* or *tra2* loci, the exceptions being a disruption in the RP4 entry exclusion factor *trbK* (Giebelhaus et al., 1996), and a disruption of *traE*, a topoisomerase III homolog (Li et al., 1997). Neither of these genes is required for the Mpf system or DNA transfer (Table 5.1) (Haase et al., 1995). Mutants in cluster 2 were completely defective in their ability to transfer DNA and did not induce the T6SS donor-directed killing response in *P. aeruginosa*. All of these insertions disrupted genes encoding Mpf structural components (Table 5.1). There were two outliers not quite in Cluster 1 or 2 that were still able to transfer DNA, but did not induce a T6SS response (Table 5.1): insertions in *trbH*, a lipoprotein believed to connect the pilus to the core complex (Schroder and Lanka, 2005); and *trbN*, a periplasmic transglycosylase that remodels the donor peptidoglycan and is required for pilus synthesis (Schroder and Lanka, 2005). Similar transposon disruptions of homologs of *trbH* (Fernandez et al., 1996) and *trbN* (Bayer et al., 1995) in heterologous T4SSs affect the formation and stability of the Mpf pili. Mutants in cluster 3 induced a greater donor-directed T6SS response than that of wild-type RP4 but were defective in DNA conjugation (Figure 5.2B). These mutants included disruptions of relaxosome components *traI* and *traJ* as well as coupling protein *traG* (Table 5.1). Like those in cluster 3, mutants in cluster 4 also induced more T6SS killing than did the wild type but exhibited no defect in conjugation. Although it remains unclear why cluster-3 and -4 mutants induce more efficient T6SS-mediated killing, it is clear that successful DNA transfer is not required to trigger a T6SS attack by *P. aeruginosa*. We next determined whether other conjugative plasmids were also able to induce donor-directed T6SS attack. IncN compatibility group plasmid pKM101 (Langer et al., 1981) induced a T6SS attack comparable with that of RP4 (Figure 5.2A), whereas *E. coli* carrying the sex factor F plasmid was unaffected

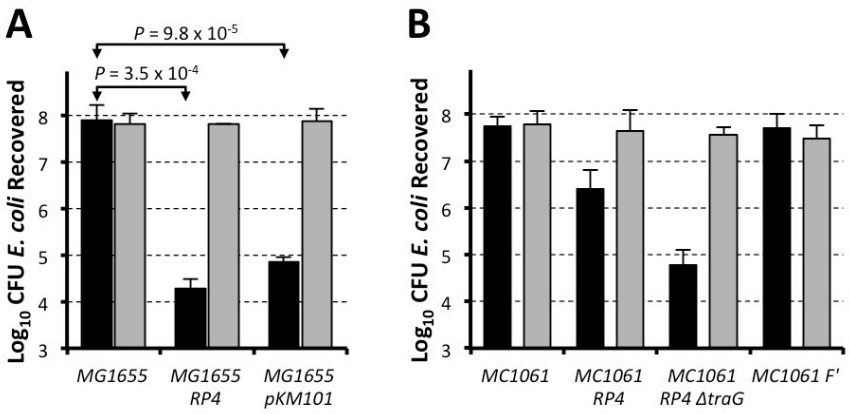

Figure 5.2 IncN but not IncF induces donor-directed T6SS attacks. (**A** and **B**) Summary of *E. coli* survival after competition with T6SS$^+$ (black bars) or T6SS$^-$ (gray bars) *P. aeruginosa*. Data are mean ± SD, $n = 3$ independent replicates. (**A**) Competition assays between *P. aeruginosa* and *E. coli* MG1655 carrying no plasmid, RP4, or pKM101. pKM101 confers streptomycin resistance so MG1655 rather than MC1061 was used. (**B**) Competition assays between *P. aeruginosa* PAO1 and *E. coli* MC1061 carrying no plasmid, RP4, RP4 hyper-inducer Tra$^-$ Mpf$^+$ mutant (Δ*traG*), or F′. F′ was confirmed to be functional by successfully mating into several different *E. coli* strains.

by T6SS$^+$ *P. aeruginosa* (Figure 5.2B). It is not known why the *E. coli* F factor cannot be successfully transferred into *P. aeruginosa* (Zhong et al., 2005), but this observation suggests that T6SS activation correlates to some degree with whether the host range of a given plasmid includes *P. aeruginosa*.

If the *P. aeruginosa* donor-directed T6SS attack could be triggered by the Mpf system of donor species, then this attack might suppress plasmid transfer into a population of T6SS$^+$ *P. aeruginosa* cells. Accordingly, we measured the frequency with which the plasmid pPSV35 (Rietsch et al., 2005) could be transferred into T6SS$^+$ or T6SS$^-$ *P. aeruginosa* from the *E. coli* donor strain SM10 (Simon et al., 1983), which carries a chromosomally-integrated RP4 plasmid. Because pPSV35 does not encode its own transfer machinery but can be mobilized by the SM10 encoded conjugation system (Rietsch et al., 2005), the frequency with which *P. aeruginosa* cells acquired pPSV35 reflects the efficiency at which this plasmid is transferred into but not between *P. aeruginosa* cells. When donor *E. coli* and recipient *P. aeruginosa* were mixed at a 1:1 ratio,

we observed an ~86% decrease in conjugation efficiency into a T6SS$^+$ strain as compared with its isogenic T6SS$^-$ *vipA* mutant (Figure 5.3A). This reduction in transfer efficiency did not match the observed magnitude of killing of RP4$^+$ MC1061 (Figure 5.1A) probably because of intrinsic differences in the ability of various donor strains to promote Mpf and T6SS activation with *P. aeruginosa*, which is similar to what we observed in our RP4 mutant analysis (Figure 5.1D). *P. aeruginosa* mutants defective in the attack-sensing pathway genes *tagT* and *pppA* (Basler et al., 2013), also exhibited greater conjugation efficiency as recipient strains (Figure 5.3A). Examination of mixtures of T6SS$^+$ *P. aeruginosa* and *E. coli* RP4$^+$ donor cells by means of fluorescence microscopy revealed rounding and blebbing of *E. coli* cells – a response that is typical of T6SS-mediated bacterial killing (Figure 5.3B). Thus inhibition of the conjugative transfer of pPSV35 was likely due to killing of *E. coli* cells through a donor-directed T6SS attack by *P. aeruginosa*.

The fact that multiple secretion systems can induce a T6SS counterattack suggested that

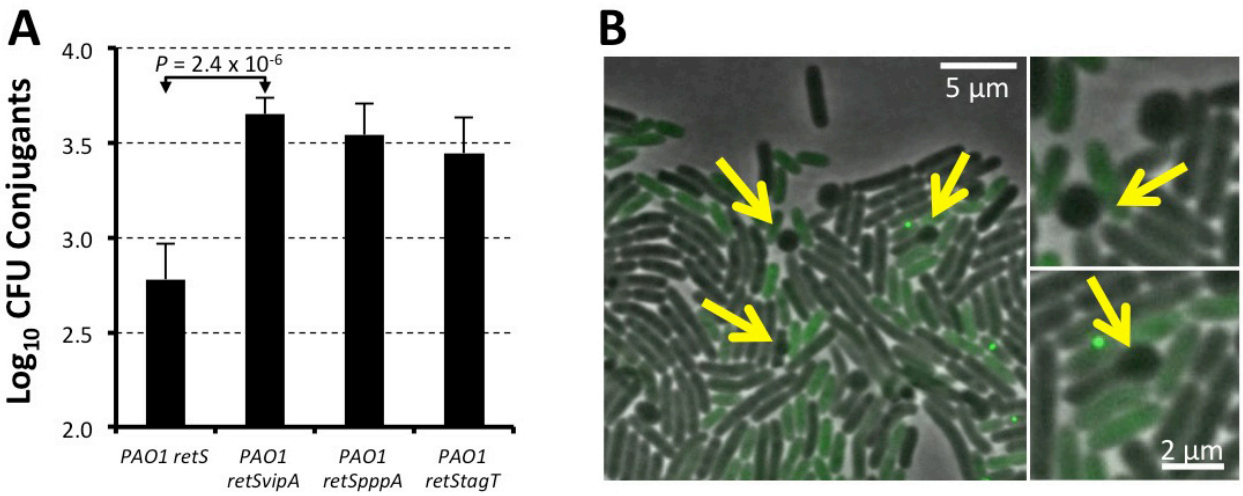

Figure 5.3 Donor-directed T6SS attack blocks heterologous transfer of DNA. (**A**) The conjugation efficiency into different *P. aeruginosa* mutants. Data are mean ± SD, $n = 7$ independent replicates. (**B**) Representative field of cells containing a mixture of *P. aeruginosa PAO1* Δ*retS clpV1-gfp* (green) and *E. coli S17-1* RP4$^+$ donor cells (non-fluorescent). *E. coli* cells exhibit cell rounding characteristic of T6SS-mediated killing (arrows). Larger magnification of rounding cells are shown in the insets.

the signal initiating this response really is a generalized disruption of the *P. aeruginosa* membrane. Accordingly, we asked whether polymyxin B, an antibiotic known to disrupt Gram-negative bacterial membranes by binding the lipid A component of lipopolysaccharides (Hankins et al., 2012; McPhee et al., 2003; Morrison and Jacobs, 1976), could induce T6SS activity in *P. aeruginosa*. We used a *P. aeruginosa* strain carrying a ClpV1-GFP and fluorescent time-lapse microscopy to monitor T6SS organelle formation and dynamics (Basler et al., 2013; Basler and Mekalanos, 2012) after exposure to polymyxin B. Cells exhibited a sixfold increase in the average number of visible ClpV1-GFP foci per cell within 90 seconds of being spotted onto agar pads containing 20 µg/mL of polymyxin B (Figure 5.4A, C and Movie S5.1). After this increase

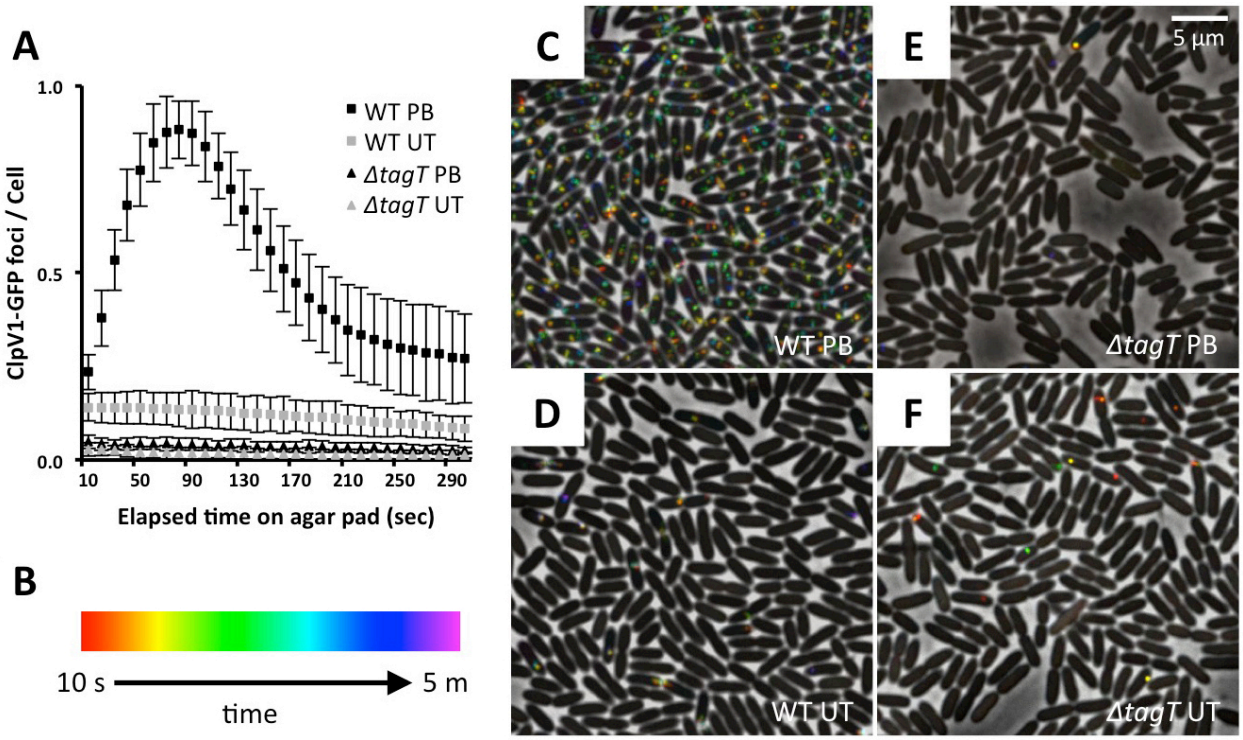

Figure 5.4 Activation of T6SS organelle formation in response to polymyxin B treatment requires TagT. (**A**) Wild type (WT) or *tagT* mutant (Δ*tagT*) *P. aeruginosa* cells were imaged every 10 seconds starting immediately after being spotted onto agar pads containing 0 µg/mL [untreated (UT)] or 20 µg/mL polymyxin B (PB). Total number of ClpV1-GFP foci was divided by the number of cells for each field of cells to determine the average number of foci per cell. Each curve represents the mean of 12 to16 fields with 250 to 600 cells in each field ± SD. (**B**) Color scale used to temporal-color code ClpV1-GFP signal. (**C-F**) ClpV1-GFP localization was followed for 5 minutes and temporally color-coded. (**C**) WT, PB. (**D**) WT, UT. (**E**) Δ*tagT* PB (**F**) Δ*tagT* UT.

in T6SS activity, most ClpV1-GFP foci disappeared over the next 3 minutes with the remaining foci becoming non-dynamic (Figure 5.4A, Movie S5.1). The loss of dynamics likely reflects consumption of intracellular adenosine 5'-triphophate pools after prolonged exposure to polymyxin B intoxication. This increase in T6SS activity was not observed when cells were spotted onto agar pads lacking polymyxin B (Figure 5.4A, D and Movie S5.1). Additionally, this increase in ClpV1-GFP foci was not observed in *tagT* mutants even in the presence of polymyxin B (Figure 5.4A, E, F and Movie S5.2), suggesting that the same attack-sensing pathway that senses T4SS and T6SS attacks is responding to this antibiotic and mediates activation of the T6SS.

These studies support a model in which the donor-directed T6SS attack response in *P. aeruginosa* likely involves detection of perturbations in the cell envelope caused by the invasive components of the T4SS conjugation machinery. T6SS may represent a type of bacterial "innate immune system" that can detect and attack invading infectious elements not by recognizing their molecular patterns [such as nucleic acid sequences, as do the clustered regularly interspaced short palindromic repeat (CRISPR) elements (Barrangou et al., 2007; Horvath and Barrangou, 2010), or unmethylated DNA as do restriction enzymes (Naito et al., 1995)] but rather by recognizing "transfer associated patterns" (TAPs), including membrane disruptions that occur during interactions with other cells deploying T6SS and T4SS translocation machines. Broad-host-range conjugative elements represent infectious bacterial "diseases" that can cause metabolic stress on their newly acquired hosts and thus represent a fitness burden to bacterial populations unable to combat their acquisition. The donor-directed T6SS attack paradigm may represent a strategy for suppressing the movement of horizontally

transferred genetic elements in bacterial populations regardless of their signature molecular patterns (such as nucleic acid chemical structures or primary sequences).

Description of Supplemental Movies

Movie S5.1 Polymyxin B induces a burst of T6SS activity in *P. aeruginosa*. Segments 1-3: Three concatenated time-lapse videos of *P. aeruginosa* PAO1 *retS* ClpV1-GFP growing on PBS agar pads containing 20 μg/mL polymyxin B. Cells exhibit a spike in T6SS activity frequently with multiple T6SS apparatuses per cell followed a gradual elimination of ClpV1-GFP dynamics. Segments 4-6: Three concatenated time-lapse videos of *P. aeruginosa* PAO1 *retS* ClpV1-GFP in the absence of polymyxin B. Cells exhibit constant levels of T6SS activity with the characteristic 'T6SS dueling' activity (Basler and Mekalanos, 2012).

Movie S5.2 Deletion of *tagT* eliminates the polymyxin B response. Segments 1-3: Three concatenated time-lapse videos of *P. aeruginosa* PAO1 *retS tagT* ClpV1-GFP growing on PBS agar pads containing 20 μg/mL polymyxin B. Cells exhibit a low, basal level of T6SS activity that is not significantly different from the cells grown in the absence of polymyxin B treatment. Segments 4-6: Three concatenated time-lapse videos of *P. aeruginosa* PAO1 *retS tagT* ClpV1-GFP in the absence of polymyxin B. Cells exhibit a low, basal level of T6SS activity. Note the absence of 'T6SS dueling' activity characteristic of this mutant (Basler et al., 2013).

Materials and Methods

Bacterial Strains. *P. aeruginosa* PAO1 and gentamicin-resistant *E. coli* MG1655 strains used in this study were described previously (Basler et al., 2013), and *E. coli* MC1061 (Casadaban and Cohen, 1980), SM10 and S17-1 (Simon et al., 1983) were obtained from our

laboratory's collection. F' plasmid was obtained from *E. coli* K12 ER2267 (New England Biolabs). pKM101 was obtained from *E. coli* K12 strain DSM-9497 (Leibniz-Institute DSMZ). Antibiotic concentrations were streptomycin, 100 μg/mL; gentamicin, 15 μg/mL; and irgasan, 20 μg/mL, kanamycin, 50 μg/mL, chloramphenicol, 15 μg/mL. Luria-Bertani (LB) broth (5 g/L NaCl) was used for all growth conditions. Liquid cultures were grown aerobically at 37 C.

Competition assay. Procedures were as previously described (Basler et al., 2013). Overnight cultures of *E. coli* or *P. aeruginosa* were washed with LB and diluted 50–200x in fresh LB and cultivated for 2.5–3.5 hr to optical density (OD) ~0.5–1.0. Cells were pelleted by centrifugation at 10,000xg for 3 min and resuspended at OD of ~10. Cell suspensions were then mixed at 1:1 ratio and 5 μL were spotted onto a dry LB agar plate. After 2 hr at 37 C, the spots were cut out, and the cells were resuspended in 1 mL LB. Serial dilutions of the resuspended cells were then spotted onto selective plates. T6SS activation efficiency defined as the Log_{10} of surviving colony forming units (CFU) of a given prey strain.

Transposon Mutagenesis. In vitro transposon mutagenesis EZ-Tn5 Custom Transposome Construction Kit (Epicentre) using manufacturer protocols. Briefly, the chloramphenicol resistance gene from pBAD33 (Guzman et al., 1995) was cloned into the multiple cloning site of pMOD-2. This vector was then linearized and incubated with EZ-Tn5 transposase and purified RP4 DNA. After heat inactivation of the reaction mixture, it was transformed into electro-competent *E. coli* MC1061 cells. Transposon mutants of RP4 were selected for growth on kanamycin and chloramphenicol. Plasmid DNA from individual colonies was prepped and sequenced. Transposon map was generated using Geneious software version 6.1.6 created by Biomatters (available from http://www.geneious.com/).

Conjugation efficiency assay. Cells used for determining conjugation efficiency were prepared as for the competition assay. Cells were mixed at OD ~10 at 1:1 ratio and 5 μL were spotted onto an LB agar plate. These spots were incubated for 1 hr at 37 C, then cut out and resuspended in 1 mL LB. Serial dilutions were spotted onto plates selective for the recipient strain and the conjugated DNA. The lower limit of detection of conjugation efficiency was ~200 conjugants per mating.

Polymyxin-response assay. *P. aeruginosa* cells were grown aerobically to OD ~ 1.0, washed with fresh LB, concentrated to OD ~10, and spotted onto 1% agarose pad (in 0.5x PBS) containing polymyxin B at the indicated concentrations. Cells were imaged 10 seconds after being spotted onto the agar pad and every 10 seconds thereafter for 5 minutes. ClpV1-GFP localization was determined as described previously (Basler and Mekalanos, 2012). Cells and ClpV1-GFP spots were counted using ImageJ function "Find Maxima", accuracy of counting was confirmed visually and function parameters adjusted accordingly for individual images.

Statistics. Student's t test was used to determine significance between indicated groups of numbers.

Chapter 6. Retrospective

In this chapter, I recount the major conclusions and insights of the work presented in this dissertation and assess their impact on the field as a whole. I also outline key unanswered questions representing potential areas for future study.

When my graduate studies began, the type 6 secretion system (T6SS) was still a complete mystery. Little was known about its genetic composition, the mechanism by which its substrates are secreted, what signals controlled its action, or what role it might play in polymicrobial communities. Over the course of this dissertation, I have recounted four different studies undertaken that have significantly advanced our understanding of the T6SS in each of these areas.

The first study involved systematically knocking out every gene in the *Vibrio cholerae* T6SS gene locus to determine each of their contributions to T6SS function (Zheng et al., 2011). This study was groundbreaking on a number of fronts. It was the first report of biological evidence for ClpV being dispensable for T6SS activity. This insight along with phenomenal biochemical work done by the Mogk laboratory (Bonemann et al., 2009; Pietrosiuk et al., 2011) revealed that ClpV did not translocate effectors down an intercellular tube, but rather ClpV remodels T6SS sheath subunits allowing for efficient turnover of T6SS compenents. This work also made a novel observation regarding the T6SS spike assembly. The T6SS in *V. cholerae* absolutely required one of the VgrG protein (VgrG-2) along with at least one of the other two VgrG proteins (VgrG-1 or VgrG-3). This observation was the first evidence suggesting that hetero-trimeric VgrG complexes not only could form but are actually required for T6SS activity. A third important observation made in this work was that the genes downstream of VgrG-1 and VgrG-2 appeared to be effector proteins. Later work from the Pukatzki laboratory (Miyata et al., 2011) and the Mekalanos laboratory (Dong et al., 2013) would confirm that these genes encode T6SS effector proteins and their cognate immunitiy proteins.

For all the advances that this first study made, it was not without its shortcomings. One of the genes encoded by the *V. cholerae* T6SS, VCA0105, seemed to not play a role in T6SS as its

deletion did not significantly affect T6SS activity. However, as was demonstrated in the second study presented in this dissertation, this protein actually plays a central role in T6SS assembly and effector delivery. The source of this discrepancy was a second copy of this gene located almost 200 kb away from the T6SS gene cluster. Deletion of both copies of this protein resulted in a substantial T6SS defect.

Through collaboration with the Leiman laboratory, a high-resolution crystal structure of this protein was obtained (Shneider et al., 2013). This crystal structure along with some biochemical analysis revealed that these PAAR-motif containing proteins served as a sharp conical tip for the VgrG trimer and are secreted along with the T6SS tube/spike complex. I preformed further bioinformatic analysis to find that many of these proteins carried N- or C-terminal extensions with identifiable enzymatic activities. These observations opened the door for the identification of a whole new class off T6SS effectors while also providing mechanistic insight into how they are secreted and translocated into target cells. Interestingly, while our manuscript was under review for publication, the Hayes laboratory independently discovered one of these PAAR-motif containing effectors in *Dickeya dadantii* (Koskiniemi et al., 2013). They were able to show that this Rhs and nuclease domain-containing protein was delivered into target cells in a T6SS-dependent manner, which served as a fitting biological confirmation of our bioinformatic and structure-based predictions.

The third study presented in this dissertation was a direct result of a brilliant insight made by a postdoc in the Mekalanos laboratory, Dr. Marek Basler. Dr. Basler, unlike others before him, not only collected static images to determine localization of subcellular bacterial structures but also observed how these structures changed over time by using time-lapse video-microscopy (Basler et al., 2012). It was through his videos that he discovered T6SS counterattacks between

Pseudomonas aeruginosa sister cells – a phenomenon he named "T6SS dueling" (Basler and Mekalanos, 2012). Based on these initial observations we worked together to characterize the T6SS-dependent killing activity associated with counterattacks toward heterologous species. In the years preceding this study, members of the Mougous and Attree laboratories had identified the components of a threonine phosphorylation pathway that post-translationally regulated the T6SS in *P. aeruginosa* (Casabona et al., 2012; Hsu et al., 2009; Mougous et al., 2007). We were able to demonstrate that this pathway was responsible for sensing exogenous T6SS assault and positioning the assembly and firing of the T6SS counterattack. Perhaps the most critical observation, however, was that these counterattacks were precisely aimed and caused no collateral damage to other neighboring cells, revealing a whole new degree of complexity in the interactions with microbial populations. For the first time, bacteria were being observed to selectively target individuals within a population not based on intrinsic sensitivities but rather based on their manifest behaviors.

Having observed this T6SS counterattack response in *P. aeruginosa* in response to its own T6SS as well as *V. cholerae* T6SS and *Acinetobacter baylyi* T6SS and having learned about a similar counterattack response to *Burkholderia thailandensis* T6SS (Leroux et al., 2012), it seemed increasingly unlikely that *P. aeruginosa* counterattacks were responding to any particular effector. Given the significant structural and mechanistic similarity to T6SS, members of our laboratory, including a very eager Professor Mekalanos, made a few attempts at observing whether bacteriophage might be able to induce *P. aeruginosa* T6SS activity as well. They, however, were met with little success. Despite these negative results, I wondered whether other forms of bacterial "poking" such as those associated with type 4 secretion system pili might transmit similar mechanical signals as the T6SS. Testing this idea was actually quite simple: mix

a conjugative donor strain with a T6SS$^+$ *P. aeruginosa* and observe under the microscope whether they round up and lyse. Taking these initial observations further, I was able to genetically determine that the type 4 secretion system structural components but not components only needed for DNA transfer itself were responsible for inducing T6SS counterattacks. That DNA transfer is not required is actually very important from a mechanistic perspective as it suggests that T6SS counterattacks might occur *before* DNA transfer is able to occur, because if it does, the T6SS would be able function as a form of bacterial innate immunity against the acquisition of foreign DNA elements. Amazingly, there was a roughly 86% decrease in DNA conjugation into T6SS$^+$ *P. aeruginosa* relative to a T6SS$^-$ mutant. Furthermore, the mechanical nature of the triggering signal means that this defense cannot simply be overcome by modifying or mutating the DNA molecule conferring both general applicability and robustness not observed in other foreign DNA resistance mechanisms like the clustered regularly interspaced short palindromic repeat (CRISPR) elements (Barrangou et al., 2007; Horvath and Barrangou, 2010) or restriction modification (RN) systems (Naito et al., 1995).

Together these last two studies have made significant insights into the mechanism of inter-bacterial communication and antagonism and have broad evolutionary and ecological implications. Unlike other systems that require specific receptors on target cells such as CDI (Aoki et al., 2008; Aoki et al., 2005; Aoki et al., 2009) and pyocins (Michel-Briand and Baysse, 2002) or that indiscriminately affect all nearby cells such as antibiotic production (Chater et al., 2010) or pH modulation (Yoon and Mekalanos, 2006), the T6SS enables *P. aeruginosa* to specifically eliminate threats while maintaining peaceful coexistence with other non-threatening bacteria. As such, it is unsurprising that *Pseudomonas* species are so widely recognized for their

ability to form multispecies biofilms (Dowd et al., 2008; Elias and Banin, 2012; Ha et al., 2012; Tashiro et al., 2013).

Despite the extensive progress and development of the T6SS field, there remain a number of outstanding unanswered questions. For example, three of the essential T6SS components identified in my systematic knockout analysis, namely TssF, TssG and TssA, still have no known structure or function. Furthermore, despite having crystal structures for the T6SS tube/spike complex components Hcp, VgrG, and the PAAR-motif proteins, we still do not know how they are assembled together in the context of a functional apparatus. We also do not know how effectors or effector extension domains fit into the assembled structure. In addition to these open questions regarding T6SS structure and assembly, we also still do not understand the role of the T6SS counterattack response outside of the laboratory setting. Given the generality of the mechanism by which the T6SS can be activated it is conceivable that host-derived signals (e.g. defensins, perforins, complement, etc.) might also induce T6SS responses. Furthermore, it is still unclear what role the antibacterial activity of T6SS might play in the context of the host microbiome. It is certainly conceivable that the T6SS might be able to modulate the resident microbiota by selectively killing certain bacterial species. Further investigation of the T6SS in the context of complex microbial communities is sure to yield exciting new insights into the study of microbial ecology both in the environment and within eukaryotic hosts.

Bibliography

Adams, P.D., Afonine, P.V., Bunkoczi, G., Chen, V.B., Echols, N., Headd, J.J., Hung, L.W., Jain, S., Kapral, G.J., Grosse Kunstleve, R.W.*, et al.* (2011). The Phenix software for automated determination of macromolecular structures. Methods *55*, 94-106.

Alteri, C.J., Himpsl, S.D., Pickens, S.R., Lindner, J.R., Zora, J.S., Miller, J.E., Arno, P.D., Straight, S.W., and Mobley, H.L. (2013). Multicellular Bacteria Deploy the Type VI Secretion System to Preemptively Strike Neighboring Cells. PLoS pathogens *9*, e1003608.

Altschul, S.F., Gish, W., Miller, W., Myers, E.W., and Lipman, D.J. (1990). Basic local alignment search tool. Journal of molecular biology *215*, 403-410.

Aoki, S.K., Malinverni, J.C., Jacoby, K., Thomas, B., Pamma, R., Trinh, B.N., Remers, S., Webb, J., Braaten, B.A., Silhavy, T.J.*, et al.* (2008). Contact-dependent growth inhibition requires the essential outer membrane protein BamA (YaeT) as the receptor and the inner membrane transport protein AcrB. Mol Microbiol *70*, 323-340.

Aoki, S.K., Pamma, R., Hernday, A.D., Bickham, J.E., Braaten, B.A., and Low, D.A. (2005). Contact-dependent inhibition of growth in Escherichia coli. Science *309*, 1245-1248.

Aoki, S.K., Webb, J.S., Braaten, B.A., and Low, D.A. (2009). Contact-dependent growth inhibition causes reversible metabolic downregulation in Escherichia coli. J Bacteriol *191*, 1777-1786.

Arisaka, F., Kanamaru, S., Leiman, P., and Rossmann, M.G. (2003). The tail lysozyme complex of bacteriophage T4. Int J Biochem Cell Biol *35*, 16-21.

Aschtgen, M.S., Bernard, C.S., De Bentzmann, S., Lloubes, R., and Cascales, E. (2008). SciN is an outer membrane lipoprotein required for type VI secretion in enteroaggregative Escherichia coli. J Bacteriol *190*, 7523-7531.

Aschtgen, M.S., Gavioli, M., Dessen, A., Lloubes, R., and Cascales, E. (2010a). The SciZ protein anchors the enteroaggregative Escherichia coli Type VI secretion system to the cell wall. Mol Microbiol.

Aschtgen, M.S., Thomas, M.S., and Cascales, E. (2010b). Anchoring the type VI secretion system to the peptidoglycan: TssL, TagL, TagP... what else? Virulence *1*, 535-540.

Aubert, D.F., Flannagan, R.S., and Valvano, M.A. (2008). A novel sensor kinase-response regulator hybrid controls biofilm formation and type VI secretion system activity in Burkholderia cenocepacia. Infection and immunity *76*, 1979-1991.

Axelrod, R., and Hamilton, W.D. (1981). The evolution of cooperation. Science *211*, 1390-1396.

Ballister, E.R., Lai, A.H., Zuckermann, R.N., Cheng, Y., and Mougous, J.D. (2008). In vitro self-assembly of tailorable nanotubes from a simple protein building block. Proc Natl Acad Sci U S A *105*, 3733-3738.

Barrangou, R., Fremaux, C., Deveau, H., Richards, M., Boyaval, P., Moineau, S., Romero, D.A., and Horvath, P. (2007). CRISPR provides acquired resistance against viruses in prokaryotes. Science *315*, 1709-1712.

Bartonickova, L., Sterzenbach, T., Nell, S., Kops, F., Schulze, J., Venzke, A., Brenneke, B., Bader, S., Gruber, A.D., Suerbaum, S.*, et al.* (2012). Hcp and VgrG1 are secreted components of the Helicobacter hepaticus type VI secretion system and VgrG1 increases the bacterial colitogenic potential. Cell Microbiol.

Basler, M., Ho, B.T., and Mekalanos, J.J. (2013). Tit-for-Tat: Type VI Secretion System Counterattack during Bacterial Cell-Cell Interactions. Cell *152*, 884-894.

Basler, M., and Mekalanos, J.J. (2012). Type 6 Secretion Dynamics Within and Between Bacterial Cells. Science.

Basler, M., Pilhofer, M., Henderson, G.P., Jensen, G.J., and Mekalanos, J.J. (2012). Type VI secretion requires a dynamic contractile phage tail-like structure. Nature *483*, 182-186.

Bayer, M., Eferl, R., Zellnig, G., Teferle, K., Dijkstra, A., Koraimann, G., and Hogenauer, G. (1995). Gene 19 of plasmid R1 is required for both efficient conjugative DNA transfer and bacteriophage R17 infection. Journal of bacteriology *177*, 4279-4288.

Benz, J., Sendlmeier, C., Barends, T.R., and Meinhart, A. (2012). Structural Insights into the Effector - Immunity System Tse1/Tsi1 from Pseudomonas aeruginosa. PLoS One *7*, e40453.

Bernard, C.S., Brunet, Y.R., Gavioli, M., Lloubes, R., and Cascales, E. (2011). Regulation of type VI secretion gene clusters by sigma54 and cognate enhancer binding proteins. J Bacteriol *193*, 2158-2167.

Bingle, L.E., Bailey, C.M., and Pallen, M.J. (2008). Type VI secretion: a beginner's guide. Current opinion in microbiology *11*, 3-8.

Bladergroen, M.R., Badelt, K., and Spaink, H.P. (2003). Infection-blocking genes of a symbiotic Rhizobium leguminosarum strain that are involved in temperature-dependent protein secretion. Mol Plant Microbe Interact *16*, 53-64.

Blondel, C.J., Jimenez, J.C., Contreras, I., and Santiviago, C.A. (2009). Comparative genomic analysis uncovers 3 novel loci encoding type six secretion systems differentially distributed in Salmonella serotypes. BMC Genomics *10*, 354.

Bonemann, G., Pietrosiuk, A., Diemand, A., Zentgraf, H., and Mogk, A. (2009). Remodelling of VipA/VipB tubules by ClpV-mediated threading is crucial for type VI protein secretion. Embo J *28*, 315-325.

Bonemann, G., Pietrosiuk, A., and Mogk, A. (2010). Tubules and donuts: a type VI secretion story. Mol Microbiol *76*, 815-821.

Boyer, F., Fichant, G., Berthod, J., Vandenbrouck, Y., and Attree, I. (2009). Dissecting the bacterial type VI secretion system by a genome wide in silico analysis: what can be learned from available microbial genomic resources? BMC Genomics *10*, 104.

Brooks, T.M., Unterweger, D., Bachmann, V., Kostiuk, B., and Pukatzki, S. (2013). Lytic Activity of the Vibrio cholerae Type VI Secretion Toxin VgrG-3 is Inhibited by the Antitoxin TsaB. The Journal of biological chemistry.

Brunet, Y.R., Bernard, C.S., Gavioli, M., Lloubes, R., and Cascales, E. (2011). An epigenetic switch involving overlapping fur and DNA methylation optimizes expression of a type VI secretion gene cluster. PLoS Genet *7*, e1002205.

Brunet, Y.R., Espinosa, L., Harchouni, S., Mignot, T., and Cascales, E. (2013). Imaging type VI secretion-mediated bacterial killing. Cell reports *3*, 36-41.

Busby, J.N., Panjikar, S., Landsberg, M.J., Hurst, M.R., and Lott, J.S. (2013). The BC component of ABC toxins is an RHS-repeat-containing protein encapsulation device. Nature.

Casabona, M.G., Silverman, J.M., Sall, K.M., Boyer, F., Coute, Y., Poirel, J., Grunwald, D., Mougous, J.D., Elsen, S., and Attree, I. (2012). An ABC transporter and an outer membrane lipoprotein participate in posttranslational activation of type VI secretion in Pseudomonas aeruginosa. Environ Microbiol.

Casadaban, M.J., and Cohen, S.N. (1980). Analysis of gene control signals by DNA fusion and cloning in Escherichia coli. Journal of molecular biology *138*, 179-207.

Cascales, E. (2008). The type VI secretion toolkit. EMBO Rep *9*, 735-741.

Cascales, E., and Cambillau, C. (2012). Structural biology of type VI secretion systems. Philos Trans R Soc Lond B Biol Sci *367*, 1102-1111.

Chakraborty, S., Sivaraman, J., Leung, K.Y., and Mok, Y.K. (2011). Two-component PhoB-PhoR regulatory system and ferric uptake regulator sense phosphate and iron to control virulence genes in type III and VI secretion systems of Edwardsiella tarda. The Journal of biological chemistry *286*, 39417-39430.

Chater, K.F., Biro, S., Lee, K.J., Palmer, T., and Schrempf, H. (2010). The complex extracellular biology of Streptomyces. FEMS Microbiol Rev *34*, 171-198.

Chou, S., Bui, N.K., Russell, A.B., Lexa, K.W., Gardiner, T.E., Leroux, M., Vollmer, W., and Mougous, J.D. (2012). Structure of a Peptidoglycan Amidase Effector Targeted to Gram-Negative Bacteria by the Type VI Secretion System. Cell Rep *1*, 656-664.

Christie, P.J., and Vogel, J.P. (2000). Bacterial type IV secretion: conjugation systems adapted to deliver effector molecules to host cells. Trends in microbiology *8*, 354-360.

Crooks, G.E., Hon, G., Chandonia, J.M., and Brenner, S.E. (2004). WebLogo: a sequence logo generator. Genome Res *14*, 1188-1190.

Das, S., and Chaudhuri, K. (2003). Identification of a unique IAHP (IcmF associated homologous proteins) cluster in Vibrio cholerae and other proteobacteria through in silico analysis. In Silico Biol *3*, 287-300.

de Berardinis, V., Vallenet, D., Castelli, V., Besnard, M., Pinet, A., Cruaud, C., Samair, S., Lechaplais, C., Gyapay, G., Richez, C.*, et al.* (2008). A complete collection of single-gene deletion mutants of Acinetobacter baylyi ADP1. Mol Syst Biol *4*, 174.

Ding, J., Wang, W., Feng, H., Zhang, Y., and Wang, D.C. (2012). Structural insights into the Pseudomonas aeruginosa type VI virulence effector Tse1 bacteriolysis and self-protection mechanisms. J Biol Chem.

Dong, T.G., Ho, B.T., Yoder-Himes, D.R., and Mekalanos, J.J. (2013). Identification of T6SS-dependent effector and immunity proteins by Tn-seq in Vibrio cholerae. Proceedings of the National Academy of Sciences of the United States of America *110*, 2623-2628.

Dong, T.G., and Mekalanos, J.J. (2012). Characterization of the RpoN regulon reveals differential regulation of T6SS and new flagellar operons in Vibrio cholerae O37 strain V52. Nucleic acids research *40*, 7766-7775.

Dowd, S.E., Sun, Y., Secor, P.R., Rhoads, D.D., Wolcott, B.M., James, G.A., and Wolcott, R.D. (2008). Survey of bacterial diversity in chronic wounds using pyrosequencing, DGGE, and full ribosome shotgun sequencing. BMC Microbiol *8*, 43.

Duda, R.L., Wall, J.S., Hainfeld, J.F., Sweet, R.M., and Eiserling, F.A. (1985). Mass distribution of a probable tail-length-determining protein in bacteriophage T4. Proceedings of the National Academy of Sciences of the United States of America *82*, 5550-5554.

Dudley, E.G., Thomson, N.R., Parkhill, J., Morin, N.P., and Nataro, J.P. (2006). Proteomic and microarray characterization of the AggR regulon identifies a pheU pathogenicity island in enteroaggregative Escherichia coli. Mol Microbiol *61*, 1267-1282.

Durand, E., Zoued, A., Spinelli, S., Watson, P.J., Aschtgen, M.S., Journet, L., Cambillau, C., and Cascales, E. (2012). Structural characterization and oligomerization of the TssL protein, a component shared by bacterial type VI and type IVb secretion systems. J Biol Chem *287*, 14157-14168.

Economou, A., Christie, P.J., Fernandez, R.C., Palmer, T., Plano, G.V., and Pugsley, A.P. (2006). Secretion by numbers: Protein traffic in prokaryotes. Molecular microbiology *62*, 308-319.

Elias, S., and Banin, E. (2012). Multi-species biofilms: living with friendly neighbors. FEMS Microbiol Rev.

Emsley, P., Lohkamp, B., Scott, W.G., and Cowtan, K. (2010). Features and development of Coot. Acta Crystallogr D Biol Crystallogr *66*, 486-501.

English, G., Trunk, K., Rao, V.A., Srikannathasan, V., Hunter, W.N., and Coulthurst, S.J. (2012). New Secreted Toxins and Immunity Proteins Encoded within the Type VI Secretion System Gene Cluster of Serratia marcescens. Mol Microbiol.

Ermolaeva, M.D., Khalak, H.G., White, O., Smith, H.O., and Salzberg, S.L. (2000). Prediction of transcription terminators in bacterial genomes. Journal of molecular biology *301*, 27-33.

Faruque, S.M., Albert, M.J., and Mekalanos, J.J. (1998). Epidemiology, genetics, and ecology of toxigenic Vibrio cholerae. Microbiology and molecular biology reviews : MMBR *62*, 1301-1314.

Felisberto-Rodrigues, C., Durand, E., Aschtgen, M.S., Blangy, S., Ortiz-Lombardia, M., Douzi, B., Cambillau, C., and Cascales, E. (2011). Towards a structural comprehension of bacterial type VI secretion systems: characterization of the TssJ-TssM complex of an Escherichia coli pathovar. PLoS Pathog *7*, e1002386.

Fernandez, D., Spudich, G.M., Zhou, X.R., and Christie, P.J. (1996). The Agrobacterium tumefaciens VirB7 lipoprotein is required for stabilization of VirB proteins during assembly of the T-complex transport apparatus. Journal of bacteriology *178*, 3168-3176.

Fey, P., Kowal, A.S., Gaudet, P., Pilcher, K.E., and Chisholm, R.L. (2007). Protocols for growth and development of Dictyostelium discoideum. Nature protocols *2*, 1307-1316.

Filloux, A. (2009). The type VI secretion system: a tubular story. The EMBO journal *28*, 309-310.

Filloux, A., Hachani, A., and Bleves, S. (2008). The bacterial type VI secretion machine: yet another player for protein transport across membranes. Microbiology *154*, 1570-1583.

Finn, R.D., Clements, J., and Eddy, S.R. (2011). HMMER web server: interactive sequence similarity searching. Nucleic Acids Res *39*, W29-37.

Flemming, H.C., and Wingender, J. (2010). The biofilm matrix. Nat Rev Microbiol *8*, 623-633.

Folkesson, A., Lofdahl, S., and Normark, S. (2002). The Salmonella enterica subspecies I specific centisome 7 genomic island encodes novel protein families present in bacteria living in close contact with eukaryotic cells. Res Microbiol *153*, 537-545.

French, C.T., Toesca, I.J., Wu, T.H., Teslaa, T., Beaty, S.M., Wong, W., Liu, M., Schroder, I., Chiou, P.Y., Teitell, M.A.*, et al.* (2011). Dissection of the Burkholderia intracellular life cycle using a photothermal nanoblade. Proc Natl Acad Sci U S A *108*, 12095-12100.

Fritsch, M.J., Trunk, K., Alcoforado Diniz, J., Guo, M., Trost, M., and Coulthurst, S.J. (2013). Proteomic identification of novel secreted anti-bacterial toxins of the Serratia marcescens Type VI secretion system. Mol Cell Proteomics.

Furste, J.P., Pansegrau, W., Frank, R., Blocker, H., Scholz, P., Bagdasarian, M., and Lanka, E. (1986). Molecular cloning of the plasmid RP4 primase region in a multi-host-range tacP expression vector. Gene *48*, 119-131.

Geer, L.Y., Domrachev, M., Lipman, D.J., and Bryant, S.H. (2002). CDART: protein homology by domain architecture. Genome Res *12*, 1619-1623.

Gibbs, K.A., Urbanowski, M.L., and Greenberg, E.P. (2008). Genetic determinants of self identity and social recognition in bacteria. Science *321*, 256-259.

Gibbs, K.A., Wenren, L.M., and Greenberg, E.P. (2011). Identity gene expression in Proteus mirabilis. J Bacteriol *193*, 3286-3292.

Giebelhaus, L.A., Frost, L., Lanka, E., Gormley, E.P., Davies, J.E., and Leskiw, B. (1996). The Tra2 core of the IncP(alpha) plasmid RP4 is required for intergeneric mating between Escherichia coli and Streptomyces lividans. Journal of bacteriology *178*, 6378-6381.

Goldova, J., Ulrych, A., Hercik, K., and Branny, P. (2011). A eukaryotic-type signalling system of Pseudomonas aeruginosa contributes to oxidative stress resistance, intracellular survival and virulence. BMC Genomics *12*, 437.

Gueguen, E., Durand, E., Zhang, X.Y., d'Amalric, Q., Journet, L., and Cascales, E. (2013). Expression of a Type VI Secretion System Is Responsive to Envelope Stresses through the OmpR Transcriptional Activator. PLoS One *8*, e66615.

Guzman, L.M., Belin, D., Carson, M.J., and Beckwith, J. (1995). Tight regulation, modulation, and high-level expression by vectors containing the arabinose PBAD promoter. J Bacteriol *177*, 4121-4130.

Ha, C., Park, S.J., Im, S.J., and Lee, J.H. (2012). Interspecies signaling through QscR, a quorum receptor of Pseudomonas aeruginosa. Mol Cells *33*, 53-59.

Haase, J., Lurz, R., Grahn, A.M., Bamford, D.H., and Lanka, E. (1995). Bacterial conjugation mediated by plasmid RP4: RSF1010 mobilization, donor-specific phage propagation, and pilus production require the same Tra2 core components of a proposed DNA transport complex. Journal of bacteriology *177*, 4779-4791.

Hachani, A., Lossi, N.S., Hamilton, A., Jones, C., Bleves, S., Albesa-Jove, D., and Filloux, A. (2011). Type VI secretion system in Pseudomonas aeruginosa: secretion and multimerization of VgrG proteins. J Biol Chem *286*, 12317-12327.

Hamburger, Z.A., Brown, M.S., Isberg, R.R., and Bjorkman, P.J. (1999). Crystal structure of invasin: a bacterial integrin-binding protein. Science *286*, 291-295.

Hankins, J.V., Madsen, J.A., Giles, D.K., Brodbelt, J.S., and Trent, M.S. (2012). Amino acid addition to Vibrio cholerae LPS establishes a link between surface remodeling in gram-positive and gram-negative bacteria. Proceedings of the National Academy of Sciences of the United States of America *109*, 8722-8727.

Hibbing, M.E., Fuqua, C., Parsek, M.R., and Peterson, S.B. (2010). Bacterial competition: surviving and thriving in the microbial jungle. Nature reviews Microbiology *8*, 15-25.

Ho, B.T., Basler, M., and Mekalanos, J.J. (2013). Type 6 Secretion System-Mediated Immunity to Type 4 Secretion System-Mediated Horizontal Gene Transfer. Science *342*, 250-253.

Hood, R.D., Singh, P., Hsu, F., Guvener, T., Carl, M.A., Trinidad, R.R., Silverman, J.M., Ohlson, B.B., Hicks, K.G., Plemel, R.L.*, et al.* (2010). A type VI secretion system of Pseudomonas aeruginosa targets a toxin to bacteria. Cell Host Microbe *7*, 25-37.

Horvath, P., and Barrangou, R. (2010). CRISPR/Cas, the immune system of bacteria and archaea. Science *327*, 167-170.

Hsu, F., Schwarz, S., and Mougous, J.D. (2009). TagR promotes PpkA-catalysed type VI secretion activation in Pseudomonas aeruginosa. Mol Microbiol *72*, 1111-1125.

Ishikawa, T., Rompikuntal, P.K., Lindmark, B., Milton, D.L., and Wai, S.N. (2009). Quorum sensing regulation of the two hcp alleles in Vibrio cholerae O1 strains. PLoS One *4*, e6734.

Kanamaru, S., Leiman, P.G., Kostyuchenko, V.A., Chipman, P.R., Mesyanzhinov, V.V., Arisaka, F., and Rossmann, M.G. (2002). Structure of the cell-puncturing device of bacteriophage T4. Nature *415*, 553-557.

Kapitein, N., and Mogk, A. (2013). Deadly syringes: type VI secretion system activities in pathogenicity and interbacterial competition. Curr Opin Microbiol.

Kikuchi, Y., and King, J. (1975). Genetic control of bacteriophage T4 baseplate morphogenesis. II. Mutants unable to form the central part of the baseplate. Journal of molecular biology *99*, 673-694.

Kitaoka, M., Miyata, S.T., Brooks, T.M., Unterweger, D., and Pukatzki, S. (2011). VasH is a transcriptional regulator of the type VI secretion system functional in endemic and pandemic Vibrio cholerae. J Bacteriol *193*, 6471-6482.

Kohanski, M.A., Dwyer, D.J., Hayete, B., Lawrence, C.A., and Collins, J.J. (2007). A common mechanism of cellular death induced by bactericidal antibiotics. Cell *130*, 797-810.

Kolenbrander, P.E., Palmer, R.J., Jr., Periasamy, S., and Jakubovics, N.S. (2010). Oral multispecies biofilm development and the key role of cell-cell distance. Nat Rev Microbiol *8*, 471-480.

Koskiniemi, S., Lamoureux, J.G., Nikolakakis, K.C., T'Kint de Roodenbeke, C., Kaplan, M.D., Low, D.A., and Hayes, C.S. (2013). Rhs proteins from diverse bacteria mediate intercellular competition. Proceedings of the National Academy of Sciences of the United States of America *110*, 7032-7037.

Kostyuchenko, V.A., Leiman, P.G., Chipman, P.R., Kanamaru, S., van Raaij, M.J., Arisaka, F., Mesyanzhinov, V.V., and Rossmann, M.G. (2003). Three-dimensional structure of bacteriophage T4 baseplate. Nat Struct Biol *10*, 688-693.

Kovach, M.E., Elzer, P.H., Hill, D.S., Robertson, G.T., Farris, M.A., Roop, R.M., 2nd, and Peterson, K.M. (1995). Four new derivatives of the broad-host-range cloning vector pBBR1MCS, carrying different antibiotic-resistance cassettes. Gene *166*, 175-176.

Krissinel, E., and Henrick, K. (2007). Inference of macromolecular assemblies from crystalline state. Journal of molecular biology *372*, 774-797.

Kyte, J., and Doolittle, R.F. (1982). A simple method for displaying the hydropathic character of a protein. Journal of molecular biology *157*, 105-132.

Langer, P.J., Shanabruch, W.G., and Walker, G.C. (1981). Functional organization of plasmid pKM101. Journal of bacteriology *145*, 1310-1316.

Leiman, P.G., Basler, M., Ramagopal, U.A., Bonanno, J.B., Sauder, J.M., Pukatzki, S., Burley, S.K., Almo, S.C., and Mekalanos, J.J. (2009). Type VI secretion apparatus and phage tail-associated protein complexes share a common evolutionary origin. Proc Natl Acad Sci U S A *106*, 4154-4159.

Leroux, M., De Leon, J.A., Kuwada, N.J., Russell, A.B., Pinto-Santini, D., Hood, R.D., Agnello, D.M., Robertson, S.M., Wiggins, P.A., and Mougous, J.D. (2012). Quantitative single-cell characterization of bacterial interactions reveals type VI secretion is a double-edged sword. Proc Natl Acad Sci U S A *109*, 19804-19809.

Lertpiriyapong, K., Gamazon, E.R., Feng, Y., Park, D.S., Pang, J., Botka, G., Graffam, M.E., Ge, Z., and Fox, J.G. (2012). Campylobacter jejuni type VI secretion system: roles in adaptation to deoxycholic acid, host cell adherence, invasion, and in vivo colonization. PLoS One *7*, e42842.

Lewis, K. (2000). Programmed death in bacteria. Microbiol Mol Biol Rev *64*, 503-514.

Li, M., Le Trong, I., Carl, M.A., Larson, E.T., Chou, S., De Leon, J.A., Dove, S.L., Stenkamp, R.E., and Mougous, J.D. (2012). Structural basis for type VI secretion effector recognition by a cognate immunity protein. PLoS Pathog *8*, e1002613.

Li, Z., Hiasa, H., Kumar, U., and DiGate, R.J. (1997). The traE gene of plasmid RP4 encodes a homologue of Escherichia coli DNA topoisomerase III. The Journal of biological chemistry *272*, 19582-19587.

Linn, T., and St Pierre, R. (1990). Improved vector system for constructing transcriptional fusions that ensures independent translation of lacZ. Journal of bacteriology *172*, 1077-1084.

Lossi, N.S., Dajani, R., Freemont, P., and Filloux, A. (2011). Structure-function analysis of HsiF, a gp25-like component of the type VI secretion system in Pseudomonas aeruginosa. Microbiology *157*, 3292-3305.

Luo, Z.Q., and Isberg, R.R. (2004). Multiple substrates of the Legionella pneumophila Dot/Icm system identified by interbacterial protein transfer. Proc Natl Acad Sci U S A *101*, 841-846.

Ma, A.T., McAuley, S., Pukatzki, S., and Mekalanos, J.J. (2009a). Translocation of a Vibrio cholerae type VI secretion effector requires bacterial endocytosis by host cells. Cell Host Microbe *5*, 234-243.

Ma, A.T., and Mekalanos, J.J. (2010). In vivo actin cross-linking induced by Vibrio cholerae type VI secretion system is associated with intestinal inflammation. Proc Natl Acad Sci U S A *107*, 4365-4370.

Ma, L.S., Lin, J.S., and Lai, E.M. (2009b). An IcmF family protein, ImpLM, is an integral inner membrane protein interacting with ImpKL, and its walker a motif is required for type VI secretion system-mediated Hcp secretion in Agrobacterium tumefaciens. Journal of bacteriology *191*, 4316-4329.

MacIntyre, D.L., Miyata, S.T., Kitaoka, M., and Pukatzki, S. (2010). The Vibrio cholerae type VI secretion system displays antimicrobial properties. Proc Natl Acad Sci U S A *107*, 19520-19524.

Mandlik, A., Livny, J., Robins, W.P., Ritchie, J.M., Mekalanos, J.J., and Waldor, M.K. (2011). RNA-Seq-based monitoring of infection-linked changes in Vibrio cholerae gene expression. Cell Host Microbe *10*, 165-174.

Marchler-Bauer, A., Zheng, C., Chitsaz, F., Derbyshire, M.K., Geer, L.Y., Geer, R.C., Gonzales, N.R., Gwadz, M., Hurwitz, D.I., Lanczycki, C.J.*, et al.* (2013). CDD: conserved domains and protein three-dimensional structure. Nucleic acids research *41*, D348-352.

Matson, J.S., Withey, J.H., and DiRita, V.J. (2007). Regulatory networks controlling Vibrio cholerae virulence gene expression. Infection and immunity *75*, 5542-5549.

McPhee, J.B., Lewenza, S., and Hancock, R.E. (2003). Cationic antimicrobial peptides activate a two-component regulatory system, PmrA-PmrB, that regulates resistance to polymyxin B and cationic antimicrobial peptides in Pseudomonas aeruginosa. Molecular microbiology *50*, 205-217.

Metzgar, D., Bacher, J.M., Pezo, V., Reader, J., Doring, V., Schimmel, P., Marliere, P., and de Crecy-Lagard, V. (2004). Acinetobacter sp. ADP1: an ideal model organism for genetic analysis and genome engineering. Nucleic Acids Res *32*, 5780-5790.

Michel-Briand, Y., and Baysse, C. (2002). The pyocins of Pseudomonas aeruginosa. Biochimie *84*, 499-510.

Miller, J.H. (1972). Experiments in molecular genetics (Cold Spring Harbor, N.Y., Cold Spring Harbor Laboratory).

Miller, V.L., and Mekalanos, J.J. (1988). A novel suicide vector and its use in construction of insertion mutations: osmoregulation of outer membrane proteins and virulence determinants in Vibrio cholerae requires toxR. Journal of bacteriology *170*, 2575-2583.

Miyata, S.T., Bachmann, V., and Pukatzki, S. (2013). Type VI secretion system regulation as a consequence of evolutionary pressure. Journal of medical microbiology.

Miyata, S.T., Kitaoka, M., Brooks, T.M., McAuley, S.B., and Pukatzki, S. (2011). Vibrio cholerae requires the type VI secretion system virulence factor VasX to kill Dictyostelium discoideum. Infect Immun *79*, 2941-2949.

Mogk, A., Haslberger, T., Tessarz, P., and Bukau, B. (2008). Common and specific mechanisms of AAA+ proteins involved in protein quality control. Biochem Soc Trans *36*, 120-125.

Morrison, D.C., and Jacobs, D.M. (1976). Binding of polymyxin B to the lipid A portion of bacterial lipopolysaccharides. Immunochemistry *13*, 813-818.

Moscoso, J.A., Mikkelsen, H., Heeb, S., Williams, P., and Filloux, A. (2011). The Pseudomonas aeruginosa sensor RetS switches type III and type VI secretion via c-di-GMP signalling. Environmental microbiology *13*, 3128-3138.

Mougous, J.D., Cuff, M.E., Raunser, S., Shen, A., Zhou, M., Gifford, C.A., Goodman, A.L., Joachimiak, G., Ordonez, C.L., Lory, S.*, et al.* (2006). A virulence locus of Pseudomonas aeruginosa encodes a protein secretion apparatus. Science *312*, 1526-1530.

Mougous, J.D., Gifford, C.A., Ramsdell, T.L., and Mekalanos, J.J. (2007). Threonine phosphorylation post-translationally regulates protein secretion in Pseudomonas aeruginosa. Nat Cell Biol *9*, 797-803.

Murdoch, S.L., Trunk, K., English, G., Fritsch, M.J., Pourkarimi, E., and Coulthurst, S.J. (2011). The opportunistic pathogen Serratia marcescens utilizes type VI secretion to target bacterial competitors. J Bacteriol *193*, 6057-6069.

Murshudov, G.N., Skubak, P., Lebedev, A.A., Pannu, N.S., Steiner, R.A., Nicholls, R.A., Winn, M.D., Long, F., and Vagin, A.A. (2011). REFMAC5 for the refinement of macromolecular crystal structures. Acta Crystallogr D Biol Crystallogr *67*, 355-367.

Naito, T., Kusano, K., and Kobayashi, I. (1995). Selfish behavior of restriction-modification systems. Science *267*, 897-899.

Nano, F.E., Zhang, N., Cowley, S.C., Klose, K.E., Cheung, K.K., Roberts, M.J., Ludu, J.S., Letendre, G.W., Meierovics, A.I., Stephens, G.*, et al.* (2004). A Francisella tularensis pathogenicity island required for intramacrophage growth. J Bacteriol *186*, 6430-6436.

Nikaido, H. (1994). Prevention of drug access to bacterial targets: permeability barriers and active efflux. Science *264*, 382-388.

Pallen, M., Chaudhuri, R., and Khan, A. (2002). Bacterial FHA domains: neglected players in the phospho-threonine signalling game? Trends in microbiology *10*, 556-563.

Pansegrau, W., Lanka, E., Barth, P.T., Figurski, D.H., Guiney, D.G., Haas, D., Helinski, D.R., Schwab, H., Stanisich, V.A., and Thomas, C.M. (1994). Complete nucleotide sequence of Birmingham IncP alpha plasmids. Compilation and comparative analysis. Journal of molecular biology *239*, 623-663.

Pell, L.G., Kanelis, V., Donaldson, L.W., Howell, P.L., and Davidson, A.R. (2009). The phage lambda major tail protein structure reveals a common evolution for long-tailed phages and the type VI bacterial secretion system. Proc Natl Acad Sci U S A *106*, 4160-4165.

Peters, B.M., Jabra-Rizk, M.A., O'May, G.A., Costerton, J.W., and Shirtliff, M.E. (2012). Polymicrobial interactions: impact on pathogenesis and human disease. Clin Microbiol Rev *25*, 193-213.

Pettersen, E.F., Goddard, T.D., Huang, C.C., Couch, G.S., Greenblatt, D.M., Meng, E.C., and Ferrin, T.E. (2004). UCSF Chimera--a visualization system for exploratory research and analysis. J Comput Chem *25*, 1605-1612.

Philippe, N., Alcaraz, J.P., Coursange, E., Geiselmann, J., and Schneider, D. (2004). Improvement of pCVD442, a suicide plasmid for gene allele exchange in bacteria. Plasmid *51*, 246-255.

Pieper, R., Huang, S.T., Robinson, J.M., Clark, D.J., Alami, H., Parmar, P.P., Perry, R.D., Fleischmann, R.D., and Peterson, S.N. (2009). Temperature and growth phase influence the outer-membrane proteome and the expression of a type VI secretion system in Yersinia pestis. Microbiology *155*, 498-512.

Pietrosiuk, A., Lenherr, E.D., Falk, S., Bonemann, G., Kopp, J., Zentgraf, H., Sinning, I., and Mogk, A. (2011). Molecular Basis for the Unique Role of the AAA+ Chaperone ClpV in Type VI Protein Secretion. J Biol Chem *286*, 30010-30021.

Pukatzki, S., Ma, A.T., Revel, A.T., Sturtevant, D., and Mekalanos, J.J. (2007). Type VI secretion system translocates a phage tail spike-like protein into target cells where it cross-links actin. Proc Natl Acad Sci U S A *104*, 15508-15513.

Pukatzki, S., Ma, A.T., Sturtevant, D., Krastins, B., Sarracino, D., Nelson, W.C., Heidelberg, J.F., and Mekalanos, J.J. (2006). Identification of a conserved bacterial protein secretion system in Vibrio cholerae using the Dictyostelium host model system. Proc Natl Acad Sci U S A *103*, 1528-1533.

Pukatzki, S., McAuley, S.B., and Miyata, S.T. (2009). The type VI secretion system: translocation of effectors and effector-domains. Curr Opin Microbiol *12*, 11-17.

Punta, M., Coggill, P.C., Eberhardt, R.Y., Mistry, J., Tate, J., Boursnell, C., Pang, N., Forslund, K., Ceric, G., Clements, J.*, et al.* (2012). The Pfam protein families database. Nucleic acids research *40*, D290-301.

Rao, P.S., Yamada, Y., Tan, Y.P., and Leung, K.Y. (2004). Use of proteomics to identify novel virulence determinants that are required for Edwardsiella tarda pathogenesis. Mol Microbiol *53*, 573-586.

Records, A.R. (2011). The type VI secretion system: a multipurpose delivery system with a phage-like machinery. Mol Plant Microbe Interact *24*, 751-757.

Rietsch, A., Vallet-Gely, I., Dove, S.L., and Mekalanos, J.J. (2005). ExsE, a secreted regulator of type III secretion genes in Pseudomonas aeruginosa. Proc Natl Acad Sci U S A *102*, 8006-8011.

Rossmann, M.G., and Blow, D.M. (1962). The detection of sub-units within the crystallographic asymmetric unit. Acta Crystallographica *15*, 24-31.

Rubires, X., Saigi, F., Pique, N., Climent, N., Merino, S., Alberti, S., Tomas, J.M., and Regue, M. (1997). A gene (wbbL) from Serratia marcescens N28b (O4) complements the rfb-50 mutation of Escherichia coli K-12 derivatives. Journal of bacteriology *179*, 7581-7586.

Russell, A.B., Hood, R.D., Bui, N.K., LeRoux, M., Vollmer, W., and Mougous, J.D. (2011). Type VI secretion delivers bacteriolytic effectors to target cells. Nature *475*, 343-347.

Russell, A.B., Leroux, M., Hathazi, K., Agnello, D.M., Ishikawa, T., Wiggins, P.A., Wai, S.N., and Mougous, J.D. (2013). Diverse type VI secretion phospholipases are functionally plastic antibacterial effectors. Nature.

Russell, A.B., Singh, P., Brittnacher, M., Bui, N.K., Hood, R.D., Carl, M.A., Agnello, D.M., Schwarz, S., Goodlett, D.R., Vollmer, W.*, et al.* (2012). A Widespread Bacterial Type VI Secretion Effector Superfamily Identified Using a Heuristic Approach. Cell Host Microbe *11*, 538-549.

Salomon, D., Gonzalez, H., Updegraff, B.L., and Orth, K. (2013). Vibrio parahaemolyticus type VI secretion system 1 is activated in marine conditions to target bacteria, and is differentially regulated from system 2. PLoS One *8*, e61086.

Sandkvist, M., Michel, L.O., Hough, L.P., Morales, V.M., Bagdasarian, M., Koomey, M., and DiRita, V.J. (1997). General secretion pathway (eps) genes required for toxin secretion and outer membrane biogenesis in Vibrio cholerae. Journal of bacteriology *179*, 6994-7003.

Schell, M.A., Ulrich, R.L., Ribot, W.J., Brueggemann, E.E., Hines, H.B., Chen, D., Lipscomb, L., Kim, H.S., Mrazek, J., Nierman, W.C.*, et al.* (2007). Type VI secretion is a major virulence determinant in Burkholderia mallei. Mol Microbiol *64*, 1466-1485.

Schindelin, J., Arganda-Carreras, I., Frise, E., Kaynig, V., Longair, M., Pietzsch, T., Preibisch, S., Rueden, C., Saalfeld, S., Schmid, B.*, et al.* (2012). Fiji: an open-source platform for biological-image analysis. Nat Methods *9*, 676-682.

Schlieker, C., Zentgraf, H., Dersch, P., and Mogk, A. (2005). ClpV, a unique Hsp100/Clp member of pathogenic proteobacteria. Biol Chem *386*, 1115-1127.

Schroder, G., and Lanka, E. (2005). The mating pair formation system of conjugative plasmids-A versatile secretion machinery for transfer of proteins and DNA. Plasmid *54*, 1-25.

Schwarz, S., Hood, R.D., and Mougous, J.D. (2010a). What is type VI secretion doing in all those bugs? Trends Microbiol *18*, 531-537.

Schwarz, S., West, T.E., Boyer, F., Chiang, W.C., Carl, M.A., Hood, R.D., Rohmer, L., Tolker-Nielsen, T., Skerrett, S.J., and Mougous, J.D. (2010b). Burkholderia Type VI Secretion Systems Have Distinct Roles in Eukaryotic and Bacterial Cell Interactions. PLoS Pathog *6*, e1001068.

Sheahan, K.L., Cordero, C.L., and Satchell, K.J. (2004). Identification of a domain within the multifunctional Vibrio cholerae RTX toxin that covalently cross-links actin. Proceedings of the National Academy of Sciences of the United States of America *101*, 9798-9803.

Shneider, M.M., Buth, S.A., Ho, B.T., Basler, M., Mekalanos, J.J., and Leiman, P.G. (2013). PAAR-repeat proteins sharpen and diversify the type VI secretion system spike. Nature *500*, 350-353.

Shrivastava, S., and Mande, S.S. (2008). Identification and functional characterization of gene components of Type VI Secretion system in bacterial genomes. PLoS One *3*, e2955.

Silverman, J.M., Agnello, D.M., Zheng, H., Andrews, B.T., Li, M., Catalano, C.E., Gonen, T., and Mougous, J.D. (2013). Haemolysin Coregulated Protein Is an Exported Receptor and Chaperone of Type VI Secretion Substrates. Mol Cell.

Silverman, J.M., Austin, L.S., Hsu, F., Hicks, K.G., Hood, R.D., and Mougous, J.D. (2011). Separate inputs modulate phosphorylation-dependent and -independent type VI secretion activation. Mol Microbiol *82*, 1277-1290.

Silverman, J.M., Brunet, Y.R., Cascales, E., and Mougous, J.D. (2012). Structure and Regulation of the Type VI Secretion System. Annu Rev Microbiol.

Simon, R., Priefer, U., and Puhler, A. (1983). A Broad Host Range Mobilization System for In Vivo Genetic Engineering: Transposon Mutagenesis in Gram Negative Bacteria. Nat Biotech *1*, 784-791.

Soding, J. (2005). Protein homology detection by HMM-HMM comparison. Bioinformatics *21*, 951-960.

Soding, J., Biegert, A., and Lupas, A.N. (2005). The HHpred interactive server for protein homology detection and structure prediction. Nucleic Acids Res *33*, W244-248.

Studholme, D.J., and Dixon, R. (2003). Domain architectures of sigma54-dependent transcriptional activators. Journal of bacteriology *185*, 1757-1767.

Suarez, G., Sierra, J.C., Erova, T.E., Sha, J., Horneman, A.J., and Chopra, A.K. (2010). A type VI secretion system effector protein, VgrG1, from Aeromonas hydrophila that induces host cell toxicity by ADP ribosylation of actin. J Bacteriol *192*, 155-168.

Suarez, G., Sierra, J.C., Sha, J., Wang, S., Erova, T.E., Fadl, A.A., Foltz, S.M., Horneman, A.J., and Chopra, A.K. (2008). Molecular characterization of a functional type VI secretion system from a clinical isolate of Aeromonas hydrophila. Microb Pathog *44*, 344-361.

Suo, Z., Avci, R., Deliorman, M., Yang, X., and Pascual, D.W. (2009). Bacteria survive multiple puncturings of their cell walls. Langmuir *25*, 4588-4594.

Tashiro, Y., Yawata, Y., Toyofuku, M., Uchiyama, H., and Nomura, N. (2013). Interspecies Interaction between Pseudomonas aeruginosa and Other Microorganisms. Microbes Environ *28*, 13-24.

Uratani, Y., and Hoshino, T. (1984). Pyocin R1 inhibits active transport in Pseudomonas aeruginosa and depolarizes membrane potential. J Bacteriol *157*, 632-636.

VanRheenen, S.M., Dumenil, G., and Isberg, R.R. (2004). IcmF and DotU are required for optimal effector translocation and trafficking of the Legionella pneumophila vacuole. Infect Immun *72*, 5972-5982.

Wenren, L.M., Sullivan, N.L., Cardarelli, L., Septer, A.N., and Gibbs, K.A. (2013). Two Independent Pathways for Self-Recognition in Proteus mirabilis Are Linked by Type VI-Dependent Export. MBio *4*.

Whitney, J.C., Chou, S., Russell, A.B., Biboy, J., Gardiner, T.E., Ferrin, M.A., Brittnacher, M., Vollmer, W., and Mougous, J.D. (2013). Identification, structure and function of a novel type VI secretion peptidoglycan glycoside hydrolase effector-immunity pair. The Journal of biological chemistry.

Wintermute, E.H., and Silver, P.A. (2010). Dynamics in the mixed microbial concourse. Genes Dev *24*, 2603-2614.

Wu, H.Y., Chung, P.C., Shih, H.W., Wen, S.R., and Lai, E.M. (2008). Secretome analysis uncovers an Hcp-family protein secreted via a type VI secretion system in Agrobacterium tumefaciens. Journal of bacteriology *190*, 2841-2850.

Yang, F., Waldor, M.K., and Mekalanos, J.J. (2013). Activation of T6SS-mediated antibacterial activity in the host revealed through Tn-seq analysis of Vibrio cholerae intestinal colonization. Cell Host Microbe *submitted*.

Yoon, S.S., and Mekalanos, J.J. (2006). 2,3-butanediol synthesis and the emergence of the Vibrio cholerae El Tor biotype. Infection and immunity *74*, 6547-6556.

Zheng, J., Ho, B., and Mekalanos, J.J. (2011). Genetic analysis of anti-amoebae and anti-bacterial activities of the type VI secretion system in Vibrio cholerae. PLoS One *6*, e23876.

Zheng, J., and Leung, K.Y. (2007). Dissection of a type VI secretion system in Edwardsiella tarda. Mol Microbiol *66*, 1192-1206.

Zheng, J., Shin, O.S., Cameron, D.E., and Mekalanos, J.J. (2010). Quorum sensing and a global regulator TsrA control expression of type VI secretion and virulence in Vibrio cholerae. Proc Natl Acad Sci U S A *107*, 21128-21133.

Zheng, J., Tung, S.L., and Leung, K.Y. (2005). Regulation of a type III and a putative secretion system in Edwardsiella tarda by EsrC is under the control of a two-component system, EsrA-EsrB. Infection and immunity *73*, 4127-4137.

Zhong, Z., Helinski, D., and Toukdarian, A. (2005). Plasmid host-range: restrictions to F replication in Pseudomonas. Plasmid *54*, 48-56.

Zoued, A., Durand, E., Bebeacua, C., Brunet, Y.R., Douzi, B., Cambillau, C., Cascales, E., and Journet, L. (2013). TssK is a trimeric cytoplasmic protein interacting with components of both phage-like and membrane anchoring complexes of the Type VI secretion system. The Journal of biological chemistry.